
The University Of Sheffield.

# Understanding interactions of barley (*Hordeum vulgare*) with soil nitrogen cycling activity and links to plant nitrogen preference.

Luke Fountain

A thesis submitted in partial fulfilment of the requirements for the degree of Doctor of Philosophy

The University of Sheffield
Faculty of Science
School of Biosciences

December 2022

# Abstract

Nitrogen is a crucial nutrient for plant survival and commonly applied as synthetic fertiliser in the form of $NH_4NO_3$ or urea in conventional agriculture. In soil, ammonium is rapidly converted to nitrate through the microbial process of nitrification. Much of the applied nitrogen is lost through leaching or release of $N_2O$, a potent greenhouse gas, through denitrification, which reduces efficiency and increases costs to the farmer. Plants generate bespoke rhizosphere microbiomes with downstream effects on function, particularly on the structure and activity of nitrifier and denitrifier communities. In this thesis I have designed a tension table system to maintain soil water-filled pore space (WFPS) that facilitated the high-throughput screening of 200 varieties of the second largest UK arable crop, spring barley (*Hordeum vulgare*) under varying WFPS conditions, for variation in ability to manipulate nitrification and denitrification, and have observed for the first time variation in gross nitrification rate between different cultivars. I have assessed using hydroponics techniques whether plant preference for ammonium or nitrate varies across select barley cultivars and whether this is influenced by changes in light intensity or carbon dioxide ($CO_2$). I demonstrated that when environmental constraints are removed, nitrogen preference tends to shift towards ammonium, and a shift to further increased ammonium uptake is observed in select cultivars when plants are exposed to short-term high light or growth at elevated $CO_2$. Moreover, I have demonstrated that nitrogen preference and plant ability to inhibit nitrification may be linked. Downstream these results will be used to assess if breeding for altered preference or manipulation of nitrification and/or denitrification represent routes to improve the sustainability of conventional agriculture.

## Acknowledgements

I would like to express my heartfelt thanks to my supervisor Professor Tim Daniell for providing me with the opportunity to study such a fascinating topic and I am forever grateful for his continuous day-to-day support throughout my PhD. I am also incredibly grateful for the support of my co-supervisor Professor Duncan Cameron who has always been there to provide advice and support when needed, and who has continued to push me to explore my wider research interests to further my research career. I would also like to express my thanks to my co-supervisor Professor Julie Gray for encouraging me to apply for this PhD, for her commitment to supporting me whenever needed and for her continuing guidance during my time in Sheffield. I am also grateful for the help and support provided by Dr. Luke Ramsay, Dr. Kelly Houston and Dr. Ken Loades at the James Hutton Institute for their help and support.

I would like to thank the BBSRC White Rose DTP for awarding me the scholarship to pursue my studies, without which I would not have been able to complete my PhD. I have been incredibly lucky to work with some incredible colleagues and friends during my studies, who have made my time here both easier and much more enjoyable. We have shared many great moments together during my PhD helping me to develop both personally and professionally, and it has been a pleasure to work and socialise with such caring and generous individuals. I would like to thank the members of the Daniell and Cameron lab groups for their continued support, in particular Robel, Sue, and Sara, without whom it would not have been possible to complete my large experiments. I would also like to thank Shifa, Harry, Jake, Maggi and other members of the AWEC research groups for their continued support and interest in my work. I am also forever grateful to

Heather, Rachel and Gemma for their support and patience in helping me to run and understand all of my IRMS samples.

Words cannot describe how grateful I am for the unwavering support of my parents throughout my academic and personal life, without their sacrifices it would not have been possible for me to finish this thesis. Their belief in me has given me the strength to carry on when I have struggled, and I am eternally grateful. I would also like to thank my grandma for her never-ending encouragement and sacrifices to make sure I have always had what I need to succeed both in my academic career and personal life, I am eternally grateful. I would also like to thank the rest of my family for continuing to support me over the past few years in pursuing my goal of completing my PhD, I appreciate you all.

Finally, I would like to thank my wife Francesca for everything she has done for me, for her undying love, care and support throughout my PhD. She is my source of encouragement and inspiration, and I would not have been able to complete my PhD without her help. I am incredibly lucky to have you in my life and want to thank you for everything that you have done for me, I am eternally grateful and love you always.

## Author's declaration

I, Luke Fountain, confirm that this thesis is my own work. I am entirely aware of the guidance of the University on the Practice of Unfair Means (www.sheffield.ac.uk/ssid/unfair-means). This work has never been previously presented for an award at this, or any other degree or any other university.

# Table of Contents

# List of Figures

# List of Tables

# Abbreviations

| | |
|---|---|
| AMO | Ammonia monooxygenase |
| ANCOVA | Analysis of co-variance |
| ANOVA | Analysis of variance |
| AOA | Ammonia oxidising archaea |
| AOB | Ammonia oxidising bacteria |
| AREs | Artificial root exudates |
| BNI | Biological nitrification inhibition |
| C | Carbon |
| $CO_2$ | Carbon dioxide |
| DCD | Dicyandiamide |
| $dH_2O$ | Deionised water |
| DMPP | 3,4-dimethylpyrazole phosphate |
| DW | Dry weight |
| DWt | Dry weight with tin cup |
| $eCO_2$ | Elevated carbon dioxide |
| FW | Fresh weight |
| FWt | Fresh weight with tin cup |
| GNR | Gross nitrification rate |
| GWAS | Genome-wide association study |
| HAO | Hydroxylamine oxidoreductase |
| JHI | James Hutton Institute |
| LMW-C | Low molecular weight carbon |
| N | Nitrogen |
| $N_2O$ | Nitrous oxide |
| $NH_4^+$ | Ammonium cation |
| NO | Nitric oxide |
| $NO_2^-$ | Nitrite anion |
| $NO_3^-$ | Nitrate anion |
| NOB | Nitrite oxidising bacteria |
| NOX | Nitrite oxidoreductase |

| | |
|---|---|
| NPK | Nitrogen, Phosphorous, Potassium fertiliser |
| NUE | Nitrogen use efficiency |
| $O_2$ | Oxygen |
| QTL | Quantitative trait loci |
| SMC | Soil moisture content |
| SNI | Synthetic nitrification inhibitor |
| Syn | Syngenta |
| T-0 | Time day 0 sample |
| T-3 | Time day 3 sample |
| T-5 | Time day 5 sample |
| TT | Tension table |
| WFPS | Water-filled pore space |
| WTW | Water to weight |

# Chapter 1: General introduction and Literature Review

## 1.1 Importance of nitrogen and agricultural sustainability

The global population is continuing to increase and is predicted to be 9.1 billion by 2050 (UN, 2017). There is therefore increased demand on food production and as a result, food insecurity is an increasing problem and achieving environmental sustainability is increasingly difficult (Wang, et al., 2018a). Nitrogen (N) is a crucial nutrient for plants and often limiting in soils. Application of large amounts of N fertiliser has increased dramatically to maximise yields and produce enough food to support the global population (Devkota et al., 2019; Galloway et al.; Peng et al., 2010), with an average increase of 1.2 % annually in N fertiliser demand (FAO, 2019). Inorganic N fertilisers are often applied as ammonium-based fertilisers such as ammonium nitrate or urea. Ammonium ($NH_4^+$) is produced by atmospherically fixing nitrogen through the Haber-Bosch process, which is an energy-intensive process, accounting for 1 % of global energy usage and 1.4% of global carbon dioxide ($CO_2$) emissions (Capdevila-Cortada, 2019).

The continued application of N fertilisers in intensive agriculture has resulted in several unintended consequences. Fertiliser application only increases crop yield to a certain level and then NUE is negatively affected (Dong & Lin, 2020; Fischer, 1993; Zhang et al., 2020). This means only 50 % of applied N is taken up by crops on average (Smil, 1999), where residual N may remain in the soil, or be lost through ammonia volatilisation, nitrification, denitrification or nitrate ($NO_3^-$) leaching (Carpenter et al., 1998), which have associated environmental impacts including pollution of groundwater sources and emission of nitrous oxide ($N_2O$). Due to extremely high costs associated with fertiliser production through Haber-Bosch, loss of applied N also causes huge economic losses. Adding appropriate amounts of fertiliser to meet demand while minimising losses through excess application remains a challenge to improve agricultural sustainability. Routes of plant N uptake and major routes of N loss from two major production systems (paddy rice system and typical dryland barley system) discussed in this chapter are

presented conceptually in Figure 1.1a and 1.1b respectively and will be referred to throughout this chapter.

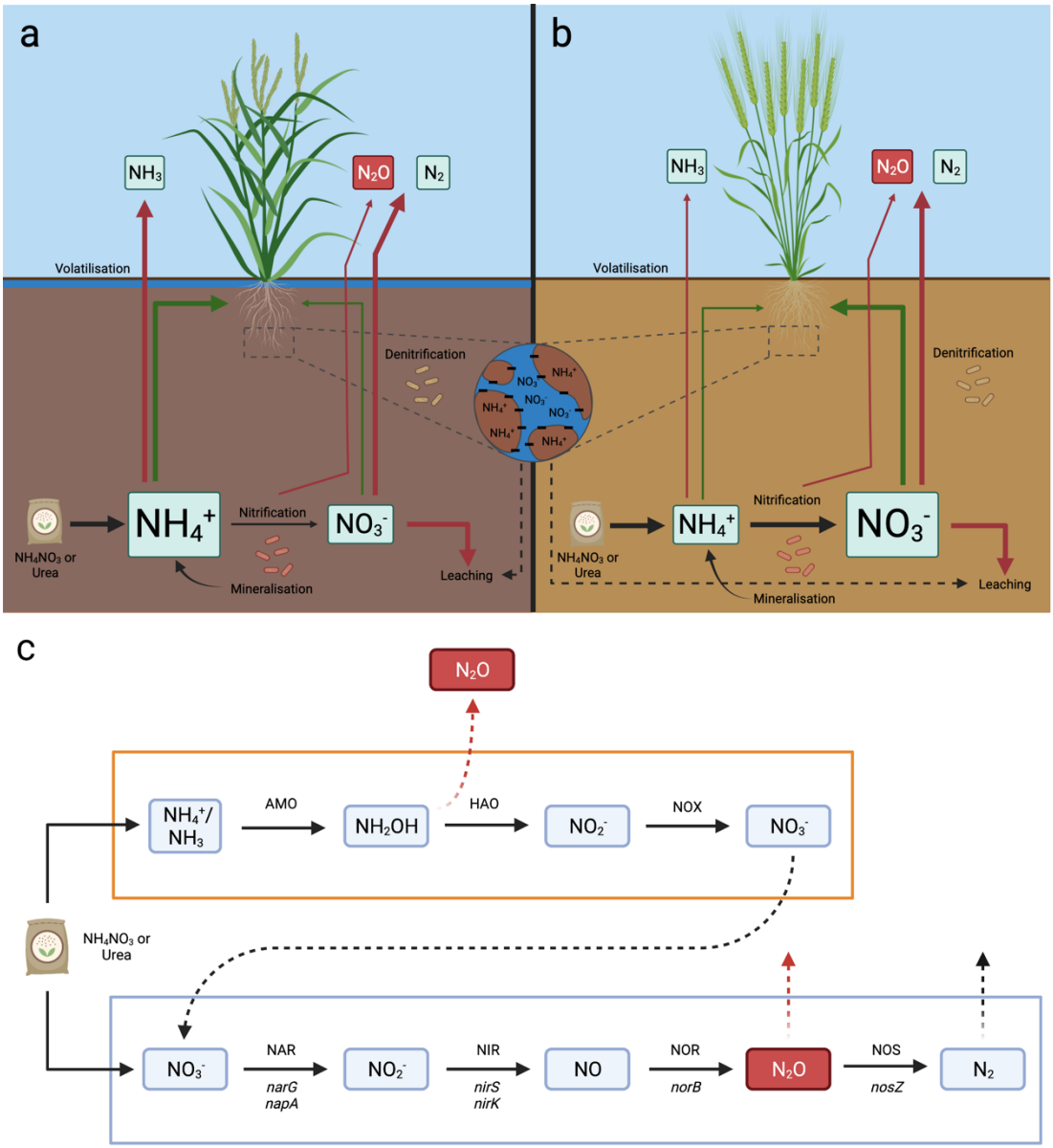


**Figure 1.1: a, b** Conceptualisation of plant N uptake and preference (green arrows), and routes of N loss (red arrows) in a typical paddy rice soil system (**a**) and a typical dryland barley soil system (**b**). Relative flux through pathways is represented by arrows and labels (for $NH_4^+$ and $NO_3^-$) of different sizes. **c** Nitrification (orange box) and denitrification (blue box) pathways including details of relevant enzymes; AMO (ammonia monooxygenase), HAO (hydroxylamine oxidoreductase), NOX (nitrite oxidoreductase), NAR (nitrate reductase), NIR (nitrite reductase), NOR (nitric oxide reductase) and NOS (nitrous oxide reductase). Corresponding genes are shown in italics. Gaseous emissions of $N_2O$ and $N_2$ are highlighted with fading dashed arrows (red for $N_2O$, black for $N_2$). The major source of $NH_4^+$ and $NO_3^-$ in arable soils is through fertilisation with $NH_4NO_3$ or urea. $NO_3^-$ produced via nitrification can also act as substrate for denitrification. Figure created in BioRender.

Major environmental problems arising as a result of increased nitrogen cycle-associated losses of fertiliser applied N include nitrate leaching and $N_2O$ emission (Cameron & Di, 2002; Gopalakrishnan et al., 2009; Mahmud et al., 2021) (Figure 1.1a, b). Nitrate leaching is a direct pathway of N loss from arable soils, causing eutrophication of surface waters and groundwater contamination (Cameron & Di, 2002; Jarvis et al., 1996; Pérez-Lucas et al., 2019; Xie et al., 2019), and is exacerbated as a result of increased nitrification driven by fertiliser addition. Both aerobic and anaerobic microsites are present in most soils (Hoorman, 2016), therefore nitrification is often coupled to the anaerobic process of denitrification, which acts as a sink of nitrate reducing availability to plants. Denitrification rates are generally very high in anaerobic systems such as paddy fields, though denitrification is also considered the major contributor of $N_2O$ emissions in drier systems (Skiba et al., 2012) (Figure 1.1a,b). Nitrification and denitrification are discussed in detail in section **1.2**.

$N_2O$ is produced both as a by-product of nitrification (Garcia-Ruiz et al., 1998; Goreau et al., 1980) and as either an intermediate or end product of denitrification (Payne, 1981; Smith & Arah, 1990). $N_2O$ is a potent greenhouse with 300x the warming potential of $CO_2$ over a 100-year period (Forster et al., 2007; Kanter et al., 2013). It is now considered the most important ozone-depleting molecule (Bouwman et al., 2013; Cicerone, 1987; Ravishankara et al., 2009) and its emission accounts for 10 % of global anthropogenic radiative forcing (Forster et al., 2007). The annual global $N_2O$ budget is estimated at 27.8 Tg $N_2O$ $yr^{-1}$ (Forster et al., 2007; Skiba et al., 2012), which is dominated by production from microbial processes in soil and aquatic systems that account for up to 89 % of emissions (Forster et al., 2007; Skiba et al., 2012). Anthropogenic emissions from agriculture account for 15.8 % or 4.4 Tg $N_2O$ $yr^{-1}$ of the global $N_2O$ budget (Skiba et al., 2012). In densely populated countries such as the UK, anthropogenic activities are the major source of $N_2O$ emissions. Emissions from agriculture accounted for 75 % of UK $N_2O$ emissions in 2008 with 23 % due to fertiliser and manure application (EEA, 2010). Denitrification is often considered the largest source of $N_2O$ in agricultural soils (Skiba et al., 2012), though the relative contribution of nitrification and denitrification to $N_2O$ emissions from a given soil is driven by a range of factors.

The processes of nitrification and denitrification and potential mitigation strategies are discussed in the following sections.

## 1.2 Nitrogen cycling processes

### 1.2.1 Nitrification

Nitrification is an aerobic process and the dominant process driving N loss from aerobic soils (Di et al., 2009; Hu et al., 2016). Nitrification can be carried out by both autotrophic and heterotrophic organisms, though autotrophic nitrification is considered the major pathway in arable soils (Anderson et al., 1993; Faeflen et al., 2016; Wang et al., 2018b) and therefore is the focus here. Autotrophic nitrification is carried out by chemolithoautotrophic ammonia oxidisers that gain energy from the oxidation of ammonia and nitrite which is used to fix carbon into biomass (Li et al., 2018; Norton & Ouyang, 2019; Xia et al., 2011). Nitrification is a three-step process whereby ammonia is oxidised to nitrite ($NO_2^-$) via the intermediate hydroxylamine ($NH_2OH$), followed by further oxidation to nitrate ($NO_3^-$) (Onley et al., 2018; Robertson & Groffman, 2006; Ward, 2013) (Figure 1.1c). The conversion of ammonia to hydroxylamine and subsequently nitrite is carried out by the ammonia monooxygenase (AMO) enzyme (Chen et al., 2010), to generate hydroxylamine, followed by conversion to nitrite by the hydroxylamine oxidoreductase (HAO) enzyme with $N_2O$ produced as a by-product (Caranto & Lancaster, 2017; Norton et al., 2002; Soler-Jofra et al., 2021). Nitrite is then converted to nitrate by nitrite oxidoreductase (NOX) (Chicano et al., 2021; Norton et al., 2002; Rani et al., 2017). Ammonia oxidation is considered the rate-limiting step of nitrification and the AMO enzyme is encoded by the *amo* operon which encodes three genes; *amoA*, *amoB*, and *amoC* (Chen et al., 2010; González-Cabaleiro et al., 2019; Wright et al., 2020). The subunit of AMO containing the active site is encoded by the *amoA* gene, and this gene is therefore usually the target when studying nitrifier community structure and activity.

Both ammonia-oxidising bacteria (AOB) and ammonia-oxidising archaea (AOA) are now understood to carry out the first step of nitrification, but the relative contribution of each to

nitrification-derived $N_2O$ emissions is thought to be dependent on soil pH (Gubry-Rangin et al., 2010; Hu et al., 2022; Offre et al., 2009) and ammonium concentration (Jia & Conrad, 2009; Ouyang et al., 2017), with AOB contributing towards a larger proportion of $N_2O$ emissions at alkaline pH and high ammonium concentration, and AOA contributing to most $N_2O$ emissions in more acidic soils with low ammonium concentration. However, the AOA *amoA* has been found to outnumber AOB *amoA* in several soils, including agricultural soils (Leininger et al., 2006).

Bacterial *amoA* genes are distinct from archaeal *amoA* genes, though conserved regions are present, and they are thought to have a common evolutionary origin (Chen et al., 2008; Ming et al., 2020). The only AOA identified to date are members of the *Crenarchaeota*, one of the four families of archaea (Venter et al., 2004). AOB can be grouped into three genera, *Nitrosomonas* (β-proteobacteria), *Nitrosospira* (β-proteobacteria) and *Nitrosococcus* (γ-proteobacteria) (Hayatsu et al., 2010). Nitrite-oxidising bacteria (NOB) are distinct from AOB and comprised of four genera; *Nitrobacter* (α-proteobacteria), *Nitrospina* and *Nitrospira* (δ-proteobacteria), and *Nitrococcus* (γ-proteobacteria) (Teske et al., 1994). It is still unclear whether nitrite-oxidising archaea exist (Hayatsu et al., 2008).

#### 1.2.1.1 Factors affecting nitrification

##### 1.2.1.1.1 Soil water-filled pore space and oxygen content

Soil oxygen content, driven in part by soil water-filled pore space (WFPS), the ratio of volumetric water content to total soil porosity, is a crucial factor driving nitrification rates and supporting nitrifier populations (Ma et al., 2020; Power & Prasad, 1997). WFPS is commonly used in nitrification and denitrification-related studies as it integrates information regarding soil porosity and water content and has been shown to be linked to microbial activity and nitrification-associated $N_2O$ emissions, which increase at WFPS below 60 % (Bateman & Baggs, 2005). WFPS below 60 % is often considered to be a largely aerobic system with enough available oxygen for nitrification. Oxygen is required both as substrate for the AMO enzyme and as a terminal electron acceptor during ammonia oxidation (Arp et al., 2002; Gilch et al., 2009; Qin et

al., 2020; Whittaker et al., 2000). High soil WFPS reduces nitrification rate by creating anaerobic conditions (Ohte et al., 1997), but most soils have sufficient oxygen to maintain nitrification at field capacity, except for paddy soils. Nitrification rates do, however, decline if soil remains sufficiently wet for several days (Liu et al., 2015; Sexstone et al., 1985; Tan et al., 2018). Contrasting nitrification rates and effects on N loss as a result of different soil WFPS are shown in Figure 1.1a and 1.1b for paddy rice systems and barley dryland systems, respectively.

#### 1.2.1.1.2 Soil pH

Soil pH is a significant controlling factor of substrate availability for nitrification. At lower pH, a larger proportion of ammonia is converted to ammonium. Given that ammonia is the substrate for ammonia oxidisers, acidic pH exponentially reduces substrate availability compared to alkaline pH (Allison & Prosser, 1993; Burton & Prosser, 2001). Soil pH also affects the relative abundance of AOB and AOA and therefore their relative contribution to $N_2O$ production from nitrification.

#### 1.2.1.1.3 Soil ammonium concentration

The concentration of ammonium in soil directly affects nitrification, with higher nitrification rates in general when ammonium substrate is more abundant. Ammonium concentration has differential effects on AOB and AOA abundance. In soils fertilised with large concentrations of ammonium (or urea which is rapidly hydrolysed to ammonium), AOB have been shown to be the dominant nitrifiers (Di et al., 2009; Jia & Conrad, 2009), whereas in soils where mineralisation of organic matter provides continual, lower supplies of ammonium, AOA have been observed to be dominant (Offre et al., 2009). A certain level of redundancy between AOA and AOB exists (Schauss et al., 2009).

#### 1.2.1.1.4 Soil temperature

Several studies have shown a significant positive relationship between temperature and nitrification rate with elevated temperature increasing nitrifier activity (Grundmann et al., 1995; Larsen et al., 2011), though the effects appear to be soil-specific (Hu et al., 2016), with studies also reporting no relationship between nitrification rate and temperature (Baer et al., 2014; Niboyet et al., 2011; Osborne et al., 2016; Shaw & Harte, 2001). Studies have also revealed that soil temperature can affect the contribution of heterotrophic and autotrophic nitrification, with autotrophic nitrification dominant at soil temperatures between 25°C to 35°C and heterotrophic nitrification dominant below 15°C (Liu et al., 2015).

#### 1.2.1.1.5 Plant presence

Plant root growth influences soil structure, aeration and oxygen content, and biological activity (Bertin et al., 2003). The chemical composition of soil, particularly the rhizosphere (the region of soil around plant roots), is affected by rhizodeposition of compounds into soil that provide carbon sources to promote microbial growth and activity (Hirsch et al., 2013; Nguyen, 2003; Philippot et al., 2013), often in the form of photosynthate (Kuzyakov and Domanski, 2000). In return, micro-organisms in the rhizosphere provide nutrients to support plant growth (Breidenbach et al., 2016). Root exudates can also have negative effects on soil microbial processes, for example exudation of compounds that inhibit nitrification, so-called biological nitrification inhibition (BNI), which act to inhibit nitrification through several mechanisms (see section **1.3** for more detail) but do not affect other micro-organisms present (Gopalakrishnan et al., 2009).

### 1.2.2 Denitrification

Denitrification is a microbial process that allows maintenance of respiration under oxygen-limiting conditions (Richardson, 2000) through the stepwise reduction of nitrate and other nitrogen oxides to $N_2O$ and $N_2$, using nitrogen oxides as alternative electron acceptors to oxygen (Zumft, 1997). Denitrification is carried out by facultative anaerobes that usually use oxygen as

the terminal electron acceptor in respiration but switch to N oxides when oxygen becomes limiting. Unlike nitrification, many bacteria and archaea from diverse groups have the potential to denitrify. Reduction of N oxides by denitrifiers is catalysed by nitrate reductase, nitrite reductase, nitric oxide reductase and nitrous oxide reductase, encoded by *narG*/*napA*, *nirK*/*nirS*, *norB* and *nosZ* genes respectively (Philippot, 2002; Zumft, 1997) (Figure 1.1c). Denitrification is a modular pathway (Graf et al., 2014), with some denitrifiers possessing only a subset of enzymes and therefore being exclusively $N_2O$ producers (K and S-denitrifiers) or $N_2O$ consumers (Z-type denitrifiers). KZ and SZ-type denitrifiers possess the full complement of enzymes and are therefore capable of reducing nitrate through to nitrogen (Graf et al., 2014; Jones et al., 2013), however the whole pathway is not always carried out depending on various abiotic and biotic factors (see below sections), often resulting in increased $N_2O$ emissions. Nitrite and nitric oxide reductases are always co-ordinately expressed as both N forms are cytotoxic (Giles et al., 2012). The types of denitrifiers that make up community structure in soil therefore affect the proportion of $N_2O/N_2$ production.

#### 1.2.2.1 Factors affecting denitrification

Denitrification in general is promoted by anaerobic conditions, readily available carbon sources and high nitrate concentrations (Philippot, 2002). However, denitrification rates and the relative proportion of $N_2O$ emission and $N_2$ production are affected by several environmental factors and their interaction, discussed in the following sections.

##### 1.2.2.1.1 Soil water-filled pore space and oxygen content

Soil water and oxygen content are intrinsically linked, as water acts as a barrier to rapid oxygen diffusion (Smith, 1990). A link between WFPS and denitrification was demonstrated by Weier et al., (1993), who showed that increased WFPS (decreasing oxygen content) increased denitrification rates but also showed increased $N_2$ production compared to $N_2O$ emissions. WFPS greater than 60-70 % is considered an anaerobic system, and denitrification-associated $N_2O$ emissions increase at this WFPS and above (Bateman & Baggs, 2005). Paddy soils are therefore

more conducive to high denitrification rates compared to dryland systems due to high WFPS creating anaerobic conditions (Figure 1.1a). The presence of oxygen reduces activity of denitrifying enzymes through inhibition of nitrate uptake systems (Hernandez & Rowe, 1987), regulating flow of electrons and suppressing expression of denitrifying genes (Berks et al., 1995). $N_2O$ reductase is the most sensitive of the N reductases to oxygen (Knowles, 1982; Morley et al., 2008), which is irreversibly damaged by oxygen, while other reductases are reversibly inhibited in the presence of oxygen (Morley & Baggs, 2010). Temporal and spatial variation in soil WFPS and oxygen content can therefore increase or decrease the proportion of $N_2O/N_2$, depending on time and length of exposure to oxygen.

#### 1.2.2.1.2 Soil pH

Alkaline soil pH between 7.0 and 8.0 is considered optimum for denitrification (Knowles, 1982), and acidic pH results in reduced denitrification rates (Brenzinger et al., 2015). Several studies have shown that $N_2O$ is the dominant denitrification product under acidic pH due to severe impairment of $N_2O$ reductase (Liu et al., 2010; Šimek & Cooper, 2002), though transcription of *nosZ* was shown to be unaffected by pH (Bergaust et al., 2010), suggesting that soil pH may have a post-translational effect on functional $N_2O$ reductase structure or activity. As a consequence of this severe effect on $N_2O$ reductase, pH is a major driver of $N_2O$:$N_2$ ratios produced via denitrification (Bakken et al., 2012; Bergaust et al., 2010; Liu et al., 2010; Šimek & Cooper, 2002). Soil pH also affects denitrifier community structure (Baggs & Philippot, 2010; Enwall et al., 2005; Herold et al., 2012), with *nirS*-type denitrifier abundance reduced under acidic pH compared to *nirK*-type denitrifiers (Herold et al., 2018). Moreover, low pH reduces available mineral nitrogen and organic carbon (Simek and Cooper, 2002; Baggs et al., 2010).

#### 1.2.2.1.3 Soil nitrate concentration

Sufficient nitrate (or other suitable forms such as nitrite or $N_2O$) is crucial for denitrification as it is used to maintain respiration as a terminal electron acceptor when oxygen is limiting. Denitrification is stimulated by fertiliser addition (Clayton et al., 1997; Webb et al., 2004).

However, if nitrate concentration is sufficiently high, $N_2O$ reduction is reduced (Firestone et al., 1979; Gaskell et al., 1981; Weier et al., 1993). It has been suggested that concentrations above 10 μg $N\text{-}NO_3^-$ g $soil^{-1}$ promote increased $N_2O$ emissions, and no $N_2O$ reduction occurred at a concentration of 44.9 μg $N\text{-}NO_3^-$ g $soil^{-1}$ (Senbayram et al., 2019). Where nitrate is limiting, such as in the rhizosphere where denitrifiers are in competition with plants for nitrate, reduced emissions of $N_2O$ have been observed (Duxbury et al., 1982).

#### 1.2.2.1.4 Soil carbon

Carbon (C) is often limited in soil through either chemical form or location (Giles et al., 2012a), but its availability is crucial for denitrification as it produces NADH via C degradation pathways and the TCA cycle, providing a source of electrons for denitrifying enzymes (Richardson, 2000). The presence of labile organic C has been shown to have a stimulatory effect on denitrification (Azam et al., 2002; Henry et al., 2008). Moreover, the quantity of C can control the efficiency of $N_2O$ reduction, altering the ratio of $N_2O$:$N_2$ produced, with the presence of labile C reducing the $N_2O$:$N_2$ ratio and therefore $N_2O$ emission (Firestone & Davidson, 1989; Morley et al., 2014; Weier et al., 1993). Effects of quantity of C on denitrification can be direct through supplying reductant to denitrifiers as described above, or indirect through stimulation of heterotrophic respiration in soil which reduces oxygen partial pressure, creating anaerobic conditions that favour denitrification (Giles et al., 2012).

The form of C also influences denitrification. Several studies have demonstrated that the addition of artificial root exudates (AREs) comprised of various sugars, amino acids and organic acids alters the ratio of $N_2O$:$N_2$ produced (e.g. Giles et al., 2017; Morley et al., 2014). Addition of high sugar concentration in AREs has been shown to increase $N_2O$ reduction (Henry et al., 2008), as has the addition of organic acids commonly exuded by plant roots (Morley et al., 2014). Addition of different low molecular weight carbon (LMW-C) compounds revealed different effects on the ratio of $N_2O$ to $N_2$ produced (Giles et al., 2017). Where C was added to soil as a single input, the authors found that differences in $N_2O$ and $N_2$ emissions were not driven by changes in denitrifier

community structure but instead were likely driven by changes in C substrate-use efficiency (Giles et al., 2017), though it is still unclear whether community structure changes would develop over longer timescales when C is supplied constantly, such as in the rhizosphere through rhizodeposition and root exudation.

## 1.3 Nitrification and denitrification mitigation strategies

It has been estimated that loss of fertiliser through processes such as nitrification, denitrification and nitrate leaching has associated economic costs of up to US$15 billion annually (Subbarao et al., 2007), in addition to the significant environmental consequences of groundwater pollution and eutrophication of surface waters. Given these major environmental and economic consequences, the regulation of nitrification and denitrification could have profound impacts for improving agricultural NUE and reducing environmental pollution and $N_2O$ emissions. Several strategies have been suggested and/or investigated to date with varying success (outlined in the following sections).

### 1.3.1 Fertiliser management

A range of fertiliser management practices have been employed to date, all of which work in a similar fashion, providing N to crops when required but managing or splitting fertiliser application to minimise surplus N in soil available for nitrification and denitrification. Applying reduced concentrations of fertiliser can be an effective method (Raun & Johnson, 1999; Wu et al., 2016), as can timing application to match periods of high plant N demand, however this approach is not always taken by farmers due to real and perceived risks (Dinnes et al., 2002). Split application is another common approach, with total fertiliser application split to apply smaller rates of N at growth stages of maximal N requirement, therefore minimising the surplus N present in soil that could subsequently be lost (Djaman et al., 2018). Controlled release fertilisers differ from traditional soluble fertiliser and are encapsulated by hydrophobic coatings that allow release of N over time, driven by soil temperature and moisture (Chandra et al., 2019). Deep placement of fertiliser can reduce N losses promoted during drying and rewetting cycles because

deeper soil layers are less prone to changes in soil moisture and reduce losses of N via leaching and denitrification (Rychel et al., 2020).

Though there are benefits of changing fertiliser management practices to improve NUE and reduce N losses, their wide-scale adoption is hindered by increased labour costs and practical difficulties which mean their use is limited on a global scale (Skiba et al., 2011).

### 1.3.2 Synthetic nitrification inhibitors

Another approach to reduce effects of nitrification is to target the pathway specifically. In addition to reducing loss of plant-available N via leaching, inhibition of nitrification reduces the substrate available for denitrification, and because the two processes are tightly coupled, this may reduce denitrification-associated N losses and $N_2O$ emissions (Subbarao et al., 2015). Nitrification inhibitors repress soil nitrification activity largely through inhibition of AMO enzyme activity i.e. the rate-limiting step of nitrification (Lu et al., 2019), and are applied to reduce N losses through nitrification and increase crop NUE (Abalos et al., 2014; Subbarao et al., 2006b; Sun et al., 2015). Commercially produced inhibitors are referred to as synthetic nitrification inhibitors or SNIs (Subbarao et al., 2006a,b). Common SNIs include nitrapyrin, dicyandiamide (DCD) and 3,4-dimethylpyrazole phosphate (DMPP), and act to directly inhibit AMO enzyme activity to reduce nitrification (Lu et al., 2019; Woodward et al., 2021). Each have their own benefits, with DMPP favoured in some countries because it is effective at lower concentrations compared to DCD and may be more effective at reducing losses due to nitrate leaching, ammonia volatilisation and $N_2O$ emission (Benckiser et al., 2013; Mahmood et al., 2011). However, DCD is favoured in countries such as New Zealand as it is less volatile, more soluble in water and cheaper (Giltrap et al., 2010). These SNIs often lead to increased ammonia volatilisation (Abalos et al., 2014; Lam et al., 2017) and their effectiveness varies across different soil types and climatic conditions (Fillery, 2007; Skiba et al., 2011; Zhang et al., 2020). High rates of microbial decay of SNIs and their leaching into surface and groundwater has also limited their effective application (Fillery, 2007; Gao et al., 2020; Skiba et al., 2011).

### 1.3.3 Biological nitrification inhibition (BNI)

More recently, plant-derived nitrification inhibitors have been identified which are released into the rhizosphere and surrounding soil through root exudation (Dayan et al., 2010; Gopalakrishnan et al., 2009; Kodama et al., 1992; Subbarao et al., 2006a,b; Sun et al., 2016). Inhibition resulting from these compounds is termed biological nitrification inhibition (BNI).

#### 1.3.3.1 BNI identity, characterisation and modes of action

BNI activity was first discovered in the roots of *Brachiaria humidicola*, a tropical pasture grass (Subbarao et al., 2006a), and further BNI activity has been found in crops such as sorghum and rice (Subbarao et al., 2007, 2013b; L. Sun et al., 2016). Key inhibitors identified from plant root exudates that demonstrate BNI activity belong to diverse functional groups and include brachialactone (diterpenoid), sorgoleone (quinone) and 1,9-decanediol (alcohol), isolated from root exudates of *Brachiaria humidicola*, *Sorghum bicolor* and *Oryza sativa* respectively (Subbarao et al., 2006a, 2013b; Sun et al., 2016). Root exudate BNI activity is thought to be composed of multiple nitrification inhibitors, each of which has a single mode or sometimes multi-mode inhibitory effect on nitrification enzymatic pathways (Subbarao et al., 2013b, 2015). The rice BNI compound 1,9-decanediol shows the same mode of action as common SNIs, inhibiting nitrifying activity of *Nitrosomonas* through blocking AMO enzyme activity (Sun et al., 2016). Other BNI compounds (e.g. brachialactone and sorgoleone) also inhibit HAO enzyme activity (Subbarao et al., 2008, 2009, 2013b). Furthermore, sorgoleone disrupts electron transfer from HAO to ubiquinone and cytochrome, which generates NADPH required for metabolic functions of *Nitrosomonas* (White, 1988, 1991).

#### 1.3.3.2 BNI release mechanisms

BNI compounds can be categorised as hydrophobic or hydrophilic (Subbarao et al., 2013a), and differ in their mobility (Subbarao et al., 2015). Hydrophobic BNI compounds (e.g. sorgoleone) are strongly adsorbed to soil organic and mineral particles which may increase their persistence in soil (Subbarao et al., 2015), and due to their movement largely being restricted to diffusion across

concentration gradients they are likely largely confined to the rhizosphere (Dayan et al., 2010; Subbarao et al., 2013a,b). In contrast, hydrophilic BNI compounds such as brachialactone are water-soluble and therefore may move out of the rhizosphere and suppress nitrifying activity in bulk soil (Subbarao et al., 2013a,b), a functional role that is complementary to hydrophobic BNI compounds (Subbarao et al., 2013a,b, 2015).

The release of BNI compounds through root exudation is strongly influenced by the form of N (i.e. ammonium or nitrate) present and stimulated by the presence of ammonium in the rhizosphere (Subbarao et al., 2007, 2013a, Gopalakrishnan et al., 2009, Zhu et al., 2012). Furthermore, only the part of the root system exposed to ammonium has been found to release BNI compounds (Subbarao et al., 2009). BNI release from roots is hypothesised to be driven by $H^+$-ATPase and associated with ammonium uptake and assimilation, at least in sorghum (Subbarao et al., 2015; Zhu et al., 2012). This regulation by ammonium suggests that release of BNIs may be an adaptive trait to help plants compete with nitrifiers for ammonium, and localised release ensures BNI concentrations are highest in areas with increased ammonium concentration and therefore nitrifying activity (Gopalakrishnan et al., 2009, Zhu et al., 2012).

There is also evidence to suggest that soil pH is another factor regulating BNI compound release (Subbarao et al., 2013a). The optimum pH for BNI compound release from sorghum roots was found to be 5.0-6.0 i.e. pH that stimulates proton pump functioning (Subbarao et al., 2013a; Zhu et al., 2012), and BNIs were not released from roots at pH ≥7.0, even in the presence of ammonium(Zhu et al., 2012). This only appears to be true for hydrophilic BNIs however, with release of hydrophobic BNIs unaffected by pH, likely because their release is not associated with proton pumping activity (Subbarao et al., 2015).

#### 1.3.3.3 Potential for genetic improvement of BNI and plant alteration of denitrification

A pre-requisite of improvement of any trait through breeding techniques is the existence of genetic variation in germplasm. Such variation has been identified for BNI activity in germplasm of *Brachiaria humidicola* (Gopalakrishnan et al., 2009; Subbarao et al., 2007a) and *Sorghum*

*bicolor* (Subbarao et al., 2013b; Tesfamariam et al., 2014), though quantitative trait loci (QTL) mapping has shown that a number of QTLs with small to moderate effects may be responsible for BNI release in *Brachiaria*, which may complicate marker-assisted selection for BNI release in this species (Subbarao et al., 2015). Nevertheless, given the associated difficulties and costs involved in screening large amounts of germplasm for BNI activity, the identification of markers associated with genetic regions affecting BNI could be useful (Subbarao et al., 2015).

BNI has the potential to improve agronomic NUE by improving soil N retention in the form of ammonium and reducing losses associated with nitrate leaching, nitrification and denitrification. This concept is illustrated in Figure 1.2a and 1.2b, which show simplified hypothesised flux through nitrification and routes of N loss without and with BNI activity respectively. The application of BNI to help mitigate N losses and improve NUE has several promising advantages over the use of SNIs. BNI compounds are released directly into the rhizosphere from plant roots and are more biologically stable, therefore their modes of action may be more efficient (Sadhukhan et al., 2022). BNI compounds are environmentally safe, and since the compounds are produced by the plant there is no need to manufacture and add inhibitors to soil, meaning BNI compounds present a more cost-effective solution than SNIs.

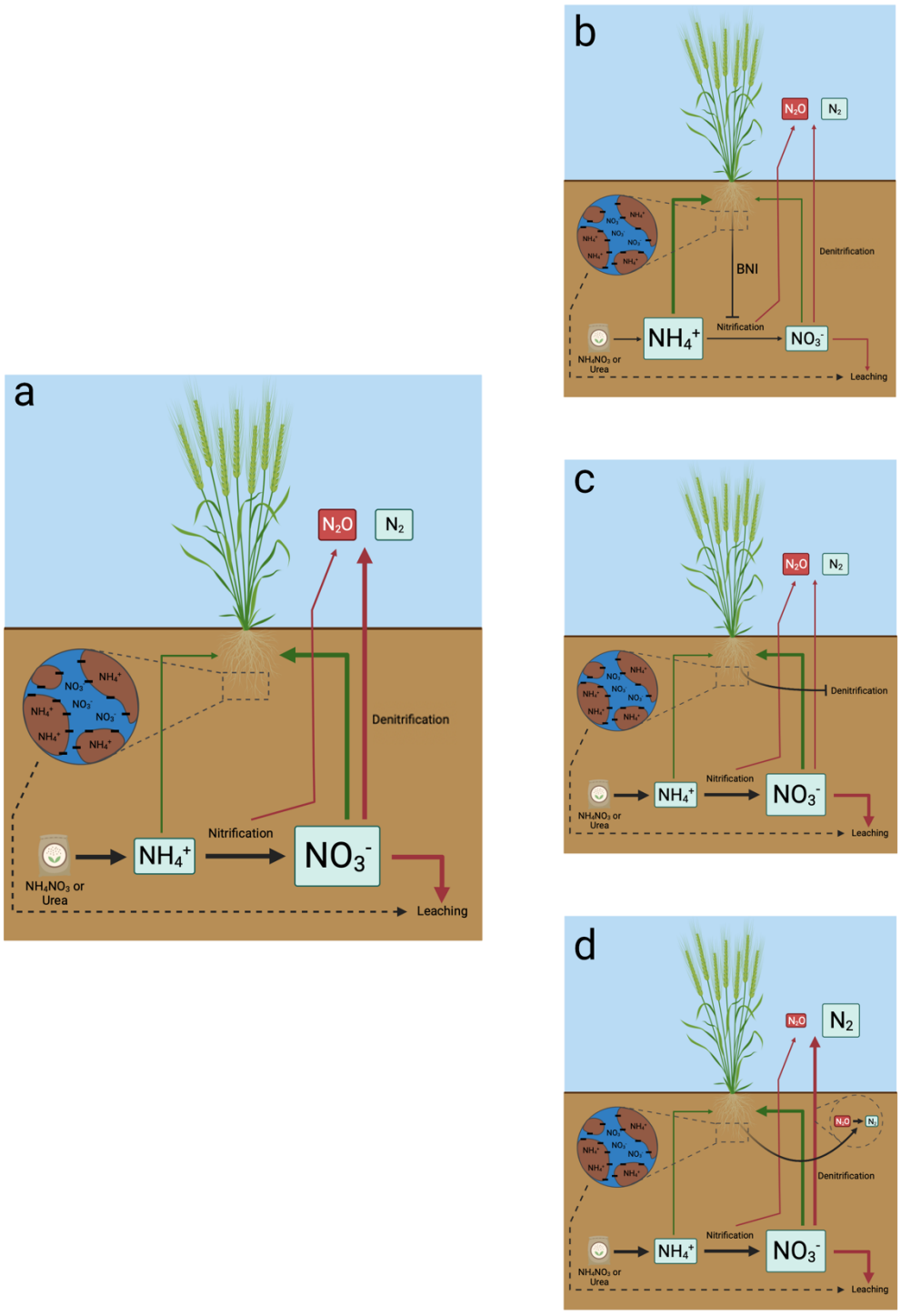


**Figure 1.2: a** Plant N uptake and preference (green arrows) and routes of N loss (red arrows) in a typical dryland barley soil system. Size of labels for $NH_4^+$ and $NO_3^-$ indicate relative pool size. **b** Hypothesised shifts in $NH_4^+$ and $NO_3^-$ pools, N preference and flux through major N pathways when plants exhibit BNI activity. Size of labels for $NH_4^+$ and $NO_3^-$ indicate relative pool size. **c** Hypothesised effect of plant inhibition of denitrification. **d** Hypothesised effect of plant promotion of $N_2O$ reduction on relative emissions of $N_2O$ and $N_2$. Size of labels for $N_2O$ and $N_2$ indicate relative emissions. For all panels, size of arrows indicates relative flux through the pathway. Figure created in BioRender.

Though significantly less research has focused on identifying germplasm variation in plant alteration of denitrification, an overall stimulatory effect of plant rhizodeposition has been observed (Philippot, 2002), though it is unclear if variation in rhizodeposition among germplasm varies in this positive rhizosphere effect, which could allow identification of germplasm that shows less of a stimulatory effect of denitrification or perhaps an inhibitory effect. Moreover, it may be possible to alter the proportion of $N_2O$:$N_2$ produced via denitrification. Several studies have shown variable effects on the proportion of $N_2O$:$N_2$ produced after addition of AREs containing different C compounds (discussed in section **1.3.1.4**). It is still unclear the extent to which root exudation of different C compounds may alter the ratio of $N_2O$:$N_2$ in arable soils, however the observation of increased $N_2O$ reductase activity and reduced $N_2O$ emissions with the addition of certain C compounds (Giles et al., 2017; Henry et al., 2008; Morley et al., 2014) suggests that plants may be able to alter denitrification rates and associated $N_2O$ emissions through root exudation. Whether this alteration would be through affecting denitrifier C substrate use efficiency, through alteration of community structure or a combination of both is still unclear (Giles et al., 2017). However, given that $N_2O$ reductase activity is the only known biological sink of $N_2O$, the characterisation of variation in germplasm to identify germplasm that regulates denitrification and/or promotes complete denitrification and production of benign $N_2$ over $N_2O$ emission could provide alternative routes to breed for improved environmental sustainability. The potential implications of reduced denitrification and increased $N_2O$ reduction driven by the plant are conceptualised in Figure 1.2c and 1.2d respectively.

## 1.4 Plant nitrogen preference

Nitrogen is considered the main limiting factor for plant growth in many temperate terrestrial ecosystems (Vitousek & Howarth, 1991). Most studies on ecosystem functioning focus on N as a single resource (Boudsocq et al., 2012) though it is well-known that plants can utilise different forms of N including nitrate, ammonium and organic N forms (Marschner, 2008). Most plants prefer inorganic forms of N (ammonium and nitrate) over organic forms of N such as amino acids

(Ashton et al., 2008; Harrison et al., 2007; Houlton et al., 2007), however plants utilise organic N in N-limited ecosystems such as alpine and arctic tundra (Chapin et al., 1993; Henry & Jefferies, 2003; Kielland, 1994; Lipson & Monson, 1998; Nordin et al., 2004; Raab et al., 1999; Schimel & Chapin, 1996), low-productivity grasslands (Bardgett et al., 2003; Streeter et al., 2000; Weigelt et al., 2003, 2005) and temperate (Finzi & Berthrong, 2005) and boreal forests (Nasholm et al., 1998; Nordin et al., 2001). Inorganic N forms are often the dominant N sources in intensive agriculture due to fertiliser addition predominantly in the form of ammonium nitrate, and N preference is therefore commonly defined as a plants choice to preferentially take up ammonium or nitrate in agricultural systems. This definition will be used hereafter when referring to 'N preference'.

Some plant species accumulate more N or produce more biomass when grown solely ammonium or nitrate, and this is where the notion of N preference originated (Britto & Kronzucker, 2013). Such variation in N preference remains poorly understood but has been attributed to various environmental, edaphic and physiological factors (Boudsocq et al., 2012; Britto & Kronzucker, 2013), discussed in the following sections.

### 1.4.1 Physiological factors affecting N preference

The uptake and assimilation of ammonium and nitrate differ in their photo-energetic cost, with a 45 % reduced cost to take up and assimilate ammonium compared to nitrate (Engels & Marschner, 1995) due to the fact that nitrate uptake occurs against a steep concentration gradient and then must be reduced to ammonium in the plant before assimilation, each of which requires a considerable expenditure of photosynthetically-fixed carbon compared to ammonium assimilation (Bloom et al., 1992; Britto & Kronzucker, 2005; Kurimoto et al., 2004). Despite this additional associated cost, most agricultural crop species (apart from rice) appear to prefer nitrate (Britto and Kronzucker, 2013). Several physiological and environmental factors may help to explain this phenomenon.

Rapid entry of ammonium into roots has been observed for both ammonium and nitrate specialists which can result in accumulation of ammonium in roots (Britto et al., 2001; Gerendás

et al., 1997), and hence ammonium toxicity can occur through suppressing the uptake of cations such as potassium ($K^+$), calcium ($Ca^{2+}$) and magnesium ($Mg^{2+}$) important for plant growth and function (Britto & Kronzucker, 2002; Kirkby, 1968; Lewis, 1992; Salsac et al., 1987; van Beusichem et al., 1988). Nitrate toxicity, however, typically occurs at much higher soil concentrations (Britto and Kronzucker, 2005). To counter effects of ammonium toxicity, plants assimilate most ammonium in the roots rapidly (Gerendás et al., 1997; Magalhães et al., 1995) but this requires elevated carbohydrate supply to the roots (Finnemann & Schjoerring, 1999; Kronzucker et al., 1998; Wang et al., 1993) which may reduce plant growth and maintenance (Lewis, 1992). Plants also increase ammonium efflux into the external medium in an energetically costly futile cycle (Britto et al., 2001; Li et al., 2012). Energy lost here may offset any energetic gain from uptake and assimilation of ammonium (Britto & Kronzucker, 2013). Plant N preference has also been observed to be dependent on growth stage, with a switch from ammonium to nitrate preference as growth progresses (Cui et al., 2017).

### 1.4.2 Environmental and edaphic drivers of N preference

#### 1.4.2.1 Interaction of N forms with soil

Ammonium is positively charged and therefore forms electrostatic interactions with soil clay particles and organic matter which have a net negative charge (Brady & Weil, 1999). Nitrate, on the other hand, does not form electrostatic attractions owing to its negative charge, and is therefore much more mobile in soil. This means that nitrate is more available to plants over a wider area but is also prone to losses through nitrate leaching and denitrification (Skiba et al., 2011) which can reduce nitrate available for uptake by plants (Figure 1.1a,b).

#### 1.4.2.2 Precipitation and soil moisture

N preference of different species has been shown to vary across precipitation gradients and therefore soil moisture gradients (Houlton et al., 2007; Wang & Macko, 2011), with ammonium-preferring species more abundant in wetter soils and nitrate-preferring species more abundant in drier soils (Houlton et al., 2007; Wang & Macko, 2011). Moreover, plant species experiencing the same precipitation did not show differences in N preference but appeared to switch N preference abruptly and in unison in response to changes in precipitation (Houlton et al., 2007; Wang and Macko, 2011), even within species. This suggests that plants do not specialise on different N forms through niche-partitioning, and instead rely on a common pool which is the most dominant in a system at a given point in time (Houlton et al., 2007). The relationship between soil moisture/precipitation and N preference is likely driven by variation in soil nitrification and denitrification (see section **1.3.3**) and may explain why paddy rice varieties, for example, are considered ammonium-preferring (Kirk, 2001) while most other crops, for example barley, tend to prefer nitrate (Figure 1.1a,b).

#### 1.4.2.3 Light intensity

The effect of light intensity on uptake of different N sources is poorly understood, however increased ammonium uptake has been observed in *Brassica chinensis* L. under long-term high light when grown under equal concentrations of ammonium and nitrate (Ma et al., 2016), possibly due to reduced intercellular $CO_2$ concentrations and photosynthesis at high light intensity brought about by stomatal closure that reduced the energy available for nitrate uptake which is more energetically demanding (Bloom et al., 1992; Britto & Kronzucker, 2005; Kurimoto et al., 2004). However, *Phaseolus vulgaris* L. plants grown solely under ammonium nutrition appear to be more sensitive to light stress than those grown solely under nitrate nutrition (Zhu et al., 2000), which the authors proposed was due to enhanced rates of photorespiration in ammonium-grown plants that reduced growth. These conflicting reports suggest that plant N

preference responses to changes in light intensity may be dependent on species and experimental conditions, and further research is necessary to fully understand this relationship.

#### 1.4.2.4 Carbon dioxide

Previous reports in the literature of plant N uptake responses to elevated $CO_2$ ($eCO_2$) have shown conflicting results (Bassirirad et al., 1996, 1997; Zerihun & Bassirirad, 2001), but more recent literature from Arnold Bloom and colleagues has suggested that $eCO_2$ may shift plants towards increased ammonium preference, with plants grown under nitrate nutrition showing reduced relative growth rate compared to those grown solely under ammonium nutrition at an elevated atmospheric $CO_2$ concentration of 720 ppm, the predicted atmospheric $CO_2$ concentration in 50 years (Bloom, 2015; Bloom et al., 2002, 2012; Cousins & Bloom, 2004; Searles & Bloom, 2003). This has been attributed to inhibition of shoot photo-assimilation of nitrate under $eCO_2$ in $C_3$ plants (Bloom et al., 2002, 2012). Nitrate reduction in leaves represents another sink for surplus reductant generated from photosynthesis when $CO_2$ is limiting (Shi-Wei et al., 2007), but under $eCO_2$ this reductant is diverted to carbon fixation which reduces a plants capacity to reduce nitrate (Bloom et al., 2002). Additionally, reductant produced via photorespiration is thought to be used for nitrate reduction in leaves, but due to the increased $CO_2$:$O_2$ ratio under $eCO_2$, rates of photorespiration are reduced and therefore reductant production from photorespiration is reduced (Bloom, 2015; Bloom et al., 2012; Cousins & Bloom, 2004; Searles & Bloom, 2003; Smart et al., 2001).

Given the reduced relative growth rate under nitrate nutrition and $eCO_2$, it is reasonable to hypothesise that $eCO_2$ would drive increased ammonium preference, and while this has been indirectly discussed in the literature (Bloom, 2015), to date the direct effect of $eCO_2$ on N preference has not been studied. A better understanding of plant N uptake responses to $eCO_2$ may help with the design of future climate-ready crops.

### 1.4.3 The influence of nitrogen cycling on N preference

In general, plants show plastic N uptake and preference responses to take up the dominant N form in a given environment at a given time (e.g. Harrison et al., 2007; Houlton et al., 2007; Wang & Macko, 2011). Relative pools of inorganic ammonium and nitrate are driven by soil N cycling processes, in particular nitrification and denitrification (described in detail in section **1.2**), which helps to explain the relationship between N preference and precipitation/soil moisture. Wetter soils that experience higher rates of precipitation and/or are managed such that soil is very wet (e.g. rice paddy soils) generally show reduced nitrification rates which is an oxygen-dependent process. Any nitrate that is produced via nitrification is rapidly denitrified either to $N_2O$ or $N_2$, removing plant-available N from the soil. Ammonium tends to dominate these low-nitrification soils and it is therefore not surprising that crops such as rice that are commonly grown in flooded paddy soils (Figure 1.1a), or more generally plants that grow in areas subjected to high amounts of rainfall tend to prefer ammonium (Houlton et al., 2007; Kirk, 2001; Wang & Macko, 2011). Conversely, plants grown in drier, well-aerated soils tend to prefer nitrate (Houlton et al., 2007; Wang and Macko, 2011) due to high nitrification rates that result in nitrate dominating the soil inorganic N pool (Figure 1.1b). This is, however, still a simplification, since N pools are dynamic and vary over both temporal and spatial scales, and pool size does not always reflect importance as some pools may be smaller due to rapid turnover (Britto & Kronzucker, 2013; Kirk & Kronzucker, 2005).

## 1.5 Relative importance of environment and genetics on N preference

Evidence continues to accumulate in the literature that plants display plasticity in uptake of different N forms in response to the dominant form available in a given time and space (Chalk & Smith, 2021). Soil nitrification rates are often considered to be the major driver (Barraclough, 1988, 1995; Barraclough et al., 1985; Barraclough & Smith, 1987; Chalk & Smith, 2021; Theory & Barraclough, 1991) of these N pools, in turn affected by environmental factors such as precipitation (see section **1.2.1.1.1** and **1.4.2.2**) and those described in section **1.2.1.1**. This body

of evidence suggests that environment appears to be of greater importance than any active 'preference' for a particular N form, leading to suggestions that the term 'N preference' is outdated and should perhaps be replaced with 'N plasticity' (Chalk & Smith, 2021).

However, there is also evidence to suggest a genetic component of N preference. Plants of different species grown in the field along a precipitation gradient showed N preference adaptations dependent on rainfall, with ammonium preference in wetter soils and nitrate preference in drier soils (Wang & Macko, 2011, see section 1.4.2.2). However, when seeds of plants across this gradient were grown under equal conditions in a greenhouse with equal supply of water, ammonium, and nitrate, they retained the N preference of the parental plant (Wang and Macko, 2011). While it is not clear whether this is a genetic effect or a maternal imprinting effect, it does suggest that while environment is a major driver of N preference, it is not the only factor to consider.

### 1.6 Aims and objectives of the thesis

Work carried out in this thesis is focused on the cereal crop spring barley (*Hordeum vulgare*). Barley is an important staple crop for animal feed and alcohol production (Newton et al., 2011). The UK is one of the world's largest producers of barley and accounts for 3.8 % of global barley production (Newton et al., 2011). Spring barley is the major cereal crop grown in Scotland and accounted for 58 % of land used for cereal crop growth in Scotland in 2019. Half of the spring barley produced in Scotland is used for malting to produce whisky, and Scotch whisky exports reached £4.37 billion in 2018 (Scottish Whisky Association, 2018), accounting for 20 % of all UK food and drink exports in the UK (O'connor, 2018). The main aims of this thesis are to assess variation in interactions of barley elite germplasm with N cycling processes, particularly nitrification and denitrification, and of N preference, to understand whether such variation exists and whether it can be exploited to improve the sustainability of barley cultivation through reduced N losses and environmental pollution such as nitrate leaching and $N_2O$ emissions.

The potential for BNI to improve the sustainability of agriculture through reduced N losses via leaching and denitrification is still being realised (Subbarao et al., 2015) (Figure 1.2b), and although variation in BNI activity in germplasm of *Brachiaria humidicola* (Subbarao et al., 2007) and *Sorghum bicolor* (Subbarao et al., 2013b; Tesfamariam et al., 2014) has been identified, the extent to which such variation exists in other major crops is poorly understood. A major aim of this thesis was therefore to assess if variation in BNI activity exists in spring barley elite germplasm to begin to understand whether such phenotypic variation could be exploited along with downstream genetic techniques such as genome-wide association studies (GWAS) to identify targets for future breeding programs to improve sustainability of barley cultivation.

Similarly, plant alteration of denitrification is a potential route for mitigation of denitrification-associated $N_2O$ emissions. The reduction of $N_2O$ by $N_2O$ reductase is the only known biological sink of $N_2O$, thus the promotion of $N_2O$ reductase activity is a logical target for reduction of $N_2O$ emissions from agricultural soils. It is well-known that plants impose a "rhizosphere effect" and affect denitrification rates through growth and activity of the root system (Philippot et al., 2013), thought to be driven by rhizodeposition (Philippot, 2002). The addition of carbon compounds as artificial root exudates has been shown to influence denitrification rates and the ratio of $N_2O$:$N_2$ emitted through alteration of denitrifier community structure (described in section **1.2.2.1.4**). It remains unclear, however, whether variation in root exudation or rhizodeposition exists across germplasm that may drive variation in the ratio of $N_2O$:$N_2$ produced via denitrification. This thesis therefore aimed to assess if variation exists in the ability of barley germplasm to alter denitrification rates (Figure 1.2c) and the ratio of $N_2O$:$N_2$ produced (Figure 1.2d). The existence of such variation, as with BNI, could help to identify future breeding targets through downstream genome-wide association study (GWAS) analyses. Screening of the influence of barley germplasm on nitrification and denitrification with enough germplasm will allow GWAS analyses to be performed downstream to identify any regions of the barley genome that may be associated with these traits.

Plant N preference is intrinsically linked with soil N cycling, and often driven by environmental conditions that determine nitrification and denitrification rates which in turn are responsible for the dominant N form in a given soil at a given time (reviewed in Chalk & Smith, 2021 and discussed in section **1.4**). Intra-species variation in N preference is poorly understood, but if such variation exists in barley germplasm, the identification of more ammonium-preferring cultivars could have similar advantages to increased BNI activity, that is reduced nitrification activity through enhanced competition with nitrifiers for ammonium (Figure 1.2b). Moreover, if such variation in N preference across barley germplasm exists, it will be important to understand how it is affected by changes in environmental conditions such as elevated $CO_2$. It has been suggested that elevated $CO_2$ may increase ammonium preference through inhibition of shoot nitrate assimilation (described in section **1.4.2.4**), though this has yet to be directly tested. If true, in addition to reducing N losses through nitrification, ammonium-preferring cultivars may be considered climate ready for a future elevated $CO_2$ environment. A further aim of this thesis was therefore to assess variation in N preference across barley germplasm and whether this is affected by changes in environmental conditions.

This thesis will provide insight into spring barley germplasm variation in BNI activity, ability to control denitrification and associated $N_2O$ production, N preference under varying environmental conditions, and their potential interactions. The objectives of the thesis chapters were:

**Chapter 2:** The aim of this chapter was to design a tension table system capable of accurately maintaining WFPS in soil microcosms to create aerobic conditions promoting nitrification or anaerobic conditions promoting denitrification, allowing high-throughput screening of barley germplasm.

**Chapter 3:** The main objective of this chapter was to utilise the tension table system developed in Chapter 2 to understand whether variation exists in the BNI activity of barley germplasm and to assess if this is related to soil factors. Sufficient germplasm was included to allow downstream GWAS analysis.

**Chapter 4:** The aim of this chapter was to use tension tables developed in chapter 2 to assess if the barley germplasm screened in Chapter 3 displays variation in ability to alter denitrification rates and/or the ratio of $N_2O$:$N_2$ emitted and whether it is affected by soil factors. Sufficient germplasm was included to allow downstream GWAS analysis.

**Chapter 5:** This chapter aimed to assess whether variation in a subset of barley germplasm included in previous chapters showed variation in 'innate' N preference, using a custom hydroponics system that removed environmental constraints of preference. This chapter also aimed to understand whether such innate N preference varied under short-term high light and growth at elevated atmospheric $CO_2$.

**Chapter 6:** The main objective of this chapter was to summarize the main research findings of the above chapters both separately and in combination, as well as potential future work that is needed to better understand the research presented in this thesis. Potential links between N preference, BNI activity and denitrification were explored.

# Chapter 2: Design and optimisation of simplified tension tables for plant growth and control of soil WFPS

## 2.1 Introduction

Despite recent advances in next-generation sequencing techniques that have facilitated large-scale generation of genetic marker information for genotyping, there is a distinct lag in the subsequent high-throughput phenotyping required to draw meaningful links between plant traits and related genes/genomic regions (Ortiz et al., 2018). Soil nitrogen cycling processes such as nitrification and denitrification are driven by soil oxygen content, with the aerobic process of nitrification requiring oxygen and therefore being the dominant $N_2O$-producing process at soil water-filled pore space (WFPS) below 60 % and denitrification, which occurs in the absence of oxygen, the dominant $N_2O$-producing process at WFPS above 70 % (Bateman & Baggs, 2005). There is therefore a need to control soil WFPS in a precise and reproducible manner to successfully study these processes.

The current standard practice for experimental control of soil WFPS is through watering to weight, where water is added to soil to a calculated weight that corresponds to a specific target WFPS. Watering to weight does however have several disadvantages. WFPS continuously decreases between watering periods, meaning a specific WFPS cannot be stably achieved but rather a range. This could present issues when studying processes sensitive to changes in WFPS where it could mean the difference between a largely aerobic or anaerobic soil, altering the dominant soil process.

Manual watering to weight is time-consuming and therefore not suited to high throughput screening experiments such as those carried out in chapters 4 and 5. Attempts have been made to automate the process, for example the PHENOPSIS system (Granier et al., 2006), which uses a robotic arm to automatically weigh pots and water to weight through an irrigation tube if below the target weight, controlled by programmable software. These technologies often require

extensive knowledge to operate and are largely cost-prohibitive. More recently, novel low-cost technologies have been leveraged to design 'DIY-style' irrigation systems using open-source modular components such as Arduino and/or Raspberry Pi calibrated moisture sensors (Ortiz et al., 2018) to maintain soil moisture, and while costs are brought down by such technologies making them more widely accessible to researchers, setup can still be complicated and costs can still be prohibitive when implemented at scale, despite their modular design.

Tension tables, sometimes referred to as suction tables, may offer a low-cost alternative to achieve homogenous and reproducible control of soil WFPS due to their passive nature and reduced reliance on electrical components. Tension tables are routinely used to determine soil water release characteristics by imposing a suction pressure to soil microcosms placed on a porous barrier (Romano et al., 2002). The maximum suction pressure achieved depends on the air entry value of the barrier material used. Several porous barriers have been implemented in the past, with early table iterations simply using Whatman filter paper (Clement, 1966) to achieve suction pressures up to 0.75 m. The technique was popularised when Stakman et al. (1969) proposed the use of fine sand for suction pressures up to 1.0 m, or a sand/kaolin mix to achieve higher suction pressures (up to 5.0 m). Silica flour and glass microfiber membranes have been used to achieve suctions up to 2.0 m (Ball & Hunter, 1988). Regardless of barrier material used, tables depend on the establishment of a continuous water column from the porous material in the table itself to a body of water in a suction control system, often referred to simply as a 'reservoir'.

Commercial tension table systems are available (e.g. Eijkelkamp Fraste UK Ltd.) but are often cost-prohibitive, therefore many research groups have opted to construct bespoke systems. Tension tables have been used in soil physics for decades, but reports of application to plant growth and high-throughput plant phenotyping are sparse. Previous work in the Daniell lab has established that simplified tension tables are capable of sustaining plant growth at variable WFPS

without the need to impose large suction pressures (Allery, 2019), but their use as a high-throughput automated watering system allowing stable control of WFPS is yet to be investigated.

The work in this chapter set out to build on previous research in the lab and past tension table iterations to design and optimise a simplified system capable of sustaining barley growth at a range of stable WFPS, using low-cost materials such that the system could be scaled up for high throughput screening of variability in nitrification and denitrification across a sufficiently large panel of barley varieties to allow subsequent genotypic analysis (Chapters 4 and 5).

## 2.2 Materials and methods

### 2.2.1 Tension table construction

#### 2.2.1.1 Table and ladder circuit construction

Tension tables were initially constructed from 10 mm thick transparent acrylic, but subsequent designs used 6 mm thick opaque green acrylic to block out light and minimise algal growth. Two end pieces of 60 mm x 390 mm and 2 side pieces of 60 mm x 790 mm were glued to a 400 mm x 790 mm base piece using Acrifix192 acrylic glue, to form a tray shape (Figure 2.1a). All acrylic and Acrifix192 glue was sourced from www.plasticsheetshop.co.uk. Leak tests were performed before proceeding.

A 6mm hole was drilled into each side piece for addition of a ladder circuit. Ladder circuits were constructed using 4 mm internal diameter (I.D.) microbore porous pipe (LBS Horticulture Ltd.) and standard aquarium airline T and elbow connectors (Amazon UK). A detailed schematic with measurements is presented in Appendix A.1. Ladder circuits were glued in place to the bottom of the tension table using standard Gorilla glue (Wilko), using small spots of glue to prevent blockages (Figure 2.1a). Ladder circuits were connected through the drilled holes to a 5-way metal aquarium manifold (Amazon UK) using opaque blue 4 mm I.D. PTFE tubing (RS Components). Tubing was sealed into the table with Gorilla glue ensuring a watertight connection. A 15 cm section of PTFE tubing was connected to one unregulated end of the

manifold, and a luer lock placed at the other end of the tubing for priming of the system (Figure 2.1b).

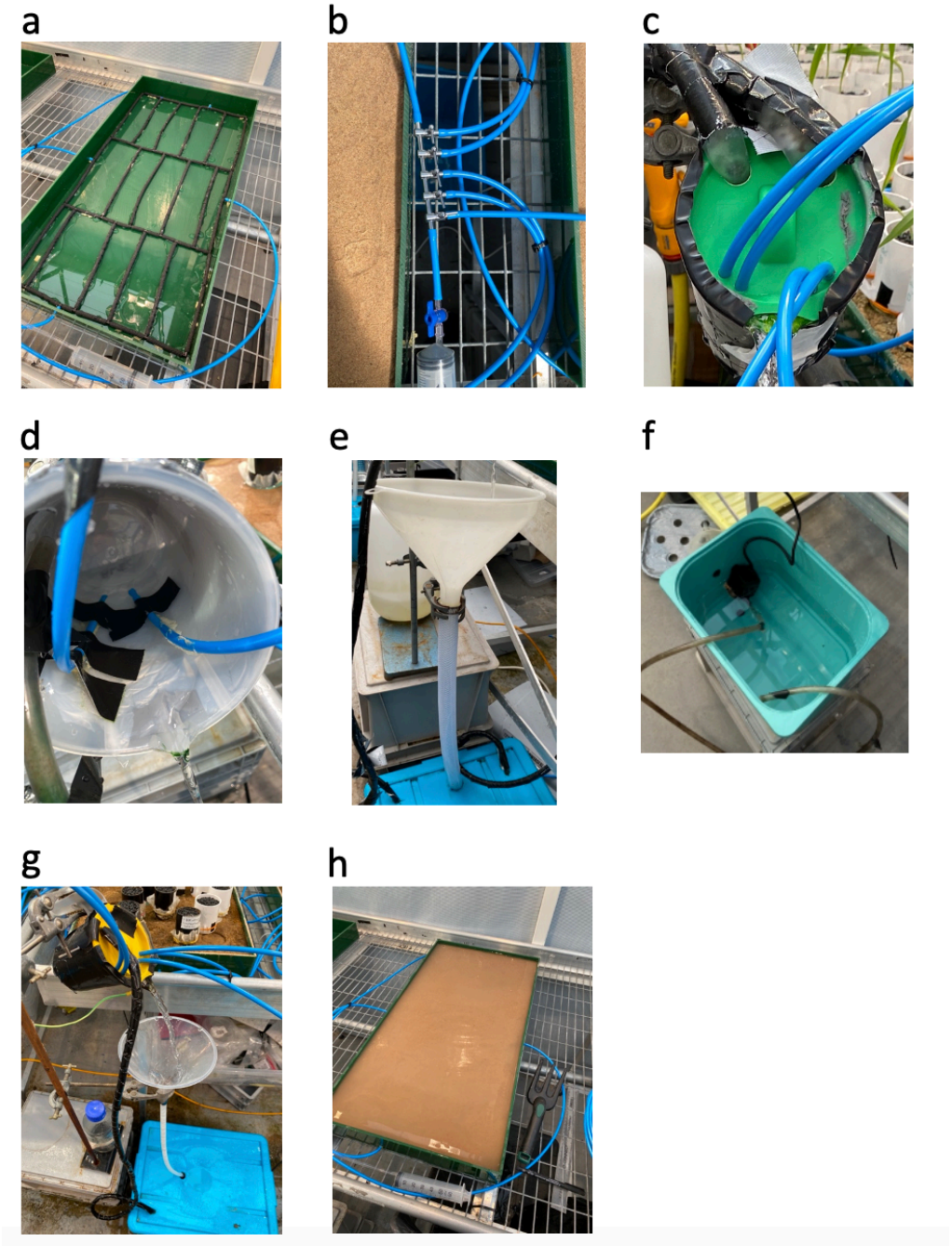


**Figure 2.1**: Tension table system assembly. **a.** Assembled green acrylic table with porous pipe ladder circuit glued to the base. **b.** Manifold with 4 controllable lines feeding the ladder circuit, and the fifth connecting the reservoir. Blue tubing containing a luer lock is attached to the unregulated end. **c.** Reservoir lid with 14 mm holes for pump tubing and 6 mm holes for blue tubing feeding the table. This photograph is from a later experiment that included additional tubing; initial designs as in this chapter contained only a single hole for each. **d.** Tubing feeding each table was fixed to the interior of the reservoir jug with Gorilla tape. **e.** Drain to minimise loss of water draining from the reservoir. **f.** water holding tank with submersible pump before addition of the lid. **g.** When switched on, the reservoir pump system constantly cycled water from the tank into the reservoir and drained it back again to ensure water always remained in the reservoir. **h.** Flooded table after addition of silica sand.

#### 2.2.1.2 Pump and reservoir system construction

Reservoirs were constructed from 500 ml plastic jugs with lids (Amazon UK). A 6 mm hole was drilled into the lid near the mouth for each table to be connected, and a single 14 mm hole drilled at the top of the lid for pump tubing (Figure 2.1c). Storage boxes with lids and a volume of 50 l were used as water holding tanks (B&M Retail Ltd., IKEA). A single 14 mm hole was drilled into the lid for pump tubing, and a single 25 mm hole for drain tubing.

Drains were constructed to minimise spillage of water flowing from the reservoir, by gluing a 40 cm length of 1 inch diameter hosing (Amazon UK) to the bottom of a 20 cm diameter plastic funnel (Amazon UK) using Gorilla glue. The glued connections were reinforced with a Jubilee clip (Amazon UK) (Figure 2.1e).

Both the reservoir and drain were secured to a retort stand with clamps, with the drain positioned below the reservoir, which was tilted to an approximate 45° angle (Figure 2.1g). A submersible aquarium pump (Amazon UK) with a maximum flow rate of 1500 l $hr^{-1}$ and maximum head height of 2 m was positioned inside the holding tank (Figure 2.1f) and 12 mm I.D. tubing connected to the pump and fed through the 14 mm hole in the lid of both the holding tank and the reservoir, where it was fixed in place with waterproof Gorilla tape. A 1 m length of 4 mm I.D. PTFE tubing (ensuring enough slack for movement of the reservoir) was connected to the remaining valve on the 5-way manifold, and the other end fed into the 6mm hole in the reservoir lid and secured with waterproof tape.

#### 2.2.1.3 System setup and priming

Tables were placed on a levelled bench in a controlled environment greenhouse cubicle at the Arthur Willis Environment Centre, University of Sheffield. The reservoir pump system was placed in front of the table, and the retort stand positioned such that the reservoir could be lifted above and dropped below the table surface. With all manifold valves closed, tables were slowly filled with tap water until the ladder circuit was completely submerged. Tap water was pushed into the

ladder circuit through the luer lock using a syringe, with valves to the table open but the reservoir valve closed. This was repeated until no air bubbles were released into the water in the table from the ladder circuit, before closing all manifold valves.

Very fine silica sand (CNHST60, supplied by Minerals Marketing) with an average grain size of 239 μm and an air-entry value of between 0.35-0.50 m (determined by the James Hutton Institute) was added to the table using a scoop, until the sand surface reached 1 cm below the top of the acrylic walls (24 kg sand per table). Sand was left to settle out in the water for 1-2 h before levelling gently avoiding compaction (Figure 2.1h).

The holding tank was filled with water and, with all manifold valves closed, the submersible pump was turned on to allow water to be pumped into the reservoir and drained back into the tank (Figure 2.1g). Reservoir height markers were added to the retort stand using a spirit level and tape measure, with reservoir height defined as the difference in height between the surface of the sand in the table and the surface of the water in the reservoir (Figure 2.2). Positive values indicate that the reservoir is above the sand surface, and negative values that the reservoir is below the sand surface.

The reservoir was raised to +2 cm and table valves opened on the manifold. Water was pulled into the ladder circuit and PTFE tubing from the table using a syringe attached to the luer lock until no air bubbles were detected in the syringe, before pushing in 180 ml de-gassed water (prepared by autoclaving deionised water ($dH_2O$) to remove dissolved gases) to allow any small remaining air bubbles to dissolve into solution. The table valves were closed, and the reservoir valve opened, and the process repeated before reopening the table valves, creating a continuous water column from the reservoir to the table. A schematic of the final tension table design is presented in Figure 2.2.

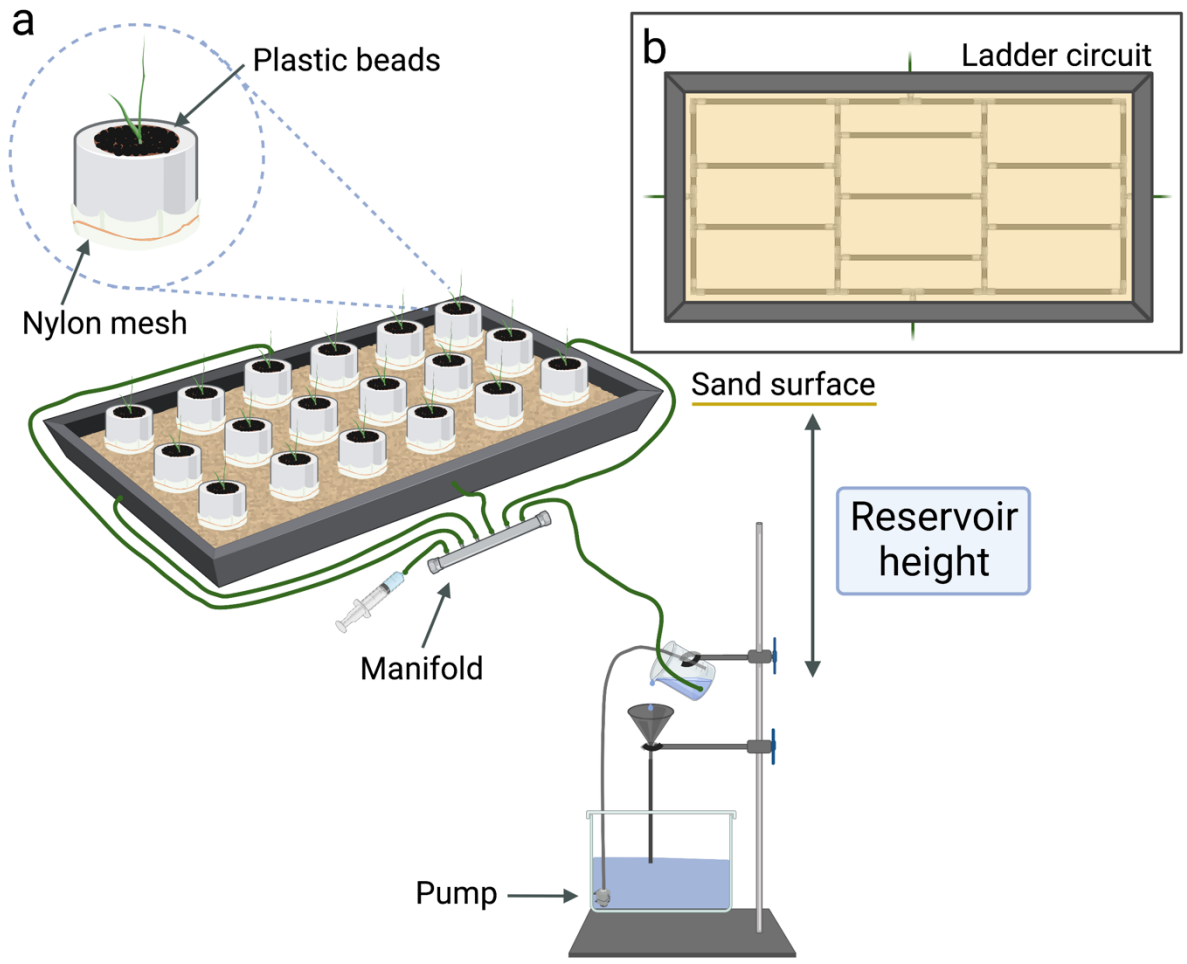


**Figure 2.2**: Schematic diagram of final tension table design. **a.** Side-on view of the final design. The table itself was placed on a levelled bench, with the pump/reservoir system placed on the floor in front. **b.** Top-down view of the tension table and porous pipe ladder circuit layout. Figure created in BioRender.

#### 2.2.1.4 Maintenance and re-priming

Holding tanks were kept topped up with water, and tension tables remained flooded when not in use to preserve the water column. If air bubbles developed during operation, the system was re-primed by pushing and pulling water into and out of the table to remove air bubbles before adding 180ml de-gassed water. With the table valves closed, water was pulled through the reservoir tubing before reopening all valves to re-establish the water column.

If the table dried out, water was manually added directly to the sand over until it began to pool on the surface, before repeating the re-priming procedure. Water was poured over 33.5 μm nylon mesh to minimise disruption of the sand surface.

### 2.2.2 Soil collection and preparation

Soil used in this work is a sandy loam cambisol collected from the East Loan field of the James Hutton Institute's Mylenfield Farm (56.455390, -3.077565). Soil was mixed to homogenise and sieved to 4 mm before packing into microcosms.

### 2.2.3 Soil moisture content

Soil moisture content (SMC) was determined by weighing out 5 c.15-20 g representative soil samples into tin cups and recording fresh weight including the weight of the tin cup (FWt). Soil was dried in an oven at 70°C for a minimum of 24 h before again weighing samples and recording dry weight (DWt). The average mass of an empty tin cup (3.17 g, calculated from an average of 20 empty tin cups) was subtracted from both fresh and dry weights (FW and DW respectively), before calculation of soil moisture content (SMC %) using ***Equation 2.1***. SMC calculation was performed each time immediately before use of the soil.

$$Soil\ sample\ moisture\ content\ (\%) = \left(\frac{FW - DW}{DW}\right) * 100 \qquad \textbf{Equation 2.1}$$

### 2.2.4 Soil microcosm preparation and packing

Microcosms were constructed from 51 mm I.D. white PVC pipe (B&Q) cut into 6 cm lengths, with a 9 $cm^2$ square of 33.5 μm nylon mesh (Cadisch Precision Meshes Ltd.) fixed to the bottom with tape and a rubber band. Mesh ensured soil and plant roots remained in the microcosm while allowing free movement of water between the soil and the sand in the tension table.

The fresh weight of soil required to pack microcosms to the target bulk density was calculated using SMC (calculated as in ***Equation 2.1***) and the volume of the microcosm/soil core with a packing height of 5 cm (106.19 $cm^2$), as in ***Equation 2.2***.

$$FW\ soil\ required\ (g) = \frac{(Volume\ of\ soil\ core * Target\ bulk\ density) * (Soil\ moisture\ content + 100)}{100} \quad \textbf{Equation 2.2}$$

Microcosms were packed in 3 equal layers to ensure equal packing throughout, using a modified rolling pin with a 50 mm diameter to compress the soil to the correct height. The surface was lightly disturbed between layers to prevent the formation of distinct layers. The soil surface was covered with black plastic beads (Polypipe Building Products) to minimise evaporative losses.

### 2.2.5 Calculation of soil WFPS

Soil microcosms were weighed to obtain a soil FW value, after subtraction of the mass of the empty microcosm and plastic beads. The dry weight (DW) of soil required to pack a microcosm to a certain height and bulk density was calculated using ***Equation 2.3***. Soil volume was calculated using DW and the absolute soil particle density (2.65 $gcm^{-3}$, constant), as in ***Equation 2.4***. Pore volume was calculated using ***Equation 2.5***, and finally WFPS (%) was calculated as in ***Equation 2.6***, using the measured soil FW.

$$DW\ soil\ required\ (g) = Bulk\ density * Core\ volume \quad \textbf{Equation 2.3}$$

$$Soil\ volume = \frac{DW\ soil\ required}{2.65} \quad \textbf{Equation 2.4}$$

$$Pore\ volume = Core\ volume - Soil\ volume \quad \textbf{Equation 2.5}$$

$$WFPS\ (\%) = \left(\frac{Measured\ soil\ FW - DW\ soil\ required}{Pore\ volume}\right) * 100 \quad \textbf{Equation 2.6}$$

### 2.2.6 Watering to weight

Microcosms were placed on a balance and watered to weight through addition of tap water from the top to a calculated target fresh weight. The target fresh weight to achieve a given WFPS (%) was calculated through rearrangement of ***Equation 2.6*** to give ***Equation 2.7*** followed by addition of the mass of an empty microcosm and beads (***Equation 2.8***).

$$Target\ soil\ FW = \left(\left(\frac{WFPS}{100}\right) * Pore\ volume\right) + DW\ soil\ required \qquad \textbf{Equation 2.7}$$

$$Actual\ target\ FW = Target\ soil\ FW + Mass\ empty\ microcosm + Mass\ plastic\ beads \qquad \textbf{Equation 2.8}$$

### 2.2.7 Seed sterilisation and germination

Spring barley (cv. Concerto) seeds were sterilised by soaking in 5 % bleach for 15 mins followed by rinsing 4 times with $dH_2O$. Seeds were germinated in 90 mm petri dishes (Thermo Fisher) on 100 mm Whatman 45 filter papers saturated with $dH_2O$. Plates were wrapped in foil with the lids on to maintain darkness and humidity and were left at room temperature for 5-6 days before planting in the centre of microcosms. Foil was removed after 3 days.

### 2.2.8 Experimental conditions

Experiments were performed in a controlled greenhouse cubicle at the Arthur Willis Environment Centre at the University of Sheffield. The cubicle provided supplementary lighting up to 200 μmol $m^{-2}$ $s^{-1}$ and was set to a 16 h/8 h day/night cycle and a 12 h/12 h temperature cycle with temperatures of 22°C/16°C. Relative humidity and $CO_2$ concentration were not monitored in the cubicle. For each experiment, 3 microcosm reps were included for each bulk density and plant status (i.e. planted or unplanted).

### 2.2.9 Initial tension table testing

Planted and unplanted microcosms were packed to a bulk density of 1.2 $gcm^{-3}$, with microcosms added to a tension table (TT) with reservoir height set to a preliminary height of -1 cm and

microcosms added to individual 10 cm diameter trays for watering to weight (WTW). TT microcosms were left for 24 h to equilibrate and weighed to determine WFPS (measured as approximately 70 %). WTW microcosms were then watered to 70 % to match TT microcosms and both sets left for a further 24 h. WTW cores were then watered back to 70 %, and TT microcosms were weighed and returned to the table (0 h timepoint). All microcosms were left undisturbed for 24 h before weighing again (24 h timepoint). WFPS was calculated for all microcosms at both time points. Plants were 1 week old when the experiment was initiated.

### 2.2.10 Determining microcosm WFPS equilibration time

Planted and unplanted microcosms were packed to 3 bulk densities (1.2 g $cm^{-3}$, 1.3 g $cm^{-3}$ and 1.4 g $cm^{-3}$) and left to equilibrate on a tension table with the reservoir height set to -4 cm. Microcosms were left to equilibrate for 24 h before lowering the reservoir to -5 cm. Microcosms were weighed immediately after lowering (0 h), then again at 1 h, 2 h, 3 h, 4 h, 5 h, 8 h and 24 h. Microcosm WFPS was calculated for each time point. Plants were 2 weeks old when the experiment was initiated.

### 2.2.11 WFPS vs. reservoir height

Planted and unplanted microcosms were packed to 3 bulk densities (1.2 g $cm^{-3}$, 1.3 g $cm^{-3}$ and 1.4 g $cm^{-3}$) and equilibrated for 24 h on a pair of tension tables set to 0 cm. Plants were 1 week old when the experiment was initiated. Microcosms were weighed to obtain 0 cm measurements and the 2 reservoirs lowered in 5 cm increments, with each table lowered to a different height, beginning with -5 cm and -10 cm. Microcosms were equilibrated at the new reservoir height for 24 h before weighing again. Tables were re-flooded, and microcosms returned to the tables before the process was repeated at a further set of 5 cm increments (-15 cm, -20 cm). This was repeated until the minimum silica sand air entry value was reached (reservoir height of -35 cm). Microcosms were returned to the tables and plants left to grow for a further 4 weeks at a reservoir height of 0 cm. The experiment was repeated at the same reservoir height increments with the 5-week-old plants.

### 2.2.12 Data visualisation and statistical analysis

All graphs in this chapter were produced using GraphPad Prism version 9.4.1. Statistical analysis performed on the results presented in 3.3.1 was carried out in RStudio version 2022.07.1+554. Prior to performing two-way analysis of variance (ANOVA), the dataset was checked to ensure it met the assumptions of ANOVA through plotting of diagnostics using the autoplot function of the ggplot2 package. The dataset met the assumptions of homogeneity of variance and that data is drawn from a normal distribution, and so the ANOVA analysis was performed on the natural, untransformed data.

## 2.3 Results

### 2.3.1 Stability of WFPS on tension tables

Two-way ANOVA revealed a significant interaction between watering system (TT or WTW) and time on microcosm WFPS ($F=201.5003$, $p<0.0001$), where WFPS in TT microcosms did not significantly change across a 24 h period but dropped significantly in WTW microcosms by approximately 25 % (Figure 2.3). This interaction was not influenced by the presence of 1 week old WT Concerto barley plants ($F=0.3879$, $p=0.5422$), and so only data showing the significant influence and interaction of watering system and time on WFPS is presented in Figure 2.3.

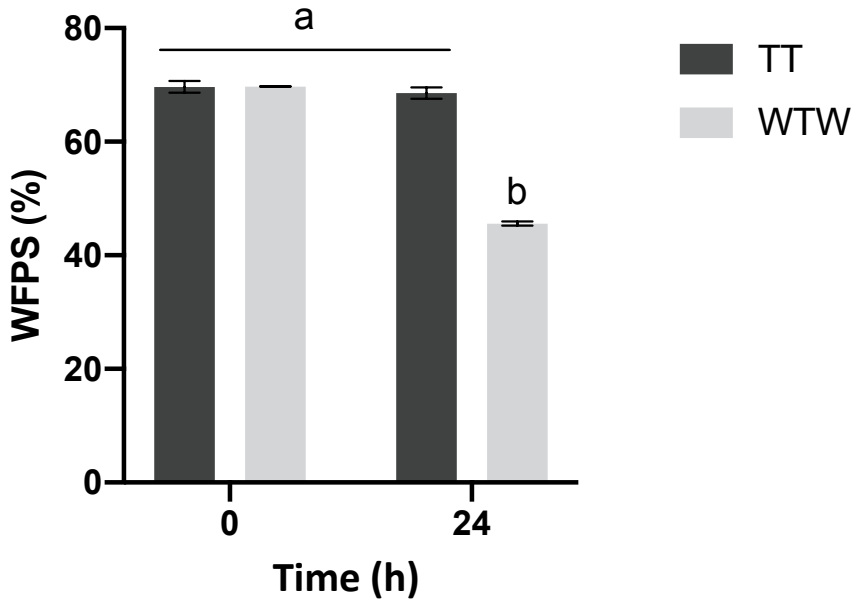


Figure 2.3: Mean ± SEM WFPS (%) of combined planted and unplanted microcosms equilibrated to 70 % either on tension tables (TT) and watered to weight (WTW) at 0 h and 24 h (n=6). Statistically significant groups are denoted by different letters (two-way ANOVA with Tukey post-hoc test).

### 2.3.2 Determining microcosm equilibration time on tension tables

This experiment was purely descriptive to inform table operation for future work, and so statistical analysis was not performed. Soil microcosm WFPS changes were only minor after dropping the table reservoir from -4 cm to -5 cm, primarily noticeable as a slight decrease of 1.7

% in planted microcosms packed to a 1.4 g $cm^{-3}$ bulk density (Figure 2.4) at 8 h after lowering. WFPS remained unchanged after 24 h, suggesting that microcosm WFPS had equilibrated by 8 h. WFPS was higher in planted microcosms than unplanted microcosms, though plant weight was not taken into account during WFPS calculation. For planted microcosms, WFPS was highest at a bulk density of 1.3 g $cm^{-3}$, followed by 1.4 g $cm^{-3}$ and 1.2 g $cm^{-3}$, however for unplanted microcosms, 1.2 g $cm^{-3}$ showed slightly higher WFPS at all time points compared to the other two bulk densities, though error bars overlapped so it is unlikely that the difference is significant.

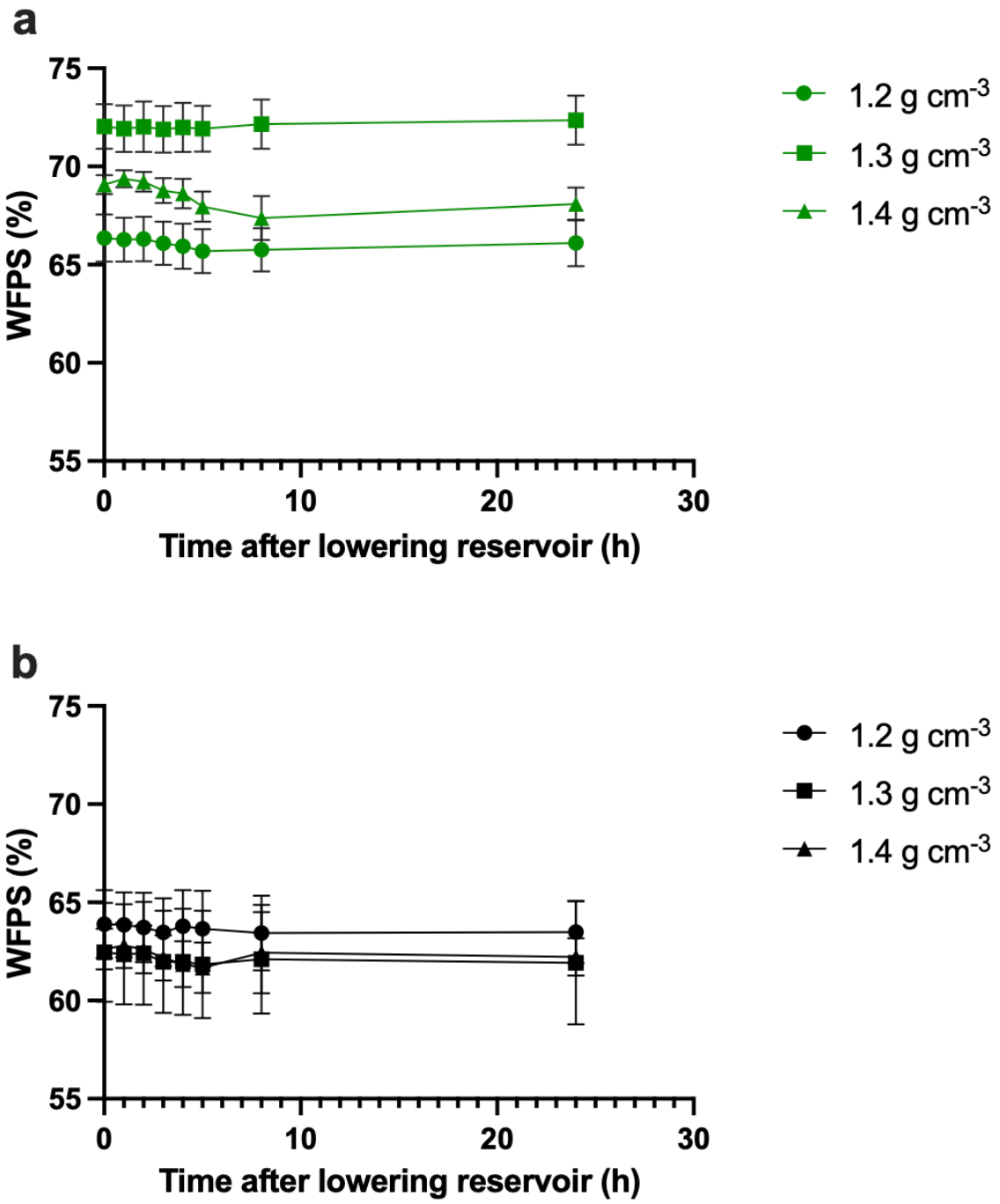


**Figure 2.4**: Mean ± SEM WFPS (%) for microcosms planted with 2 week old WT Concerto barley plants (**a**) and unplanted microcosms (**b**) over a period of 24 h after lowering tension table reservoir from -4 cm to -5 cm. The reservoir was lowered at time 0 h. a. Different symbols indicate different soil bulk densities.

### 2.3.3 The relationship between WFPS and reservoir height

Overall, microcosm WFPS was highest in microcosms with the highest bulk density (1.4 g $cm^{-3}$) at all reservoir heights and time points both with and without plant presence, followed by 1.3 g $cm^{-3}$ and 1.2 g $cm^{-3}$ respectively (Figure 2.5a-f). WFPS decreased with decreasing reservoir height across all bulk densities irrespective of plant presence in an approximately linear fashion (Figure 2.5a-f). When plants were 1 week old, WFPS did not differ between planted and unplanted microcosms (Figure 2.5a, c, e), but there was larger disparity between planted and unplanted microcosms when plants were 5 weeks old (Figure 2.5b, d, f). However, discrepancies in the data collected from tables 1 and 2 during the second part of the experiment made it difficult to disentangle any potential differences between unplanted and planted microcosms from the systematic issues faced, with microcosms placed on table 2 higher than those on table 1, particularly at the lower bulk densities (Figure 2.5b, d). For this reason, no statistical analysis was conducted on the data. Aerobic WFPS (<60 %) was achieved in planted microcosms at all reservoir heights below -5 cm with a bulk density of 1.2 g $cm^{-3}$ when plants were 1 week old (Figure 2.5a), however this becomes less clear at 5 weeks old due to the table discrepancy (Figure 2.5b). Anaerobic WFPS (>70 %) was largely achieved only with a bulk density of 1.4 g $cm^{-3}$, at heights of -10 cm and above when plants were 1 week old, and at all reservoir heights when plants were 5 weeks old.

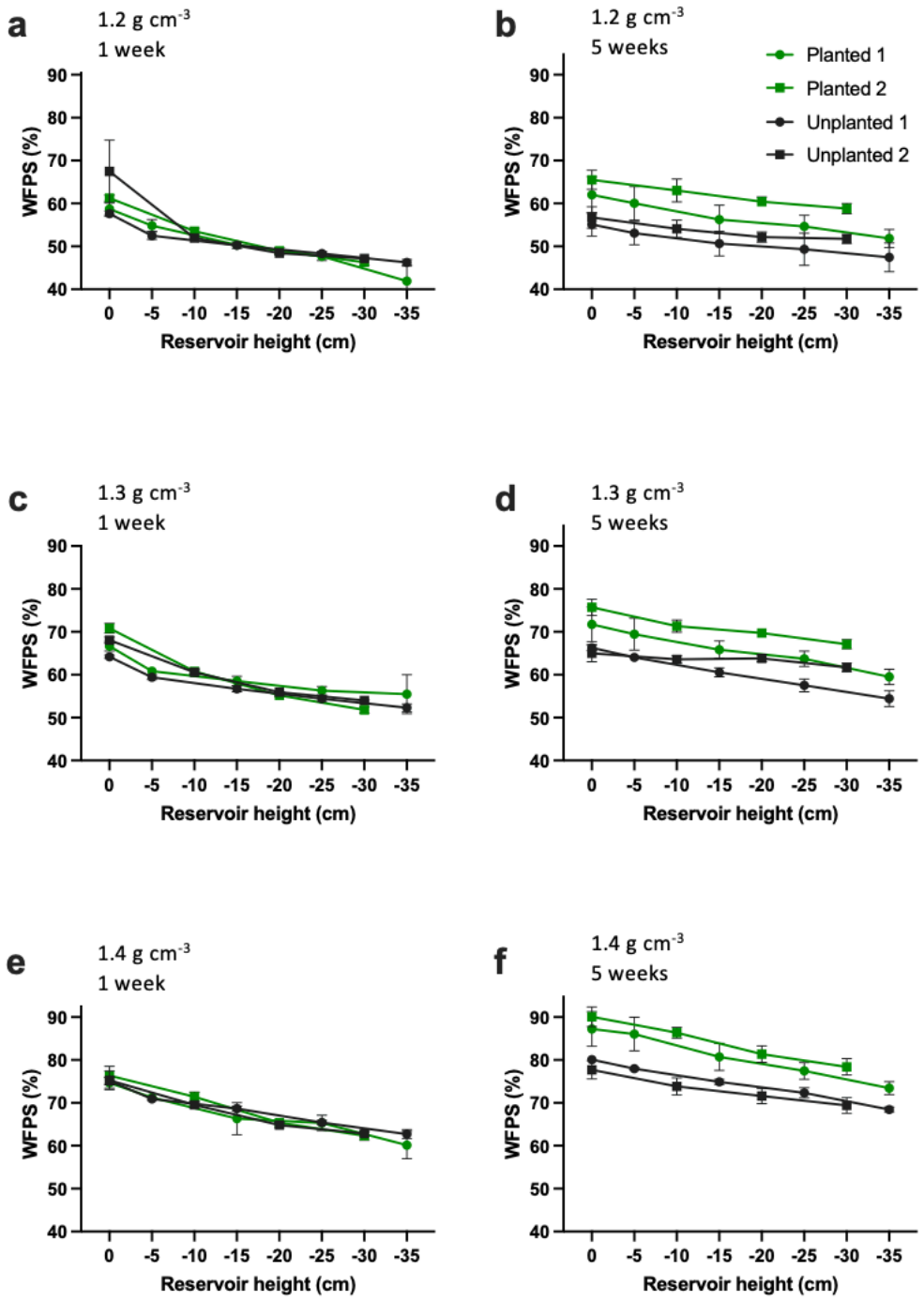


**Figure 2.5**: Mean ± SEM WFPS (%) plotted against reservoir height (cm) for microcosms planted with 1 week old Concerto barley plants and equivalent unplanted microcosms, packed to 1.2 g cm$^{-3}$ (**a**), 1.3 g cm$^{-3}$ (**c**) and 1.4 g cm$^{-3}$, and the same microcosms with 5 week old Concerto barley plants and equivalent unplanted microcosms at 1.2 g cm$^{-3}$ (**b**), 1.3 g cm$^{-3}$ (**d**) and 1.4 g cm$^{-3}$ (**f**). Different colours represent planted (green) and unplanted (black) microcosms, and the two tension tables used in the experiment indicated by different symbols, with table 1 indicated with circles and table 2 with squares.

## 2.4 Discussion

The study of processes sensitive to soil WFPS and/or soil oxygen content such as nitrification and denitrification requires reliable and stable control of soil WFPS. Watering to weight is the gold standard for controlling soil WFPS in small-scale experiments but is very time-consuming and not suited to high-throughput studies without considerable resources. Automating WFPS through the use of robotics (e.g. Granier et al., 2006) can increase experimental throughput whilst reliably controlling WFPS, however these technologies are cost-prohibitive and not accessible to a majority of research groups. The use of low-cost soil moisture sensors and open-source technologies like Raspberry Pi and Arduino have reduced costs (Ortiz et al., 2018), but often remain unsuitable when employed at large scale owing to their setup time and required expert knowledge. Tension tables create a continuous water column from soil placed on a porous barrier through to a suction control system, generating a static WFPS equilibrium dependent on the amount of suction pressure applied (Romano et al., 2002). In this work we set out to create a simplified tension table system that could generate sufficient suction pressure to create both aerobic (<60 %) and anaerobic (>70 %) WFPS, could sustain plant growth, and is sufficiently low-cost to scale up for a large screen of nitrification and denitrification across a panel of 200 spring barley cultivars (Chapters 3 & 4).

### 2.4.1 Tension table design and construction

The tension table design described here (Figure 2.2) was based on past iterations developed for determination of soil water release characteristics (Stakman et al., 1969, Ball & Hunter, 1988) and previous work in the lab that built on these concepts and made several modifications to reduce costs (Allery, 2019). Tables were initially assembled from transparent acrylic to facilitate rapid detection of air bubbles that could disrupt the water column and prevent the system from functioning as intended, as suggested by Ball & Hunter (1988). However, algal growth rapidly became a problem within 1-2 weeks of table operation, with growth initially seen on the surface of the sand, but quickly spreading into the sand (particularly at the edges of the acrylic) and

eventually into the opaque tubing, where blockages regularly occurred that acted to disrupt the water column. Transparent acrylic was therefore replaced with opaque green acrylic (Figure 2.1a) that acted to block out light from the sand in the table, reducing algal growth. Similar issues were observed with the reservoir/pump system, which was initially kept open to allow easy drainage of the water from the reservoir into the tank, but significant algal growth in the reservoir and holding tank quickly clogged tubing and caused issues with the system. The addition of a lid to both the water tank and the reservoir significantly reduced algal growth. A drain system was designed to allow water to flow back into the tank after addition of lids (Figure 2.1g), which also acted to minimise spillage of water via splashing when raised directly underneath the reservoir, reducing the number of times the water tank required re-filling, further reducing the time required to maintain the system.

The construction of a porous pipe ladder circuit (Figure 2.1a) removed the need for channels to be cut into the base of the table with a laser as in Ball & Hunter (1988) and cut costs significantly. A silt/air trap was not included, and instead was replaced with a manifold that allowed sectioning off either ladder circuit/table tubing or reservoir tubing (Figure 2.1b), allowing air bubbles to effectively be removed and easy addition of de-gassed water into the system as required. A limitation of the system remains that the presence of air bubbles cannot be effectively detected until either the sand dries out or an unexpected decrease in soil WFPS is detected.

Total costs for previous tension table iterations are not available, however the cost to construct a complete tension table as described in this chapter was approximately £90, and as such does not become cost-prohibitive even when several tables are constructed for larger experiments. Four tension tables can be constructed and set up by a single person in one day after initial construction of the table itself, with minimal maintenance required once the system is up and running, making the system ideal for application to high-throughput screening experiments.

### 2.4.2 Tension table performance compared to watering to weight

To assess the ability of the tension table to maintain WFPS over time, soil microcosms equilibrated to 70 % WFPS on a tension table were compared to equivalent soil microcosms watered manually to 70 % over a period of 24 h. While WFPS dropped significantly by approximately 25 % over the 24 h period in microcosms watered to weight, WFPS remained constant in microcosms placed on the tension table (Figure 2.3). The large decrease in WFPS of WTW microcosms was surprising given the measures taken to minimise losses via evaporation such as the addition of plastic beads to the soil surface, but the stability of WFPS across the 24 h period in TT microcosms indicated that, at least over this short time period, the tension table could replace any evaporative losses from the microcosms to maintain the static WFPS equilibrium. These results were not affected by the presence of a 7-day-old barley plant, suggesting that the table could replace water lost by plant transpiration in addition to evaporative losses. Since plants were relatively small during this experiment (approximately 10 cm tall) with only 1-2 relatively small leaves, losses via transpiration were likely small, and may have had more of an effect if plants were larger.

### 2.4.3 Understanding tension table WFPS dynamics

To assess the necessary time period for microcosms to equilibrate to a new WFPS after lowering the reservoir to alter applied suction pressure, WFPS was tracked in a set of both planted and unplanted microcosms packed to 3 bulk densities (1.2 g $cm^{-3}$, 1.3 g $cm^{-3}$, 1.4 g $cm^{-3}$) over a period of 24 h and used to generate time courses to investigate WFPS dynamics (Figure 2.4). Only very minor changes in WFPS were observed after lowering the reservoir from -4 to -5 cm, likely because the reservoir was not lowered far enough to sufficiently increase suction pressure to generate any detectable changes. The most noticeable change in WFPS was detected in planted 1.4 g $cm^{-3}$ soil microcosms, with a decrease of approximately 1.7 % at 8 h (Figure 2.4a). WFPS did not drop any further after this point, suggesting that a minimum of 8 h is required for soil microcosms to equilibrate at a new WFPS after a 1 cm drop in reservoir height. This was a simple

descriptive experiment to start to understand the dynamics of WFPS changes during transition to different reservoir heights, but further experiments will be necessary to determine whether 8 h is enough equilibration time if the reservoir is lowered more than 1 cm, and if it holds true when the reservoir is lifted higher up. This was outside the scope of this work. Subsequent experiments and application to high-throughput screening used a minimum equilibration time of 24 h regardless of the distance the reservoir was moved.

WFPS differed between planted and unplanted microcosms in this experiment, with planted microcosms generally having higher WFPS values than unplanted microcosms at all time points. Plants were two weeks old in this experiment, and plant weight was not taken into account during calculation of WFPS. It is likely that the additional mass of the plant, reflected in the measured total core fresh weight, led to an overestimation of WFPS in planted microcosms, and in reality the difference in WFPS may be much smaller. It remains a possibility, however, that plant transpiration acted to pull water into the microcosm, which would also increase microcosm WFPS, though transpiration also acts as a route of water loss from the microcosm. This highlights the need for plant weight to be taken into account to accurately calculate soil WFPS as in watering to weight experiments, where it is common practice to grow a separate set of plants and harvest regularly to measure plant weight which can then be accounted for during WFPS calculation.

### 2.4.4 The relationship between WFPS and reservoir height

After establishing that the tension table could maintain WFPS over time and identifying the minimum required equilibration time, a final experiment was set up to understand the relationship between WFPS and reservoir height. A linear decrease in WFPS with decreasing reservoir height was observed (Figure 2.5) irrespective of plant presence and soil bulk density, as increasing suction pressure was applied to the soil. This should allow for easy identification of the required reservoir height to achieve a specific WFPS at a certain bulk density. WFPS generally increased with increasing bulk density, irrespective of reservoir height and plant presence. Larger pores are drained more easily than small pores and so the bulk density trend in WFPS can

be explained by the pore size distribution of the soil, with more loosely packed microcosms (1.2 g $cm^{-3}$) with larger average pore sizes having a reduced capacity to hold water and therefore having the lowest WFPS (Figure 2.5a,b), and more densely packed soil (1.4 g $cm^{-3}$) with a smaller average pore size retaining more water at any given reservoir height and therefore having higher WFPS. Soil bulk density is therefore an important factor to consider when determining the experimental conditions necessary to achieve a specific target WFPS.

The influence of the plant itself is another important factor to consider. Small plants that are only 1 week old appear to have very little effect on soil WFPS (Figure 2.5a,c,e), with little difference in WFPS compared to unplanted soil microcosms packed to the same bulk density. As plants increase in size, their influence on WFPS also appears to increase, with larger disparity between planted and unplanted microcosms observed when plants are 5 weeks old (Figure 2.5b,d,f). As in the previous experiment, this is likely due to the fact that plant weight was not taken into account when calculating WFPS, as planted microcosms appeared to show increased WFPS. If the plant itself were having a direct effect on WFPS, it would likely decrease WFPS compared to an equivalent unplanted microcosm as plant transpiration acts as an additional route of water loss from the microcosm, though transpiration could also act to pull water into the microcosm from the table. Differences in WFPS between microcosms on the two tension tables used in the experiment made it difficult to interpret the magnitude of the difference between unplanted and planted microcosms and to perform any meaningful statistical analysis. This discrepancy between tables could have arisen from a difference in plant size across the two tables; if plants on table 2 were larger at 5 weeks, this could have led to a greater overestimation of WFPS. However, plant size/weight was not recorded in this experiment. Nevertheless, control measures should be put in place to allow for adjustments in WFPS to be made on an individual table basis when running experiments for longer than a few days. Ideally, a separate set of plants should be grown on each tension table and harvested weekly to allow plant size and influence on WFPS to be taken into account. This may be impractical for larger scale experiments however, but as a

minimum an unplanted 'control' microcosm should be included on each individual table to allow WFPS to be tracked in equivalent soil without plant weight leading to overestimation of WFPS.

### 2.4.5 Application to high-throughput nitrogen cycling screening and conclusion

The tension table system described in this chapter was designed specifically for the purpose of facilitating high-throughput screening of variation in soil nitrification and denitrification, which are aerobic and anaerobic processes respectively. Nitrification is the dominant $N_2O$-producing nitrogen cycling process at WFPS <60 % (Bateman & Baggs, 2005). WFPS <60 % can be achieved with a soil bulk density of 1.2 g $cm^{-3}$ and a reservoir height of -5 cm or lower (Figure 3.5a). Denitrification is the dominant $N_2O$-producing process at WFPS >70 % (Bateman & Baggs, 2005), which can be achieved with soil packed to a bulk density of 1.3 g $cm^{-3}$ or 1.4 g $cm^{-3}$ if the reservoir is not lowered below 0 cm (Figure 2.5c,e). WFPS values much higher than 70 % however are difficult to achieve with this system and soil type, and flooding of the tables may be necessary to achieve sufficiently high WFPS. Each table can hold up to 60 microcosms with a 55mm external diameter (as used in this work), meaning a large number of plants can be included in a screening experiment with a relatively small number of tables.

Further work will be necessary to determine the broader scope of application of this system, with several key factors to consider, including the plant species of interest, soil bulk density and soil type. The sandy loam soil used in this work showed lower WFPS values compared to a silt loam used in preliminary testing of the tension table (data not shown), presumably because silt loams have a lower average particle size and therefore pore size distribution when compared to a sandy loam. Testing of any system constructed should be carried out with the specific soil type, bulk density and plant species before proceeding with any experimental studies.

# Chapter 3: Screening for variation in soil gross nitrification rates across a large panel of *Hordeum vulgare* (spring barley) germplasm.

## 3.1 Introduction

The microbial process of nitrification is a key determinant of the forms of N present in many ecosystems and can have profound impacts on both the environment and plant productivity. During nitrification ammonium is converted to nitrate via oxidation to nitrite. The rate of nitrification therefore influences relative plant uptake and utilisation of ammonium and nitrate (Chalk & Smith, 2021). Edaphic factors can add further complexity, with the cation ammonium electrostatically attracted to soil particles in many soils, but no such interaction present with the anion nitrate (Brady and Weil, 1999). While this means that nitrate is more mobile in soil and also therefore more readily available for plant uptake, it is susceptible to leaching and loss from the root zone (Glass, 2003; Raun & Johnson, 1999; Subbarao et al., 2006b) with significant associated economic costs of up to US$15 billion annually solely from fertiliser loss (Subbarao et al., 2007) in addition to environmental consequences such as eutrophication of surface water and pollution of groundwater sources (Subbarao et al. 2006b). Moreover, nitrate can be denitrified to various gaseous N products under anoxic or partially anoxic conditions, further contributing to loss of N from soil and producing the potent greenhouse gas $N_2O$, which is also produced as a by-product of nitrification. Nitrification is the dominant producer of $N_2O$ in aerobic soils (Bateman & Baggs, 2005).

Nitrification rates are often exacerbated in intensive agricultural systems where large quantities of N fertiliser, often in the form of $NH_4NO_3$ or urea, are added to soil, providing ample substrate for nitrification in largely aerobic soils (Wang et al., 2018). Excessive fertilisation often results in reducing nitrogen use efficiency (NUE), with only 30 % of applied N sometimes recovered by plants (Subbarao et al. 2006b). Regulation of nitrification could therefore be an important

strategy for improving agronomic nitrogen use efficiency where nitrification contributes significantly to N losses.

Several strategies have been suggested to limit soil nitrification and reduce N losses, including optimised N fertiliser management such as split-application or point application, ensuring enough N is added to meet plant N demand while reducing losses, or foliar application of urea which removes the need for addition of N directly to soil (Dinnes et al., 2002; Skiba et al., 2011). Synthetic nitrification inhibitor (SNI) application has also been trialled and successfully implemented as a strategy to minimise nitrification and improve plant NUE (Jarvis et al., 1996; Power & Prasad, 1997; Sahrawat & Keeney, 1985; Slangen & Kerkhoff, 1984; Subbarao et al., 2006). Effectiveness of SNI application, however, is often varied and lower than expected under field conditions (Davies & Williams, 1995), possibly due to leaching from the rhizosphere and/or microbial degradation (Puttanna et al., 1999; Schwarzer & Haselwandter, 1991). SNIs are often cost-prohibitive, and performance is varied across different environments (Fillery, 2007).

More recently, suppression of soil nitrification has been found to occur naturally in some ecosystems and has been termed biological nitrification inhibition (BNI) (Subbarao et al. 2006a). BNI was first characterised in pasture grasses such as *Brachiaria humidicola* (Subbarao et al. 2006a) and several BNI mechanisms have been proposed, including plant modulation of soil pH and plant competition with nitrifying microorganisms for ammonium. However, a major BNI mechanism is the release of low molecular weight carbon compounds into the rhizosphere through root exudation, which act to directly inhibit the AMO pathway responsible for the rate-limiting step of nitrification, the reduction of nitrate to nitrite (Subbarao et al. 2006b, 2007; Sun et al., 2016, see section **1.3.3.1**).

Research has extended to different crop species to assess the extent to which BNI could be applied as a strategy to improve NUE in agricultural systems (e.g. Subbarao et al., 2007). Rice (*Oryza sativa*) has received particular interest, and research has resulted in identification of new BNI compounds (Sun et al., 2016) in addition to intraspecies variation in BNI activity (Li et al., 2008;

Sun et al., 2016). Previous work in the Daniell lab has shown that soil nitrification rate is significantly affected by rice cultivar (Pervin, 2022). Other cereal crops have received less attention, particularly important crops such as barley (*Hordeum vulgare*). To my knowledge, there is only one published report of an assessment of barley BNI activity, performed on a single cultivar (cv. Shunrai), which did not demonstrate detectable BNI activity (Subbarao et al., 2007). Unpublished results from Tim Daniell, Tim George and colleagues at the James Hutton Institute and previous results in the Daniell lab have demonstrated that root exudates of different barley cultivars may display variable BNI activity (Baker, 2019), but intraspecies variation in BNI activity in barley (among other species) is still poorly understood.

It has been proposed that a key research need in the development of BNI as a strategy for mitigation of N losses is to systematically screen agronomically important crops for BNI potency (de Klein et al., 2022). We therefore designed a large-scale screening experiment, spanning a wide range of 200 spring barley cultivars, to assess variation in soil gross nitrification rate (GNR) as influenced by barley cultivar. The aim was to use GNR as a proxy for BNI activity, where reduced GNR could be an indicator of increased BNI activity, to determine whether intraspecies variation exists in barley BNI activity that could identify direct targets for improved NUE, reduced nitrification and associated N losses and environmental damage in barley cultivation. Measurement of GNR is a powerful technique that allows measurement of nitrification while taking into account other N transformation processes (de Klein et al., 2022; Drury et al., 2007), therefore any variation observed across cultivars in GNR is as a result of a direct interaction of the plant with nitrification and not driven by indirect effects on other N transformation processes.

**Research aims**

- To assess whether barley cultivars will have variable effects on soil gross nitrification rate as a proxy for variation in BNI activity.
- To assess whether soil ammonium concentration, nitrate concentration and pH will vary across cultivars.

## 3.2 Materials and methods

### 3.2.1 Soil type and barley cultivar selection

Soil used in this experiment was the same as that used in Chapter 2 (see section **2.2.2**) and is a sandy loam cambisol. Soil was mixed to homogenise and sieved to 4mm before packing into microcosms. A total of 200 spring barley (*Hordeum vulgare*) cultivars (listed in appendix table A.1), selected based on their available genetic information for downstream GWAS analysis, were included. Cultivars were provided by The James Hutton Institute and Syngenta. The screen was carried out between July to August 2021 and consisted of 4 replicate blocks. Each block contained. a T-5 plant (harvested 5 days after fertilisation with enriched $NH_4{}^{15}NO_3$) for all 200 cultivars (i.e. 200 plants) and 20 randomly selected T-0 plants (harvested immediately after fertilisation with enriched $NH_4{}^{15}NO_3$). A T-0 plant should ideally be included for each cultivar when assessing gross nitrification rate, but this was not possible within the confines of this experiment. For this reason, a different random set of 20 T-0 plants was included in each block with no cultivars repeated, with the assumption that soil $NO_3^-$ concentration and $^{15}NO_3^-$ atom% would not vary across cultivars or blocks. Each block consisted of 4 tension tables (see section **3.2.2** below), and each tension table contained 50 random T-5 plants, 5 random T-0 plants and a single unplanted control. Blocks were planted one week apart from each other on a separate set of 4 tension tables to facilitate harvest (see section **3.2.4**).

### 3.2.2 Tension table setup

Plants were grown on tension tables constructed and set up as described in **3.2.1**, with some adjustments. A set of 4 tables was used for each block, connected to a single reservoir/pump system to minimise variation in WFPS across tables within a block. A separate set of 4 tension tables was assembled for each block due to overlap in plant growth. Reservoir height was set to -5 cm to achieve largely aerobic WFPS of 50-55 % for a microcosm packed to a bulk density of 1.2 g $cm^{-3}$ (based on Chapter 3 results, see Figure 3.5a,b). WFPS was monitored frequently by

weighing an unplanted control microcosm (one per table), and re-priming of the table was carried out, when necessary, as described in section **2.2.1.4**.

### 3.2.3 Soil microcosm preparation and plant growth

Microcosms were assembled and packed as described in **3.2.4**. Soil was packed to a bulk density of 1.2 g $cm^{-3}$ to achieve largely aerobic WFPS when tension table reservoir height was set to -5 cm (see above section **3.2.2**). Microcosms were left to rest on tension tables for 5 days with reservoir height set to 0 cm before planting. Barley seeds were sterilised with bleach and germinated on petri dishes as described in **2.2.7** for 5 days before planting in the centre of microcosms. Seedlings were planted over 2 days for each block to facilitate harvest. Immediately after planting, table reservoirs were dropped to -5 cm to ensure microcosm WFPS of 50-55 %. The screen was carried out in a controlled greenhouse cubicle at the Arthur Willis Environment Centre, Sheffield, UK. The cubicle provided supplementary lighting to 200 μmol $m^{-2}$ $s^{-1}$ and was set to a 16 h/8 h day/night cycle and a 16 h/8 h temperature cycle with temperatures of 22°C/16°C.

N fertilisation was applied at the recommended optimum barley application rate of 150 kg N $hectare^{-1}$ (Overthrow, 2005) with ratios of 22:4:14 $N:P_2O_5:K_2O$ as in the Yara Mila Sulphurcut fertiliser used by the James Hutton Institute for barley field growth. Following standard agricultural practice, NPK (Nitrogen, Phosphorous, Potassium) fertilisation was split across 2 equal treatments and contained $NH_4NO_3$, $KH_2PO_4$ and $KHSO_4$ supplying a total of 250.43 mg N kg dw $soil^{-1}$, 20.01mg P kg dw $soil^{-1}$ and 132.39 mg K kg dw $soil^{-1}$. The 1st fertiliser treatment was applied at planting and the 2nd at maximum tillering at 35 DAP (days after planting). N was 5 % enriched with $NH_4{}^{15}NO_3$ in the 2nd fertilisation and considered day T-0, T-0 plants were harvested at this point. T-5 plants were grown for a further 5 days before harvest. Fertiliser was applied at 5 points (1 ml at each point) in each microcosm at the 4 cardinal points and close to the centre of the microcosm, for a total of 5 ml fertiliser in each microcosm at each fertilisation event. Fertiliser was added directly to soil after destruction of soil cores for T-0 plants (see **3.2.4** for more detail).

### 3.2.4 Harvest and soil sampling

T-0 microcosms were destructed at 35 DAP. Soil was removed from microcosms and plant material separated. Shoots were separated from roots and dried at 70°C for 48 h to determine shoot dry weight. Roots were collected and dried but due to issues with removal of soil from root material during harvest, root dry weight was not measured. Soil was sieved to 4 mm before direct addition of 5 ml $^{15}N$-enriched fertiliser to ensure sampling accurately captured the amount of N added. Soil was mixed and sieved again to homogenise before sampling for chemical analyses. Soil moisture content was determined as described in **2.2.3**. T-5 plants were harvested at 40 DAP using the same procedure apart from soil was sieved once before sampling.

### 3.2.5 Soil chemical analyses

Soil pH was determined by addition of 0.01 M $CaCl_2$ (Sigma-Aldrich, USA) to soil in a 1:5 soil:$CaCl_2$ ratio and shaking vigorously for 30 seconds. The suspension was agitated with a magnetic flea during measurement and pH measured with a Jenway 3510 benchtop pH meter (Jenway, Cole-Parmer Ltd., UK). Soil inorganic $NH_4^+$ and $NO_3^-$ concentration and gross nitrification rate was determined after soil KCl extraction. Briefly, 2 M KCl (VWR) was added to soil in a 1:4 soil:KCl ratio in 200 ml plastic bottles (RS Components Ltd., Northants, UK) for T-0 plants and 60 ml plastic bottles (RS Components Ltd., Northants, UK) for T-5 plants (using 25 g and 9 g soil respectively) and mixed at 180 rpm for 1 h using a custom shaker. Extracts were then filtered using Whatman 42 filter paper and extracts stored at -80°C until analysis. Filtered extracts were used for analysis of soil $NH_4^+$ and $NO_3^-$ concentration (**3.2.5.1**) and gross nitrification rate (**3.2.5.2**) determination.

#### 3.2.5.1 Soil $NH_4^+$-N concentration analysis

Soil $NH_4^+$ concentration was determined through a colourimetric assay described by Baethgen & Alley (1989) with volumes adjusted for microplate format, based on the reaction of $NH_4^+$ ions with a weakly alkaline mixture of sodium salicylate and hypochlorite in the presence of sodium nitroprusside. Briefly, sodium salicylate (Sigma-Aldrich, USA), (tri)sodium citrate (Sigma-Aldrich,

USA), sodium tartrate (Sigma-Aldrich, USA) and sodium nitroprusside (Sigma-Aldrich, USA) were combined to make a sodium salicylate cocktail solution. A separate NaOH/hypochlorite solution was made by diluting sodium hypochlorite (Thermo-Fisher) with NaOH (VWR). Standard curve solutions of 0-200 μM were prepared by serial dilution of a 200 μM $NH_4^+$ ($NH_4Cl$) solution with 2 M KCl, and 40 μl each dilution added to a 96-well, flat-bottomed polystyrene microtitre plate (Thermo-Fisher). Standards and samples were mixed with 80 μl salicylate cocktail and 80 μl NaOH/hypochlorite solution and incubated at room temperature for 45 minutes. Absorbance was measured at 650 nm with a Tecan Spark 10M microplate reader (Tecan, Switzerland). Standard curves were produced by linear regression of standard absorbance and concentration (μM) values and the line equation used to calculate sample $NH_4^+$ concentration in μM. Concentration in (μM) was re-expressed as mg $NH_4^+$-N kg dw $soil^{-1}$. Samples were diluted with 2 M KCl and re-run as necessary to ensure absorbance fell within the range of the standard curve.

#### 3.2.5.2 Soil $NO_3^-$-N concentration analysis

Solution $NO_3^-$ concentration was determined through reduction of sample $NO_3^-$ by vanadium(III) followed by detection via the acidic Griess reaction (Miranda et al., 2001). Briefly, a saturated vanadium(III) chloride (Sigma-Aldrich, USA) solution was combined with 2 % sulphanilamide solution (Sigma-Aldrich, USA) and 0.1 % N-(1-napthyl) ethylene diamine dihydrochloride solution (Sigma-Aldrich, USA) to form a vanadium cocktail solution. Standard curve solutions of 0-200 μM were prepared by serial dilution of a 200 μM $NO_3^-$-N ($KNO_3$) solution with 2 M KCl. A volume of 100 μl of each dilution was added to a 96-well, flat-bottomed polystyrene microtitre plate (Thermo-Fisher). Vanadium cocktail (100μl) was added to standards and diluted samples, mixed and incubated at room temperature for 2 h before measuring absorbance at 540 nm with a Tecan Spark 10M microplate reader (Tecan, Switzerland). Standard curves were produced by linear regression of standard absorbance and concentration (μM) values and the line equation used to calculate sample $NO_3^-$ concentration in μM. Concentration in (μM) was re-expressed as

mg $NO_3^-$-N kg dw $soil^{-1}$. Samples were diluted with 2 M KCl and re-run as necessary to ensure absorbance fell within the range of the standard curve.

### 3.2.5.3 Gross nitrification rate determination

Soil gross nitrification rate was determined using a $^{15}NO_3^-$ pool dilution technique based on methods described by Brooks et al., (1989) and Drury et al., (2007). This method allows estimations of gross nitrification rate accounting for nitrate losses from other processes such as denitrification, leaching and plant uptake.

Soil nitrate was isolated from soil KCl extracts through diffusion. The process is summarised in Figure 3.1 and described below.

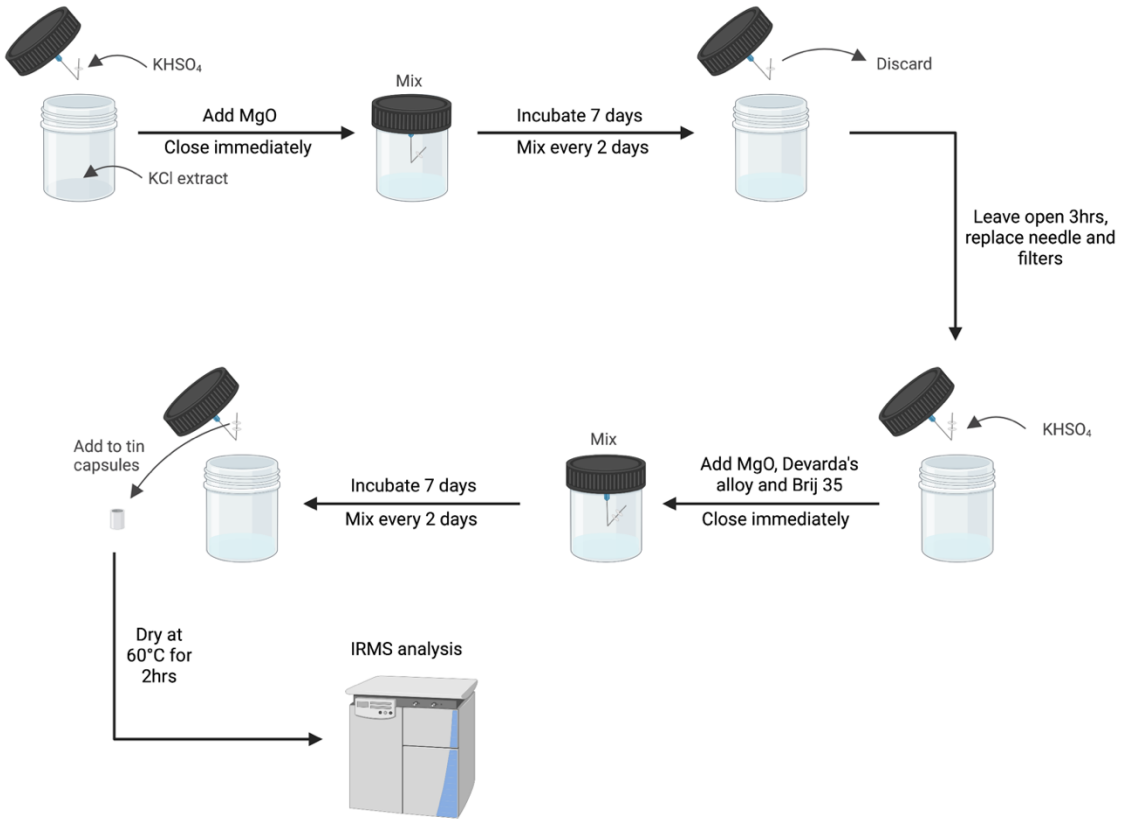


**Figure 3.1:** Overview of nitrate pool dilution method to isolate $NO_3^-$-N from solution. Figure created in BioRender.

Briefly, 25 ml sample KCl extract was added into a 60 ml airtight plastic bottle (RS Components Ltd., Northants, UK). A bent syringe needle was attached to the bottom of the lid with Blu Tack to suspend a 6 mm glass microfibre filter disc (Whatman GF/A) spiked with 2 M $KHSO_4$ (Sigma-Aldrich, USA) above the KCl extract in the bottle. Alkaline conditions were created by addition of 0.3 g anhydrous MgO (Sigma-Aldrich, USA) to convert $NH_4^+$ to $NH_3$ gas. Bottles were immediately closed to trap liberated $NH_3$. PTFE tape was added to the threads of the bottle to ensure an airtight seal. $NH_3$ was captured on the filter disc due to the acidic conditions created by the $KHSO_4$. Bottles were incubated for 7 days and mixed 3 times over the diffusion period. After 7 days the $NH_4^+$ filters were removed and discarded. Bottles were left open for 3 h to allow any remaining $NH_3$ to diffuse before replacing the syringe needle and filter.

A pair of $KHSO_4$ treated filters were added for the second diffusion with a new needle and Blu tack. Devarda's alloy (0.25 g) was added to convert $NO_3^-$ to $NH_4^+$ along with a further 0.05 g anhydrous MgO (Sigma-Aldrich, USA) to maintain alkaline conditions and allow $NH_4^+$ to be converted to $NH_3$ and captured on the acidic filter discs. A few drops of Brij 35 solution (Thermo-Fisher, USA) were added to prevent formation of bubbles. Bottles were immediately closed and incubated for a further 7 days, mixing 3 times over the incubation period. After 7 days, filter discs were removed and added to tin cups (Sercon, UK). Discs were dried for 2 h at 60°C and stored in a desiccator until analysis via isotope ratio mass spectrometry (IRMS).

Filter discs were analysed through IRMS for $^{15}N$ atom % with an elemental analyser connected to an ANCA GSL 20-20 Mass Spectrometer (Sercon PDZ Europa, Cheshire). Gross nitrification rate was calculated for each sample using ***Equation 3.1*** (Drury *et al*., 2007). Individual T-5 $NO_3^-$ concentration values and $^{15}N$ atom % values were used for T-5 values, but since a paired T-0 plant was not present for every cultivar in the 1st screen, the average T-0 $NO_3^-$ concentration value and $^{15}N$ atom % value was used for the relevant block, i.e. for block 1 samples, the individual T-5 values for each sample were used but the block 1 averages were used for T-0 values. This gave

the best approximation of T-0 $NO_3^-$ concentration and $^{15}N$ atom % experienced by all plants in each block.

$$GNR = \left(\frac{[NO_3^-]_0 - [NO_3^-]_5}{5}\right) x \left(\frac{log\left(\frac{APE_0}{APE_5}\right)}{log\left(\frac{[NO_3^-]_0}{[NO_3^-]_5}\right)}\right) \qquad \textbf{Equation 3.1}$$

Where;

GNR = Gross nitrification rate (mg N $kg^{-1}$ soil $day^{-1}$)

APE = $^{15}N$ atom % enrichment of a $^{15}NO_3^-$ pool minus natural $^{15}N$ abundance (0.3663 %)

$APE_0$ = Atom % excess at time T-0

$APE_5$ = Atom % excess at time T-5

$[NO_3^-]_0$ = $NO_3^-$ concentration at time T-0 (mg N $kg^{-1}$)

$[NO_3^-]_5$ = $NO_3^-$ concentration at time T-5 (mg N $kg^{-1}$)

A summarised workflow of the approach taken to screen gross nitrification rate is shown in Figure 3.2.

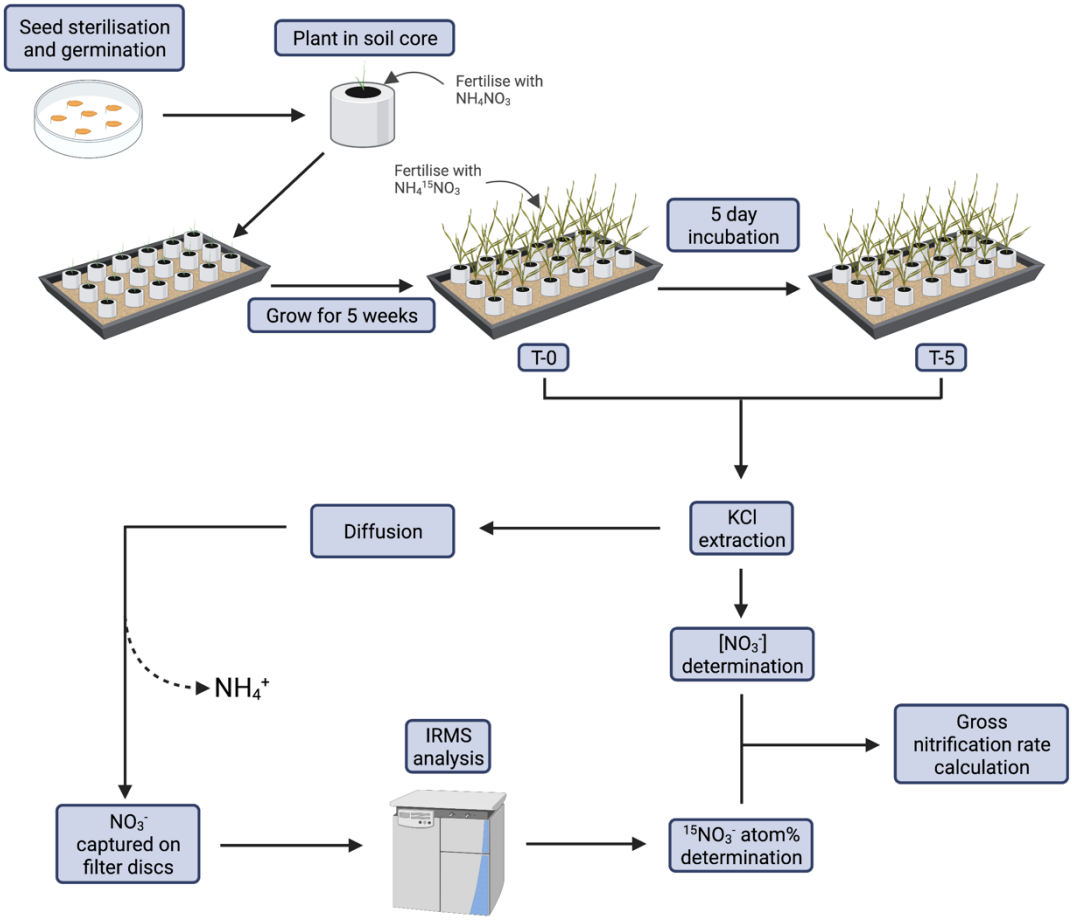


**Figure 3.2:** Summary of approach taken to screen for variation in soil gross nitrification rate using tension tables and $^{15}N$ nitrate pool dilution. Figure created in BioRender.

### 3.2.6 Data visualisation and statistical analysis

All graphs in this chapter were produced using GraphPad Prism version 9.4.1. Type II ANOVA analysis was performed using the Anova() function in R statistical software (v3.5.1; R Core Team 2018) with RStudio. Prior to performing ANOVA, datasets were checked to ensure they met the assumptions of ANOVA through plotting of diagnostics using the autoplot function of the ggplot2 package. Datasets met the assumptions of homogeneity of variance and that data is drawn from a normal distribution except for $NH_4^+$ concentration data, which deviated from a normal distribution. ANOVA analysis for this data was therefore performed on square root-transformed values, though natural data is presented. All two-way ANOVA analysis included both cultivar and block as dependent variables, but interactions were not investigated because only a single rep was present in each block for each cultivar.

Analysis of covariance (ANCOVA) was performed on $log_{10}$-transformed gross nitrification rate data with WFPS as a covariate. Prior to computing the ANCOVA test, data was checked to ensure the assumptions of the test were met. Two-way ANOVA analysis was performed as described above to assess whether there was a significant interaction between the covariate (WFPS) and dependent variable (Cultivar), but no significant interaction was detected so the assumption was met. A Shapiro test was carried out to check whether residuals were normally distributed, and this was significant ($p<0.05$), therefore data was log10-transformed to meet this assumption. All future analysis was carried out on this transformed data. A Levene test was used to ensure equal variance within the data, and this was not significant ($p=0.40$), therefore the assumption was met. Finally, the data was examined for potential outliers that may affect interpretation of the model. Outliers were identified by analysing standardized residuals (the residual divided by its estimated standard error). Values with standardised residuals with an absolute value of 3 or greater were classed as outliers. No outliers were detected so all observations were included in the ANCOVA. ANCOVA was computed using the aov() function. After computation of the ANCOVA test, estimated marginal means and standard errors of the mean were computed using the

emmeans_test() and get_emmeans() functions of the RStatix package. Data was presented as log10-transformed estimated marginal means of gross nitrification rate.

Computation of Pearson's r was performed in Microsoft Excel (Version 16.68) using the PEARSON function.

## 3.3 Results

All variables presented were tested for significant differences through two-way ANOVA analysis (ANCOVA for gross nitrification rate) with cultivar and block as dependent variables. Only main effects are displayed because it was not appropriate to test for significant interactions between cultivar and block, since each block only contained a single rep for each cultivar.

### 3.3.1 Soil gross nitrification rate

One-way ANCOVA analysis performed on log10-transformed gross nitrification rate revealed significant variation across cultivars when including WFPS as a covariate ($F=1.2458$, $p<0.05$) (Figure 3.3). Nitrification rate varied almost 8-fold with the highest gross nitrification rate associated with barley cultivar Westminster (cultivar number 198) (original non-transformed mean & SEM of 6.08±2.09 mg N kg soil$^{-1}$ day$^{-1}$) and the lowest nitrification rate associated with barley cultivar Barke (cultivar number 18) (original non-transformed mean & SEM of 0.78±0.17 mg N kg soil$^{-1}$ day$^{-1}$). Nitrification rate varied significantly across block ($F_{(3, 196)}=8.9544$, $p<0.001$, two-way ANOVA), with an increased nitrification rate in block 2 compared to blocks 1, 3 and 4 (Table 3.1).

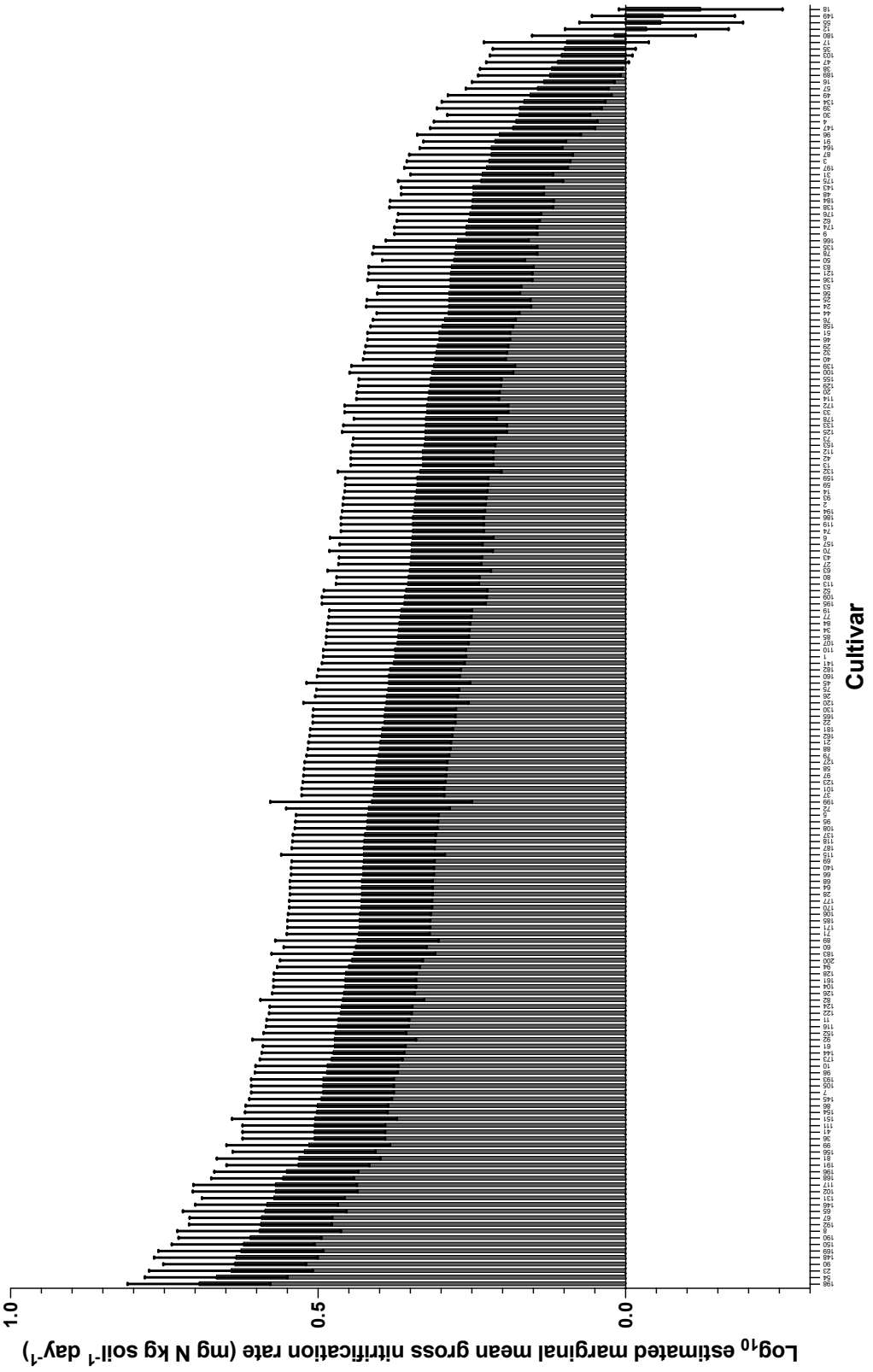


**Figure 3.3:** Estimated marginal mean ± SEM from one-way ANCOVA of log10-transformed gross nitrification rate (mg N kg soil$^{-1}$ day$^{-1}$) with WFPS as a covariate, ranked from highest to lowest gross nitrification rate. n=4 for each cultivar.

**Table 3.1:** Comparison of mean and SEM gross nitrification rate across blocks.

| Block | Mean gross nitrification rate (mg N kg soil$^{-1}$ day$^{-1}$) | SEM |
|---|---|---|
| **B1** | 2.77 | 0.12 |
| **B2** | 3.47 | 0.15 |
| **B3** | 2.78 | 0.13 |
| **B4** | 2.54 | 0.17 |

### 3.3.2 Soil WFPS

Two-way ANOVA analysis revealed a significant effect of block on WFPS ($F_{(3,\ 196)}$=144.2885, p<0.001) but no effect of cultivar ($F_{(3,\ 196)}$=0.6401, p=0.4239). WFPS was considered low enough to maintain largely aerobic conditions (<60 %) for all blocks and fell within the target range of 50-55 % in block B1 (Table 3.2). WFPS fell below the expected range for blocks B2, B3 and B4, and was lowest in B2, almost 15 % below the target WFPS range, though no plants wilted during the experiment.

**Table 3.2:** Comparison of mean and SEM WFPS (%) across blocks.

| Block | Mean WFPS (%) | SEM |
|---|---|---|
| **B1** | 54.26 | 0.56 |
| **B2** | 36.04 | 0.52 |
| **B3** | 44.59 | 0.54 |
| **B4** | 48.08 | 0.81 |

### 3.3.3 Soil pH

Two-way ANCOVA analysis of square root-transformed data showed a significant difference in soil pH between blocks ($F_{(3, 196)}$=66.0189, p<0.001), but pH did not vary significantly across cultivar ($F_{(3, 196)}$=0.7449, p=0.39). Soil pH was consistent across blocks 1 to 3 but lower in block 4 (Table 3.3).

**Table 3.3:** Comparison of mean and SEM soil pH across blocks.

| Block | Mean soil pH | SEM |
|---|---|---|
| **B1** | 4.93 | 0.01 |
| **B2** | 4.98 | 0.01 |
| **B3** | 4.96 | 0.01 |
| **B4** | 4.77 | 0.01 |

### 3.3.4 Soil $NH_4^+$-N concentration

Soil $NH_4^+$-N concentration was below detection limits in a large number of samples, particularly for block 2, where $NH_4^+$ was only detectable in 6 samples. Only 72 samples had detectable $NH_4^+$ in block 1, but blocks 3 and 4 were less affected, with 168 and 171 samples having detectable $NH_4^+$ respectively. Two-way ANOVA analysis revealed significant differences in soil $NH_4^+$-N concentration across blocks ($F_{(3, 196)}$=190.4744, p<0.001) (Table 3.4), but no significant difference across cultivars ($F_{(3, 196)}$=1.1686, p=0.09) was detected.

**Table 3.4:** Comparison of mean and SEM soil $NH_4^+$-N (mg N kg $soil^{-1}$) concentration across blocks.

| Block | Mean $NH_4^+$ concentration (mg N kg $soil^{-1}$) | SEM |
|---|---|---|
| **B1** | 0.99 | 0.15 |
| **B2** | 0.09 | 0.04 |
| **B3** | 3.07 | 0.22 |
| **B4** | 4.11 | 0.24 |

### 3.3.5 Soil $NO_3^-$-N concentration

Two-way ANOVA analysis showed significant differences in soil $NO_3^-$-N concentration across blocks ($F_{(3, 196)}$=9.1987, p<0.001). Soil $NO_3^-$-N concentration was lowest in block 1 (Table 3.5) and highest in block 3. Significant variation was seen across cultivars ($F_{(3, 196)}$=1.4374, p<0.001) (Figure 3.4) with $NO_3^-$-N concentration highest for barley cultivar Georgie (number 67) and lowest for barley cultivar Kassima (number 79), with means & SEMs of 22.62±13.41 mg N kg soil$^{-1}$ and 0.34±0.11 mg N kg soil$^{-1}$ respectively. However, computation of Pearson's r revealed no significant linear relationship between soil $NO_3^-$-N concentration and GNR ($r_{(740)}$=0.02, p=1.00).

**Table 3.5:** Comparison of mean and SEM soil $NO_3^-$-N (mg N kg soil$^{-1}$) concentration across blocks.

| Block | Mean $NO_3^-$ concentration (mg N kg soil$^{-1}$) | SEM |
|---|---|---|
| **B1** | 2.29 | 0.30 |
| **B2** | 2.85 | 0.61 |
| **B3** | 4.44 | 0.62 |
| **B4** | 4.19 | 0.46 |

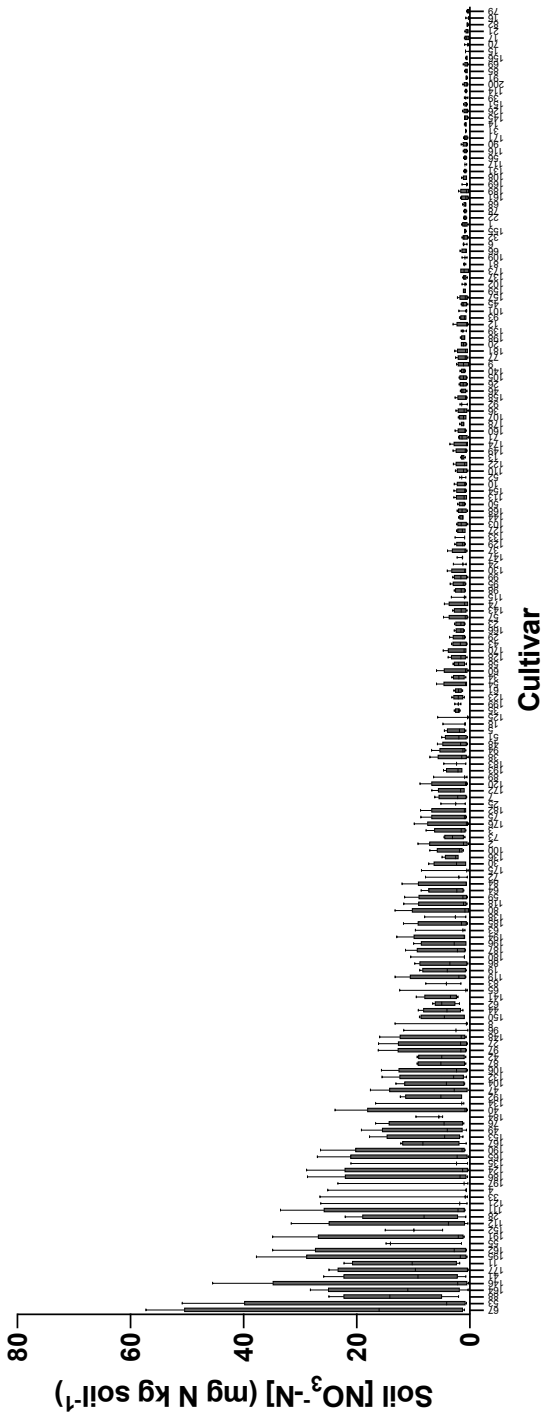


**Figure 3.4:** Comparison of soil $NO_3$-N concentration (mg N kg soil$^{-1}$) across cultivar.

### 3.3.6 Plant shoot dry weight

Two-way ANOVA analysis revealed a significant effect of block on plant shoot dry weight ($F_{(3, 196)}$=64.1234, p<0.001), with shoot dry weight highest in block 3 and lowest in block 2 (Table 3.6). Shoot dry weight also significantly varied across barley cultivar ($F_{(3, 196)}$=1.9206, p<0.001) (Figure 3.5), with barley cultivar Syn 23 (number 175) displaying the highest shoot dry weight (mean & SEM of 1.43±0.11 g) and barley cultivar Tyne (number 193) displaying the lowest shoot dry weight (mean & SEM of 0.75±0.07 g). Computation of Pearson's r revealed no significant linear relationship between shoot dry weight and GNR ($r_{(740)}$=-0.009, p=1.00).

**Table 3.6:** Comparison of mean and SEM plant shoot dry weight (g) across blocks.

| Block | Plant shoot dry weight (g) | SEM |
|---|---|---|
| **B1** | 0.96 | 0.02 |
| **B2** | 0.93 | 0.01 |
| **B3** | 1.16 | 0.02 |
| **B4** | 1.09 | 0.02 |

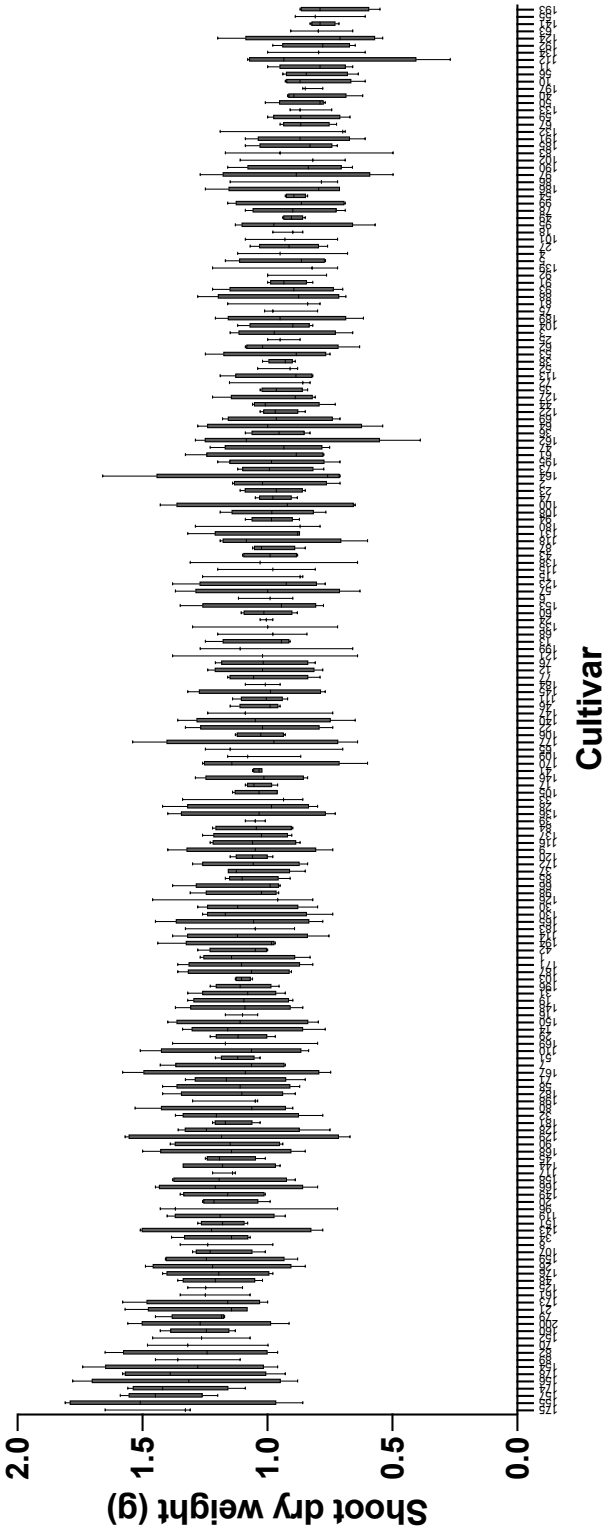


**Figure 3.5:** Comparison of shoot dry weight across cultivars.

## 3.4 Discussion

Nitrification is a major contributor to N losses from agricultural soils and a source of environmental pollution through nitrate leaching and $N_2O$ emission (Skiba et al., 2011). Plants are known to display BNI activity which acts to inhibit nitrification, often through exudation of low molecular weight compounds into the rhizosphere which may allow plants to better compete with nitrifiers for ammonium. The extent to which this BNI activity is present in crops remains unclear, but its identification is a key research need to assess the potential for BNI as a strategy to mitigate N losses (de Klein et al., 2022). A previous study investigating the BNI potential of various crops showed that barley (*Hordeum vulgare* cv. Shunrai) displayed no detectable BNI activity (Subbarao et al., 2007), though this study focused on many crops and did not investigate intraspecies variation in crop BNI activity. In this study we screened 200 spring barley cultivars, under nitrifying conditions, for variation in nitrification activity to assess whether intraspecies variation exists in barley germplasm that could be exploited to reduce N losses and improve NUE.

Tension tables developed in Chapter 2 were used in this screen to maintain aerobic WFPS in soil microcosms, ensuring oxygen was available for nitrification. Despite all microcosms experiencing aerobic conditions (WFPS <60 %) for the duration of the experiment, cracks appeared at the corner joints of several tables, notably in block B2 tables. These tables were repaired as soon as the break was detected, but this was often not until the sand and microcosms had dried out. Tables were re-flooded and reset to resolve the issue but not in enough time for soil WFPS to fully revert to the target range of 50-55 %. This could explain why B2 displayed an increased gross nitrification rate (Table 3.1) and therefore why $NH_4^+$ was lowest in block B2 (Table 3.4) and only detectable in 6 samples in B2. Interestingly, this did not result in decreased soil pH in block B2, rather soil pH was lowest in block B4 (Table 3.3). These results further highlight the importance of accurately maintaining constant WFPS when screening processes such as nitrification that are sensitive to soil oxygen content (and therefore WFPS).

To account for the observed variation in WFPS, a one-way ANCOVA analysis was performed including WFPS as the covariate and used to calculate estimated marginal means for gross nitrification rate if WFPS was consistent. This analysis revealed significant variation in gross nitrification rate across barley cultivars, with barley cultivar Barke (number 18) showing an 8-fold reduction in nitrification rate compared to barley cultivar Westminster (number 196), which showed the highest nitrification rate (Figure 3.3). These results clearly demonstrate the capability of barley to suppress soil nitrification, contrary to the results reported by Subbarao et al. (2007).

These results represent, to my knowledge, the first report of the existence of variation in BNI activity within barley germplasm. Variation in BNI activity can be attributed to the cultivar since the same soil type, bulk density, WFPS and growth conditions were used for all microcosms, with the only difference being the cultivar. Only soil $NO_3^-$-N concentration and shoot dry weight varied significantly across cultivar, though neither showed a significant linear relationship with GNR (see sections **3.3.5** and **3.3.6** respectively). This is unexpected for $NO_3^-$-N concentration, which theoretically should correlate with GNR as the main producer of nitrate in this system. Moreover, measurement of GNR through nitrate pool dilution is a powerful technique because it accounts for other N transformation processes that may be occurring in soil (Drury et al., 2007), indicating that the reduction in GNR i.e. increase in BNI activity is through direct interaction of the plant with nitrification, and not indirectly through another N transformation process.

Whether this apparent BNI activity occurs through root exudation or through some other mechanism such as enhanced competition with nitrifiers for ammonium cannot be resolved with the results from this experiment alone, but the possibility that BNI activity is related to plant N preference is explored in Chapter 6. A logical next step for this work is to collect root exudates from barley cultivars with contrasting BNI activity and add them to soil. If the same contrasting GNR as seen in this experiment is observed, for example high GNR for Westminster and low GNR for Barke, then it could be concluded that the root exudates are responsible for BNI activity. The

hydroponics system developed in Chapter 5 could be used to collect root exudates to perform such an experiment. Metabolomics analysis of root exudates displaying contrasting BNI activity would help to shed light on the compounds responsible and may lead to the identification of novel BNIs.

Cultivars were chosen for this screening experiment based on their available genetic data, and the next step for this work is to perform GWAS to identify any potential regions of the genome associated with BNI activity that can be targeted in future breeding programs and may shed further light on potential barley BNI mechanisms. It is also important to understand nitrifier community structure and activity since nitrification is a microbial process. Downstream quantitative polymerase chain reaction (qPCR) analysis will allow an assessment of *amoA* (coding for the active site of AMO, the enzyme responsible for the first step of nitrification, see section **1.2.1**) transcript abundance in soils with high and low BNI activity. I would predict that *amoA* transcript abundance would be reduced in soil with higher BNI activity. Understanding the nitrifier community structure and the contribution of bacterial and archaeal nitrification is also important. Bacteria are the dominant ammonia oxidisers at high ammonium concentration, as in this experiment which was fertilised at the standard agricultural rate of 150 kg N hectare$^{-1}$, however archaea are often the dominant ammonia oxidisers at acidic pH, and the pH of this soil was acidic with an average pH of 4.91±0.01. Performing 16S rRNA sequence analysis could therefore help to understand the relative contributions of pH and substrate availability to nitrifier community structure in this system. Samples of soil were snap-frozen in liquid nitrogen during the experiment which will allow such an assessment of nitrifier community structure and activity to be performed in future work.

Screening for variation in $N_2O$ emissions across barley germplasm with contrasting BNI activity under aerobic, nitrifying conditions will be important to assess whether the observed variation in BNI activity drives variation in $N_2O$ emissions as has been observed with the application of SNIs (Bozal-Leorri et al., 2021; Dai et al., 2013; Lam et al., 2017; Lan et al., 2018; Wang et al., 2016) and

through BNI activity (Bozal-Leorri et al., 2021), providing additional support for the development of BNI as a potential $N_2O$ mitigation strategy.

The results in this chapter have fulfilled an imminent research need for systematic screening of agronomically important crops (in this case Barley) for BNI activity (de Klein et al., 2022), and will help inform decisions on crop selection to improve NUE and reduce N losses. However, further work will be necessary to determine whether yield can be maintained (or improved) with reduced fertiliser application.

# Chapter 4: Screening for variation in soil denitrification rates across a large panel of *Hordeum vulgare* (spring barley) germplasm.

## 4.1 Introduction

$N_2O$ is a potent greenhouse with 300x the warming potential of $CO_2$ over a 100-year period (Forster et al., 2007; Kanter et al., 2013) and has the potential to deplete the ozone layer (Cicerone, 1987). Its emission accounts for 10% of global anthropogenic radiative forcing (Forster et al., 2007). Agriculture is the major anthropogenic source of $N_2O$ in many countries, driven by intensive fertiliser application (Skiba et al., 2012). In the UK, agriculture accounts for 75 % of $N_2O$ emissions (Skiba et al., 2012). Spikes in $N_2O$ emissions are seen after fertiliser addition (Skiba et al., 2012) due to addition of $NH_4NO_3$ and/or urea fertiliser that provides substrate for the microbial processes of nitrification and denitrification. Both processes produce $N_2O$ and account for most $N_2O$ emissions from agriculture. The relative contribution of nitrification and denitrification to $N_2O$ emissions varies over temporal and spatial scales and is driven by abiotic factors such as soil oxygen content, WFPS, pH and carbon availability in addition to soil ammonium and nitrate concentration. Periods of heavy rainfall can temporarily create anaerobic conditions favouring denitrification, which cause spikes in $N_2O$ emissions that are often short-lived but can contribute over 50 % of annual $N_2O$ emissions from soils (Skiba et al., 2012). Even in largely aerobic soils, nitrification and denitrification can occur simultaneously in different microsites of the same soil (Stevens et al., 1997), and the two processes are tightly coupled with nitrate, the substrate for denitrification, produced as the end product of nitrification (see Chapter 1, Figure 1.1b for further detail). Denitrification is therefore an important driver of $N_2O$ emissions from soils.

Denitrification is a microbial pathway that allows facultative anaerobes to continue to respire under oxygen-limiting conditions (Richardson, 2000), using $NO_3^-$ and other nitrogen oxides as

alternative electron acceptors (Zumft, 1997). Complete denitrification produces $N_2$ as the end-product but $N_2O$ is produced if the final step is not completed (termed incomplete denitrification). The ratio of $N_2O$ to $N_2$ production is dependent on a range of biotic and abiotic factors. Denitrification is a modular pathway, and although some denitrifiers possess the complete suite of enzymes required to carry out all reduction steps in the denitrification pathway, they are not all necessarily expressed at the same time (Graf et al., 2014; Jones et al., 2013). Furthermore, there are certain groups that do not possess an $N_2O$ reductase and therefore cannot carry out the final step to produce $N_2$ (Graf et al., 2014). Conversely, other denitrifiers possess only an $N_2O$ reductase and therefore can only carry out the final reaction. The composition of the denitrifier community therefore drives the ratio of $N_2O$ to $N_2$ production (see section **1.2.2** for further detail).

A number of abiotic factors can drive changes in the ratio of $N_2O$ to $N_2$ emission. The presence of oxygen represses expression of denitrification genes (Berks et al., 1995), reducing flux through the denitrification pathway. Oxygen irreversibly damages $N_2O$ reductase through oxidative stress (Morley & Baggs, 2010) but reversibly alters activity of other enzymes in the pathway, therefore temporal shifts from aerobic to anaerobic or vice versa through fluctuations in WFPS can increase incomplete denitrification and $N_2O$ emissions. Soil pH is another influencing abiotic factor. Alkaline pH between 7.0 to 8.0 is considered optimum for denitrification (Knowles, 1982), and acidic pH alters the abundance of different denitrifier communities and reduces activity of N oxide reductases (Brenzinger et al., 2015). $N_2O$ reductase is most affected by acidic pH (Liu et al., 2010; Šimek & Cooper, 2002), therefore low pH can promote increased $N_2O$ emissions compared to $N_2$ (Bakken et al., 2012; Bergaust et al., 2010; Liu et al., 2010; Šimek & Cooper, 2002). Soil nitrate concentration is a further abiotic factor affecting denitrification. Nitrate is required for denitrification to occur, but higher nitrate concentrations promote incomplete denitrification (and therefore $N_2O$ production) over $N_2$ production, as less energy is gained from reduction of $N_2O$ compared to other nitrogen oxides (Firestone et al., 1979; Gaskell et al., 1981; Weier et al., 1993). Carbon is also crucial for denitrification as it produces reducing power and a source of electrons for denitrifying enzymes (Richardson, 2000), and carbon addition has been shown to

stimulate denitrification (Azam et al., 2002; Henry et al., 2008). In addition to the quantity of carbon, the form of carbon can also influence denitrification and $N_2O$:$N_2$ product ratios (Giles et al., 2017; Morley et al., 2014).

The inhibition of denitrification or the promotion of complete denitrification could provide routes to improve nitrogen use efficiency through reduced N losses and reduce $N_2O$ emissions. The reduction of $N_2O$ to $N_2$ by $N_2O$ reductase is the only know biological sink of $N_2O$, so the promotion of complete denitrification could be key to reducing $N_2O$ emissions from agriculture. Plants are known to influence soil denitrification through root growth and activity (Philippot et al., 2013), and higher denitrification rates are observed in rhizosphere soil compared to bulk soil (Bakken, 1988; Klemedtsson et al., 1987; Mahmood et al., 1997) due to root exudation of various carbon compounds. Addition of artificial root exudates drives distinct responses in different denitrifier communities (Langarica-Fuentes et al., 2018), suggesting the possibility of manipulation of denitrifier community structure and/or activity through root exudation to promote complete denitrification. Previous work in by Tim Daniell, Tim George and colleagues at the James Hutton Institute has suggested that barley cultivars have variable effects on soil $N_2O$ emissions, but the extent of variation in the capacity of barley germplasm to alter incomplete and complete denitrification rates is still poorly understood. In this experiment we utilised the tension table system developed in Chapters 2 and 3 to screen the same panel of 200 barley cultivars, chosen because of their available genetic data for downstream genome-wide association studies, for variation in complete and incomplete denitrification rates, under anaerobic WFPS (>70 %) conditions. The identification of barley cultivars that suppress denitrification and/or drive increased complete denitrification could help to reduce $N_2O$ emissions from agriculture. Downstream GWAS analysis may identify future breeding targets to help mitigate denitrification-associated $N_2O$ emissions.

**Research aims**

- To assess whether there is significant variation across barley germplasm driving altered incomplete denitrification, complete denitrification, total denitrification and incomplete to complete denitrification ratios.
- To assess whether soil pH and $NO_3^-$ concentration in a common soil will have significant effects on incomplete denitrification, complete denitrification, total denitrification and the ratio of incomplete to complete denitrification.

## 4.2 Materials and methods

A summarised workflow of the approach taken to screen variation in soil denitrification rate across barley cultivars is shown in Figure 4.1 and described in detail in the following sections.

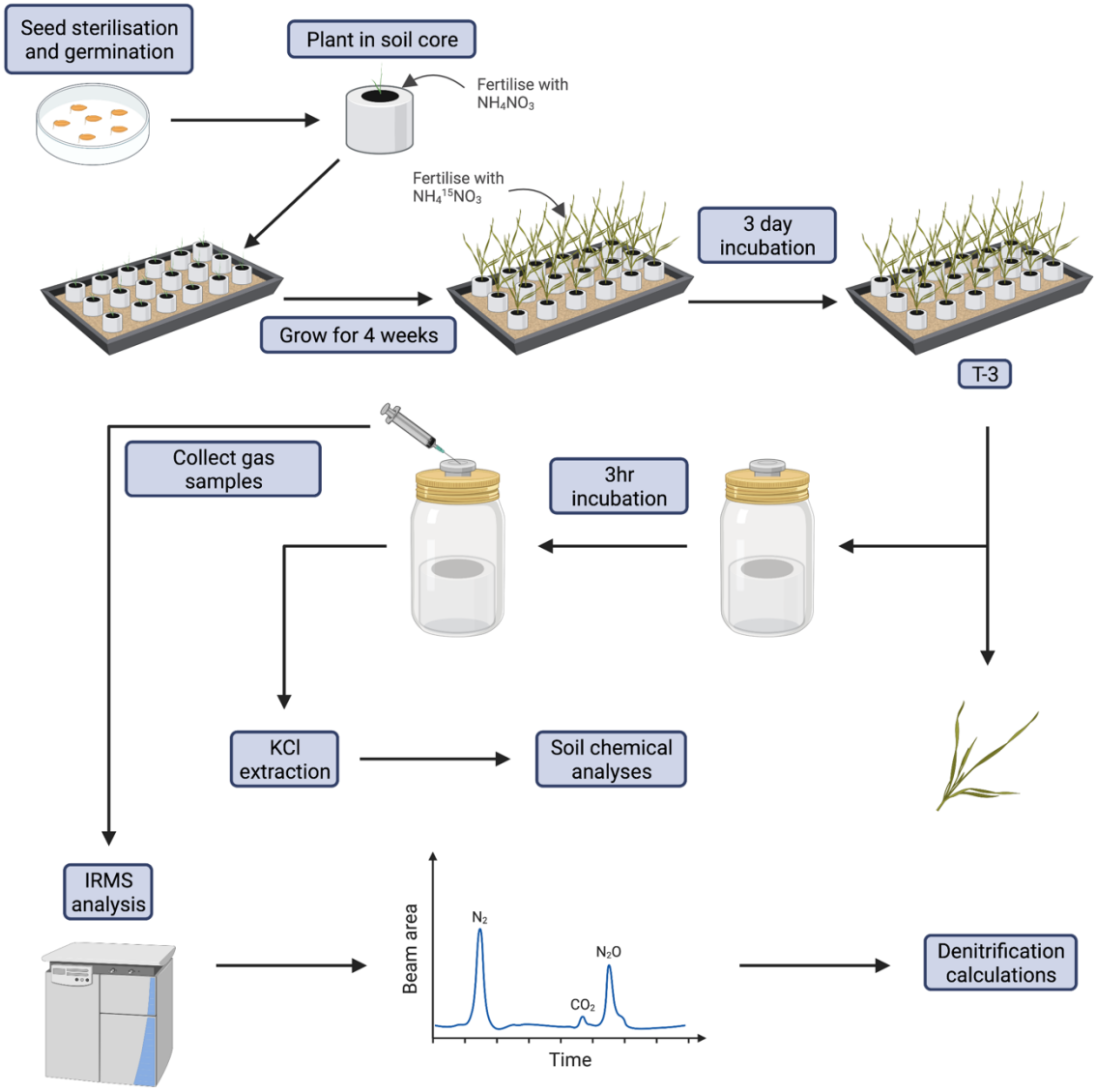


**Figure 4.1:** Summary of approach taken to screen for variation in soil denitrification rates using tension tables, $^{15}N$ enrichment and isotope ratio mass spectrometry. Chromatograph peaks are not to scale. Figure created in BioRender.

### 4.2.1 Soil type and barley cultivar selection

Soil used in this experiment was the same as that used in Chapters 2 and 3 (see section **2.2.2**) and is a sandy loam cambisol collected from the East Loane field of the James Hutton Institute's Mylnefield farm. This screen included the same 200 spring barley (*Hordeum vulgare*) cultivars from the nitrification screen carried out in Chapter 3 (listed in appendix table A.1). The screen was carried out between August to September 2021 and folowed the same experimental design as in Chapter 3 (see section **3.2.**1), consisting of 4 replicate blocks spaced one week apart from each other. Each block contained a single T-5 plant for each cultivar.

### 4.2.2 Tension table setup

Plants were grown using the same tension table setup described in **3.2.2**. Reservoir height was initially set to 0 cm to achieve a largely anaerobic WFPS of 75-80 % based on results from Chapter 3 (see Figure 3.5) and a preliminary test before the screen (data not shown), but this WFPS could only be achieved in this experiment by raising reservoirs to +2 cm to keep tension tables flooded. WFPS was monitored frequently by weighing an unplanted control microcosm (one per tension table), and re-priming of the table was carried out, when necessary, as described in **3.2.1.4**.

### 4.2.3 Soil microcosm preparation and plant growth

Microcosms were assembled and packed as described in **3.2.4**. Soil was packed to a bulk density of 1.3 g $cm^{-3}$ to achieve largely anaerobic WFPS. Microcosms were left to rest on tension tables for 5 days before planting. Barley seeds were sterilised with bleach and germinated on petri dishes as described in **3.2.7** and germinated for 5 days before planting in the centre of microcosms. Plants were planted over 2 days for each block to facilitate harvest. The screen was carried out in a controlled greenhouse cubicle at the Arthur Willis Environment Centre, Sheffield, UK, set to the same conditions as described in **2.2.8**.

N fertilisation was applied at the recommended optimum barley application rate of 150 kg N $hectare^{-1}$ (Overthrow, 2005) as described in **3.2.3**. The 1st fertiliser treatment was applied at

planting and the 2nd at 28 DAP. The 2nd fertiliser treatment was planned to be applied at maximum tillering at 35 DAP as in **3.2.3**, but plants began to show signs of N starvation at 28 DAP so fertilisation and subsequent harvest was brought forward a week. N was 5 % enriched with $NH_4{}^{15}NO_3$ in the 2nd fertilisation, considered day T-0, with gas collection and harvest carried out three days later at T-3 (31 DAP). Fertiliser was applied at 5 points in the microcosm as described in **3.2.3**.

### 4.2.4 Plant harvest and gas sample collection

Harvest and gas sampling took place on DAP 31, 3 days after the 2nd fertilisation treatment. Plant shoots were cut at the base of the plant and dried at 70°C for 48 h to obtain shoot dry weight. Intact microcosms were placed in 500 ml kilner jars and sealed with lids containing a Suba seal. Microcosms were incubated for 3 h before collection of 2 gas samples from the headspace of the jar, taken by inserting a syringe into the Suba seal. Air was mixed with the syringe 2-3 times before removal of gas samples to ensure representative samples were taken. Gas samples were immediately added to evacuated gas vials and stored at room temperature until analysis. Only 1 gas sample was taken for block 1 samples due to logistical issues.

### 4.2.5 Soil sampling

Microcosms were destructed at 31 DAP after collection of gas samples. Soil was removed from microcosms and separated from plant roots. Plant roots were initially collected for analysis but due to issues described in **3.2.1** root dry weight was not collected. Soil was sieved to 4 mm to homogenise before sampling for chemical analyses. Soil moisture content was determined as described in **2.2.3**.

### 4.2.6 Soil chemical analyses

Soil pH was determined by addition of soil to 0.01 M $CaCl_2$ (Sigma-Aldrich, USA) as described in **3.2.5**. Soil inorganic $NH_4^+$ and $NO_3^-$ concentration was determined after soil KCl extraction,

described in **3.2.5**. Filtered extracts were used for analysis of soil $NH_4^+$ and $NO_3^-$ concentration (**4.2.6.1**).

#### 4.2.6.1 Soil $NH_4^+$-N and $NO_3^-$-N concentration analysis

$NH_4^+$-N and $NO_3^-$-N concentration of soil KCl extracts was determined through the colourimetric methods described in **3.2.5.1** and **3.2.5.2** respectively. 2 M KCl was used as the matrix when preparing serially diluted standards. Samples were diluted with 2 M KCl and re-run as necessary to ensure absorbance fell within the range of the standard curve.

### 4.2.7 Gas sample $N_2O$ analysis

Gas samples were analysed for $N_2O$ concentration (ppm) using an ANCA GSL 20-20 Mass Spectrometer (Sercon PDZ Europa, Cheshire). Within the instrument, $CO_2$ was stripped from samples before cryo-concentration with liquid nitrogen and separation by gas chromatography to separate any residual $CO_2$ from $N_2O$. This step was crucial as $N_2O$ and $CO_2$ have the same molecular weight. Signal was detected as beam area, with peaks detected for $N_2$, $CO_2$ and $N_2O$. $N_2O$ standards ranging from 0-100 ppm were run at the start of each batch, with a subset of standards run at the end of each batch (5 ppm and 100 ppm). Standard curves were produced from standard ppm and beam area values, and line equations from each individual batch used to calculate sample ppm from beam area values. Samples were run in October 2021 and January 2022, and the majority of samples were run between June and July 2022.

Instrumentation issues were encountered during analysis of samples in October 2021, with a large shoulder observed on $N_2O$ peaks which led to large beam area measurements and a subsequent underestimation of sample $N_2O$ ppm concentration. Loss of samples from these issues led to 35 cultivars being removed before analysis.

### 4.2.8 Denitrification rate calculations

#### 4.2.8.1 Calculation of $N_2O$ emission rate (incomplete denitrification)

$N_2O$ ppm values were converted using the ideal gas law (***Equation 4.1***) to calculate moles of gas (calculated as 0.01449267 moles) and ***Equation 4.2*** to convert to mass of N-$N_2O$ in μg. $N_2O$ emission rate was expressed as μg N-$N_2O$ g dry weight soil$^{-1}$ hr$^{-1}$.

$$PV = nRT \qquad \textbf{Equation 4.1}$$

*Where;*

*P = Atmospheric pressure in pascals (101325 pascals)*

*V = Volume of the jar in $m^3$ (0.00051 $m^3$)*

*N = Number of moles of gas*

*R = Gas constant (8.31441 J $K^{-1}$ $mol^{-1}$)*

*T = Temperature (292.25 K)*

$$N_2O\ (\mu g) = \frac{Calculated\ ppm\ value\ x\ 0.01449267\ x\ N_2O\ Mw\ x\ 1000000}{1000000} \qquad \textbf{Equation 4.2}$$

#### 4.2.8.2 Calculation of $N_2$ emission rate (complete denitrification)

The % $N_2$ gas derived from soil was calculated using ***Equation 4.3*** as described by (Morley et al., 2014), with $^{15}NO_3$ atom % excess (APE) substituted for $^{15}N_2O$ APE measured by IRMS. This was done because $^{15}NO_3$ APE from soil was not measured during the experiment due to logistical and financial constraints and assumes that all $N_2O$ was produced by denitrification and that no isotopic fractionation occurs during denitrification. The number of moles of N was calculated using ***Equation 4.4***, followed by calculation of the mass of N in the jar (g) using ***Equation 4.5***. The

mass of N-$N_2$ derived from $NO_3^-$ in g was then calculated using ***Equation 4.6***. $N_2$ emission rate was expressed as μg N-$N_2$ g dry weight $soil^{-1}$ $hr^{-1}$.

$$\%\ N\ gas\ soil\ derived = \left(\frac{APE\ N_2\ in\ headspace}{APE\ in\ NO_3^-}\right) x\ 100 \qquad \textbf{Equation 4.3}$$

$$Moles\ N\ in\ jar = Moles\ gas\ in\ jar\ x\ Proportion\ N_2\ in\ atmosphere \qquad \textbf{Equation 4.4}$$

*Where;*

*Moles gas in jar = 0.01449267*

*Proportion $N_2$ in atmosphere = 0.7809*

$$Mass\ N\ in\ jar\ (g) = Moles\ N\ in\ jar\ x\ Mw\ of\ N \qquad \textbf{Equation 4.5}$$

*Where;*

*Moles N in jar = 0.011317326*

*Mw of N = 14.067*

$$Mass\ N\ derived\ from\ NO_3^-(g) = \left(\frac{\%\ N\ soil\ derived}{100}\right) x\ Mass\ N\ in\ jar \qquad \textbf{Equation 4.6}$$

#### 4.2.8.3 Calculation of total denitrification rate and ratio of incomplete to total denitrification

Total denitrification was calculated as the sum of the $N_2O$ and $N_2$ emission rate, i.e. incomplete and complete denitrification rate, expressed as μg N g dry weight $soil^{-1}$ $hr^{-1}$. The ratio of incomplete to total denitrification was calculated using ***Equation 4.7***. Ratio values vary from 0 to 1, with a value of 0 indicating that complete denitrification accounts for 100% of total

denitrification and a value of 1 indicating that incomplete denitrification accounts for 100% of total denitrification.

$$Ratio\ incomplete\ to\ total\ denitrification = \frac{N_2O(\mu g\ g\ dw\ soil^{-1}hr^{-1})}{N_2\ (\mu g\ g\ dw\ soil^{-1}hr^{-1}) + N_2O\ (\mu g\ g\ dw\ soil^{-1}hr^{-1})} \qquad \textbf{\textit{Equation 4.7}}$$

### 4.2.9 Data visualisation and statistical analysis

All graphs in this chapter were produced using GraphPad Prism version 9.4.1. Type II ANOVA analysis was performed using the Anova() function in R statistical software (v3.5.1; R Core Team 2018) with RStudio. Prior to performing ANOVA, datasets were checked to ensure they met the assumptions of ANOVA through plotting of diagnostics using the autoplot function of the ggplot2 package. Datasets were $log_{10}$-transformed (incomplete denitrification rate, complete denitrification rate and total denitrification rate) or square root-transformed (ratio incomplete to total denitrification) to meet the assumptions of homogeneity of variance and that data is drawn from a normal distribution. All two-way ANOVA analysis included both cultivar and block as dependent variables, but interactions were not investigated because only a single rep was present in each block for each cultivar.

Analysis of covariance (ANCOVA) was performed on $log_{10}$-transformed data for incomplete, complete and total denitrification rate and square root-transformed $N_2O/(N_2+N_2O)$ ratio data including soil WFPS as a covariate. Prior to computing the ANCOVA test, data was checked to ensure the assumptions of the test were met as described in section **3.2.6**. ANCOVA was computed using the aov() function and performed on square root-transformed $N_2O/(N_2+N_2O)$ ratio data.

## 4.3 Results

### 4.3.1 Denitrification rates

Two-way ANOVA analysis was performed for $N_2O$ emission rate (a measure of incomplete denitrification), $N_2$ emission rate (a measure of complete denitrification), $N_2+N_2O$ emission rate (a measure of total denitrification), and $N_2O/(N_2+N_2O)$ ratio (the ratio of incomplete denitrification to total denitrification). Analysis revealed a significant effect of block but no significant effect of barley cultivar on all measures of denitrification (F and p values are reported in Table 4.1). Mean and SEM ratio values for each block are displayed in Table 4.2. All ratio values fall between 0 and 1, where 0 indicates that complete denitrification (conversion to $N_2$) accounts for 100 % of total denitrification, and a value of 1 indicates that incomplete denitrification (conversion to $N_2O$) accounts for 100 % of total denitrification. Only $N_2O/(N_2+N_2O)$ ratio values are displayed because this describes each of the 3 distinct denitrification rates in a single value. The $N_2O/(N_2+N_2O)$ ratio was notably lower in block D1 (Table 4.2), indicating that a greater proportion of incomplete denitrification occurred in block D1.

Because WFPS varied across block (see section **4.3.2**), ANCOVA analysis was performed including WFPS as a covariate. Soil WFPS had a significant effect on each denitrification rate and the $N_2O/(N_2+N_2O)$ ratio (Table 4.3), however cultivar did not have a significant effect (Table 4.3).

**Table 4.1:** Results (F and p-values) of two-way ANOVA analysis testing for significant differences in incomplete denitrification rate, complete denitrification rate, total denitrification rate and the ratio of incomplete to total denitrification across block and barley cultivar. Statistical analysis was performed on $log_{10}$-transformed data for incomplete, complete, and total denitrification rate, and on square root-transformed data for the ratio of incomplete to total denitrification. *** denotes significance at the p<0.001 level.

| | | F value $_{(3, 164)}$ | p value | Significance |
|---|---|---|---|---|
| **Incomplete** | Block | 75.1138 | <0.001 | *** |
| | Cultivar | 0.9193 | 0.7817 | |
| **Complete** | Block | 51.6159 | <0.001 | *** |
| | Cultivar | 1.1848 | 0.0930 | |
| **Total** | Block | 42.9971 | <0.001 | *** |
| | Cultivar | 1.1859 | 0.0918 | |
| **Ratio** | Block | 82.9683 | <0.001 | *** |
| | Cultivar | 0.9701 | 0.5840 | |

**Table 4.2:** Comparison of mean and SEM ratio of incomplete to total denitrification across the 4 blocks included in the experiment.

| Block | Ratio mean | Ratio SEM |
|---|---|---|
| **D1** | 0.038 | 0.004 |
| **D2** | 0.110 | 0.011 |
| **D3** | 0.180 | 0.009 |
| **D4** | 0.156 | 0.008 |

**Table 4.3:** Results (F and p-values) of ANCOVA analysis testing for significant differences in incomplete denitrification rate, complete denitrification rate, total denitrification rate and the ratio of incomplete to total denitrification across block and barley cultivar. Statistical analysis was performed on log10-transformed data for incomplete, complete, and total denitrification rate, and on square root-transformed data for the ratio of incomplete to total denitrification. * denotes significance at the p<0.05 level, *** denotes significance at the p<0.001 level.

| | | F value $_{(1, 164)}$ | p value | Significance |
|---|---|---|---|---|
| **Incomplete** | Block | 31.6970 | <0.001 | *** |
| | Cultivar | 0.7580 | 0.9800 | |
| **Complete** | Block | 10.358 | <0.001 | *** |
| | Cultivar | 0.9700 | 0.5860 | |
| **Total** | Block | 5.762 | <0.05 | * |
| | Cultivar | 0.9690 | 0.5870 | |
| **Ratio** | Block | 46.924 | <0.001 | *** |
| | Cultivar | 0.8510 | 0.8840 | |

### 4.3.2 Soil WFPS

Soil WFPS remained above 70 % in all 4 blocks for the duration of the experiment, however two-way ANOVA analysis revealed significant differences in soil WFPS across blocks ($F_{(3,164)}$=30.7330, p<0.001), with the highest WFPS in block D1 (Table 4.4). It should be noted that tension tables were kept flooded for the duration of the experiment in order to maintain this high WFPS and therefore did not actively control WFPS. Soil WFPS did not vary significantly across barley cultivars ($F_{(3,164)}$=1.0080, p=0.4681).

**Table 4.4:** Comparison of soil WFPS (%) across the 4 blocks included in the experiment.

| Block | WFPS mean (%) | WFPS SEM |
|---|---|---|
| **D1** | 84.39 | 0.51 |
| **D2** | 80.33 | 0.46 |
| **D3** | 78.88 | 0.32 |
| **D4** | 78.77 | 0.45 |

### 4.3.3 Soil pH

Two-way ANOVA analysis showed significant variation in soil pH across block ($F_{(3,164)}$=149.0941, p<0.001), with pH lower in blocks D1 and D2 compared to blocks D3 and D4 (Table 4.5). Soil pH did not vary significantly across cultivar ($F_{(3,164)}$=1.0395, p=0.3761).

**Table 4.5:** Comparison of soil pH across the 4 blocks included in the experiment.

| Block | pH mean | pH SEM |
|---|---|---|
| **D1** | 5.10 | 0.02 |
| **D2** | 5.10 | 0.02 |
| **D3** | 5.41 | 0.01 |
| **D4** | 5.42 | 0.02 |

### 4.3.4 Soil $NH_4^+$-N concentration

Soil $NH_4^+$-N concentration varied significantly across block ($F_{3,164)}$=11.6039, p<0.001, two-way ANOVA), with $NH_4^+$-N concentration lower in blocks D1 and D2 compared to blocks D3 and D4 (Table 4.6). Soil $NH_4^+$-N concentration did not vary significantly across barley cultivar ($F_{(3,164)}$=1.2213, p=0.0611).

**Table 4.6:** Comparison of soil $NH_4^+$-N concentration (mg N kg $soil^{-1}$) across the 4 blocks included in the experiment.

| Block | $NH_4^+$ mean (mg N kg $soil^{-1}$) | $NH_4^+$ SEM |
|---|---|---|
| **D1** | 21.06 | 0.78 |
| **D2** | 19.71 | 0.97 |
| **D3** | 24.74 | 0.75 |
| **D4** | 25.15 | 0.56 |

### 4.3.5 Soil $NO_3^-$-N concentration

Soil $NO_3^-$-N concentration varied significantly across block ($F_{(3,164)}$=13.0610, p<0.001), with lower concentrations observed in blocks D1 and D3 compared to blocks D2 and D4 (Table 4.7). Concentration also varied across barley cultivar ($F_{(3,164)}$=1.2356, p<0.05) (Figure 4.2), with the highest $NO_3^-$-N concentration observed for barley cultivar Meltan (cultivar number 99, mean±SEM of 20.54±11.05 mg N kg $soil^{-1}$), and the lowest $NO_3^-$-N concentration observed for barley cultivar Atlas (cultivar number 13, mean±SEM of 0.5±0.1 mg N kg $soil^{-1}$).

**Table 4.7:** Comparison of soil $NO_3^-$-N concentration (mg N kg $soil^{-1}$) across the 4 blocks included in the experiment.

| Block | $NO_3^-$ mean (mg N kg $soil^{-1}$) | $NO_3^-$ SEM |
|---|---|---|
| **D1** | 8.33 | 0.54 |
| **D2** | 5.56 | 0.79 |
| **D3** | 7.98 | 0.47 |
| **D4** | 5.90 | 0.38 |

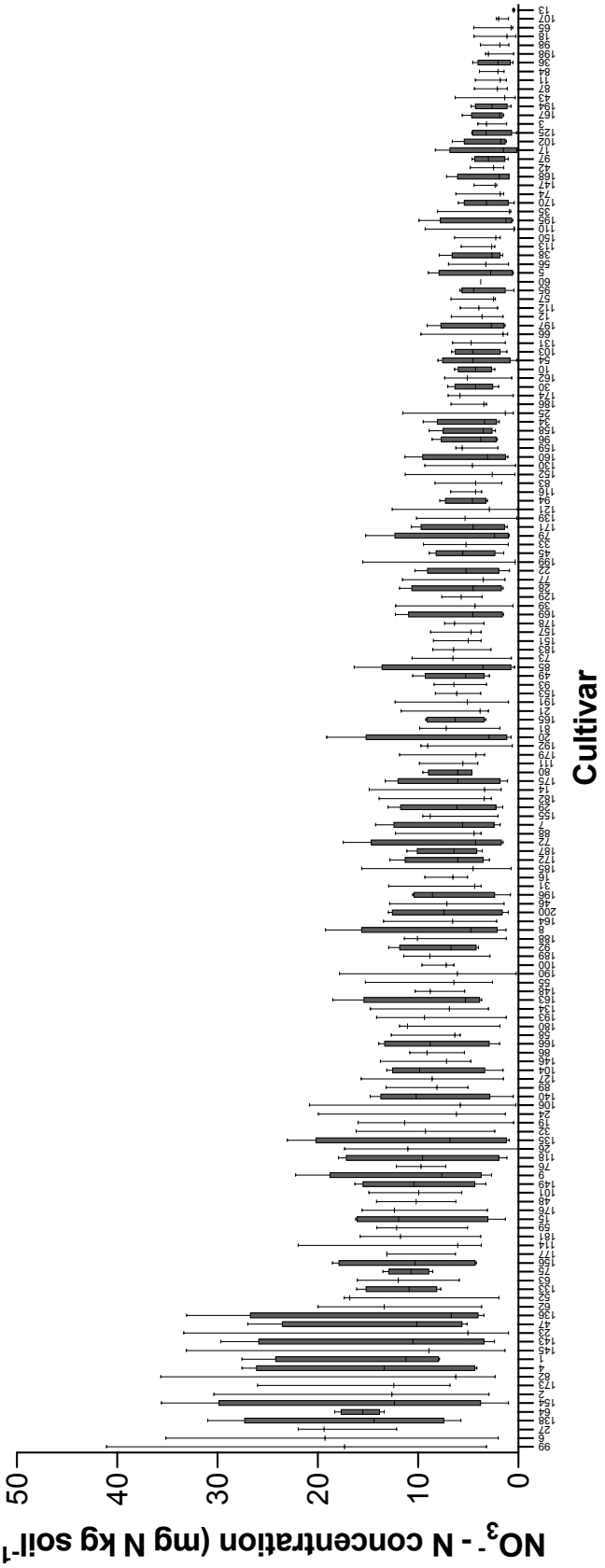


**Figure 4.2:** Comparison of soil $NO_3^-$-N concentration (mg N kg soil$^{-1}$) across cultivar.

### 4.3.6 Plant shoot dry weight

Two-way ANOVA analysis revealed significant differences in shoot dry weight across block ($F_{(3,164)}$=175.0465, p<0.001), with shoot dry weight larger in block D2 compared to other blocks (Table 4.7). Plants were visibly smaller for block D4 when the experiment was run, and this is reflected in the average shoot dry weight for this block (Table 4.8). Shoot dry weight did not vary significantly across cultivar ($F_{(3,164)}$=1.1779, p=0.0995).

**Table 4.8:** Comparison of plant shoot dry weight (g) across the 4 blocks included in the experiment.

| Block | Shoot dry weight mean (g) | Shoot dry weight SEM |
|---|---|---|
| **D1** | 0.50 | 0.01 |
| **D2** | 0.85 | 0.02 |
| **D3** | 0.51 | 0.01 |
| **D4** | 0.44 | 0.01 |

## 4.4 Discussion

Denitrification is one of the two main sources of $N_2O$ from agriculture, which accounts for 75 % of UK $N_2O$ emissions (Skiba et al., 2012). $N_2O$ is produced by incomplete denitrification when the final step, the reduction of $N_2O$ to $N_2$, is not carried out. The ratio of incomplete to complete denitrification is a major driver of $N_2O$ emissions and is driven by various biotic and abiotic factors (Brenzinger et al., 2015; Giles et al., 2012; Morley & Baggs, 2010). Previous work at the James Hutton Institute (Tim Daniell, Tim George and colleagues, unpublished) has shown that barley cultivars may affect $N_2O$ emissions from denitrification, though the extent to which this plant influence of denitrification is present in barley germplasm and any underlying genetic components remain poorly understood. In this study, 200 barley cultivars previously screened for variation in soil nitrification rates were screened under anaerobic (WFPS >70 %), denitrifying conditions for variation in incomplete denitrification ($N_2O$ emissions), complete denitrification ($N_2$ emissions), total denitrification ($N_2O$+$N_2$ emissions), and the ratio of incomplete denitrification to total denitrification ($N_2O/(N_2+N_2O)$).

During analysis of gas samples, several issues were encountered with the IRMS instrument. A large number of block D1 samples run during early batches were lost after a large shoulder was observed on the $N_2O$ peak of these samples. This was later attributed to a loose fitting on the cryo-concentration loop that allowed air to enter the sample. Since $CO_2$ (present in the air) has the same molecular weight as $N_2O$, the peak from this large amount of $CO_2$ overlapped with the $N_2O$ peak, resulting in an underestimate of sample $N_2O$ ppm concentration compared to samples run later when the issue was fixed. As a result, these samples were omitted from the dataset. Furthermore, machine errors were common in which the connection to the computer was interrupted during a sample run, leading to the gas sample entering the instrument but no data being recorded. Where possible, the second rep for these samples was run, but these issues combined with missing data and/or samples inevitable with an experiment of this scale led to the omission of 35 cultivars from the analysis. It should also be noted that many samples displayed

$N_2O$ ppm values above 100 ppm (the most concentrated standard). Due to issues related to the COVID-19 pandemic and Brexit, it was not possible to source a more concentrated standard. The assumption was therefore made that the relationship between beam area and $N_2O$ ppm remains linear above 100ppm, but as soon as a more concentrated standard becomes available this should be verified.

No significant differences were detected across barley cultivar via two-way ANOVA analysis for any of the above rates or $N_2O/(N_2+N_2O)$ ratio, though significant differences across block were observed for all (Table 4.1). The tension table system developed in Chapter 2 and modified in Chapter 3 for large-scale screening was used to maintain anaerobic WFPS across the experiment. Though anaerobic WFPS >70 % was maintained across blocks, significant variation in WFPS was seen across block, with block D1 WFPS falling outside of the target 75-80 % target (Table 4.4). This was likely due to issues experienced with the tension tables. Table reservoirs were originally set to a reservoir height of 0cm to maintain WFPS of approximately 70 %, based on results from Chapter 2 Figure 2.5. However, sufficiently high WFPS could not be maintained, and the only way to achieve the target WFPS was through raising the reservoir to +2 cm and keeping the sand surface flooded. This allowed anaerobic conditions to be maintained in microcosms but at the expense of the fine control the tables should have allowed if imposing a suction pressure.

WFPS, a proxy for soil oxygen content, drives differences in the $N_2O/(N_2+N_2O)$ ratio, with $N_2O$ reductase irreversibly damaged by oxygen (Morley & Baggs, 2010). Higher WFPS should therefore promote reduced $N_2O$ emissions through reduced oxidative damage of $N_2O$ reductase and increased complete denitrification. In line with this, the $N_2O/(N_2+N_2O)$ ratio was lowest in block D1 (Table 4.2), which displayed the highest average WFPS (Table 4.4), suggesting incomplete denitrification contributed the most to total denitrification in this block. Given that WFPS appeared to influence the $N_2O/(N_2+N_2O)$ ratio despite efforts to maintain consistent WFPS in the experiment, an ANCOVA analysis was conducted including WFPS measured at harvest as a covariate. However, even when controlling for variation in WFPS, no significant differences were

observed across cultivar for the $N_2O/(N_2+N_2O)$ ratio, nor for incomplete, complete or total denitrification rate (Table 4.3). This suggests other factors were more important than cultivar in controlling denitrification rates under the conditions of this experiment.

In addition to WFPS, soil pH and nitrate concentration can affect the $N_2O/(N_2+N_2O)$ ratio, with both acidic pH and high $NO_3^-$ concentration favouring incomplete denitrification over complete denitrification. Both soil pH and nitrate concentration varied across block (Table 4.5 and 4.7 respectively) in addition to ammonium concentration and shoot dry weight (Table 4.6 and 4.8 respectively), however no obvious relationship between these factors and $N_2O/(N_2+N_2O)$ ratio was observed. It is likely that complex interactions between these abiotic factors drove the observed variation in $N_2O/(N_2+N_2O)$ ratio across blocks. It is clear that under the conditions of this experiment, no variation in $N_2O/(N_2+N_2O)$ ratio can be attributed to barley cultivar.

The lack of variation in $N_2O$ emissions across barley cultivar does not support previous unpublished results from the James Hutton Institute where it was observed that $N_2O$ emissions varied across cultivar under fluctuating WFPS conditions (i.e. between largely aerobic and largely anaerobic). However, WFPS was held consistently anaerobic for the duration of this screen which may favour complete denitrification due to the prolonged absence of significant oxygen which would act to irreversibly damage $N_2O$ reductase (Morley & Baggs, 2010). This suggests that total denitrification rates are not affected by barley cultivars but may be driving variation in $N_2O$ emissions and $N_2O/(N_2+N_2O)$ ratio through alteration of denitrifier community structure to promote or suppress $N_2O$ reducers, or through alteration of $N_2O$ reductase activity. In this study, complete denitrification was favoured due to the sustained anaerobic WFPS >70 %, and this may have masked any variation across cultivar affecting $N_2O$ reductase activity. A future screen should be set up to fluctuate between aerobic and anaerobic WFPS to generate conditions that are more similar to the conditions of the previous work, and which simulate periods of heavy rainfall where $N_2O$ emissions often spike, to reveal any potential variation in $N_2O$ reductase activity when $N_2O$ production is generally favoured. If variation is observed across barley germplasm under these

fluctuating conditions, GWAS analysis could be carried out to potentially identify future breeding targets that promote complete denitrification.

# Chapter 5: Investigating variation in nitrogen preference in a range of *Hordeum vulgare* (spring barley) cultivars under variable environmental conditions

## 5.1 Introduction

Nitrogen (N) is crucial for plant survival and its availability is a key driver of crop productivity. Plants can take up both organic and inorganic N forms, though inorganic forms are often preferred (Ashton et al., 2008; Harrison et al., 2007), particularly in agriculture where large amounts of inorganic N are added as fertiliser. The concept of N preference is as such commonly described as a plants choice to preferentially take up either ammonium or nitrate. Variation in N preference can be attributed to a range of plant physiological, environmental and edaphic factors (Boudsocq et al., 2012, Britto & Kronzucker, 2013). The photo-energetic costs of ammonium and nitrate uptake differ, with a 45 % reduced cost to assimilate ammonium (Raven, 1985) because it can be directly incorporated into amino acids, whereas nitrate must first be reduced to ammonium before it can be assimilated (Engels & Marschner, 1995). Ammonium becomes toxic to plants at much lower concentrations than does nitrate, leading to the majority of ammonium being assimilated in plant roots at the site of uptake, whereas nitrate is also assimilated in plant shoots (Ali et al., 2001; Engels & Marschner, 1995; Lewis & Chadwick, 1983). This leads to enhanced carbohydrate demand to the roots for ammonium assimilation (Finnemann & Schjoerring, 1999; Haynes & Goh, 1978; Wang et al., 1993). Nitrate is usually more available for plant uptake in most systems, owing to its higher mobility due to its negative charge and reduced electrostatic interactions with soil (Brady & Weil, 1999).

Environment is a key driver of relative pools of inorganic N in a system and can often determine whether ammonium or nitrate is the dominant N form. Changes in precipitation drive soil oxygen availability and in turn soil nitrification and denitrification rates. This relationship between soil moisture and key nitrogen cycling processes explains why paddy rice varieties, for example, are

generally considered to be ammonium-preferring (Kirk, 2001), where flooded soil conditions limit oxygen availability and thus nitrification. High denitrification rates also act as a sink for nitrate in flooded soils, limiting availability for plant uptake. Well-aerated soils, however, are often dominated by nitrate due to high nitrification rates, particularly in agricultural soils when large quantities of ammonium and/or urea are added as fertiliser. Plants in these drier soils tend to favour nitrate as an N source to reflect this (Houlton et al., 2007, Wang & Macko, 2011). It is important to remember, however, that this is still a simplified view of the effects of environment on the presence of different N forms. N pools are dynamic and vary over both temporal and spatial scales, and pool size does not always equal importance, as some pools may be small due to rapid turnover (Kirk & Kronzucker, 2005, Britto & Kronzucker, 2013).

Light intensity can affect uptake of different N sources; Ma et al. (2016) observed increased ammonium uptake in *Brassica chinensis* L. under long-term high light when supplied with equal amounts of ammonium and nitrate. However, ammonium-grown *Phaseolus vulgaris* plants have been shown to be more sensitive to light stress than nitrate-grown plants (Zhu et al., 2000), suggesting different responses to high light dependent on plant species and/or experimental conditions. N source and preference may also be affected by changes in atmospheric $CO_2$. Previous studies have shown conflicting N preference results under elevated $CO_2$ (Bassirirad et al., 1996, 1997; Zerihun & Bassirirad, 2001), but recent literature has suggested that elevated $CO_2$ could alter N preference in favour of ammonium through inhibition of shoot nitrate assimilation. This may be due to surplus photosynthetic reductant no longer being available for nitrate reduction and instead being used for carbon fixation at $eCO_2$ (Bloom et al., 2002), or decreased reductant production through photorespiration, which is inhibited at $eCO_2$ (Bloom, 2015; Bloom et al., 2012; Cousins & Bloom, 2004; Searles & Bloom, 2003; Smart et al., 2001). To date, the direct effect of $eCO_2$ on N preference has not been extensively studied, though plants often show decreased growth with nitrate as the sole N supply compared to ammonium under $eCO_2$ conditions (Bloom et al., 2002, 2012).

Taken together, the above considerations have made it difficult to provide a firm definition of N preference, despite extensive use of the term in the literature. At its simplest, N preference is often defined as preference for either ammonium or nitrate (as in this thesis), though it is important to recognise that this is often not a rigid classification but rather specific to a plant species under a defined set of experimental conditions. Given that this measured preference is often driven by the relative proportions of ammonium and nitrate available, it has recently been suggested that perhaps it would be more appropriate to use the term 'N plasticity', since 'preference' implies an inherent benefit to a plant actively taking up a particular N form (Chalk & Smith, 2021). However, plants have been shown to retain the N preference of their parents when grown under consistent experimental conditions and equal ammonium and nitrate supply (Wang & Macko, 2011), suggesting that when environmental constraints are removed a genetic component driving an 'innate' N preference is revealed, and that perhaps the term 'preference' should not be completely discarded.

In this chapter, a hydroponics system was developed to allow screening of innate N preference when environmental constraints of preference were removed, allowing assessment of shifts in preference in response to changes in individual environmental conditions such as light intensity and atmospheric $CO_2$ across a range of cultivars of the UK staple crop barley (Figure 5.1). Through this simplified approach we hoped to understand 1.) whether 'innate' N preference (N preference when all factors that could drive a particular form to be preferentially taken up are removed) is common across genetically distinct barley cultivars, 2.) whether this innate preference is shifted under short-term exposure to high light or long-term exposure to $eCO_2$, and 3.) whether observed changes in preference in response to these environmental pressures are common across all barley cultivars.

**Research hypotheses**

- Innate N preference will be for ammonium rather than nitrate and will be common across all barley cultivars.
- Innate N preference will be shifted further towards ammonium for all cultivars when exposed to short-term high light or long-term $eCO_2$.

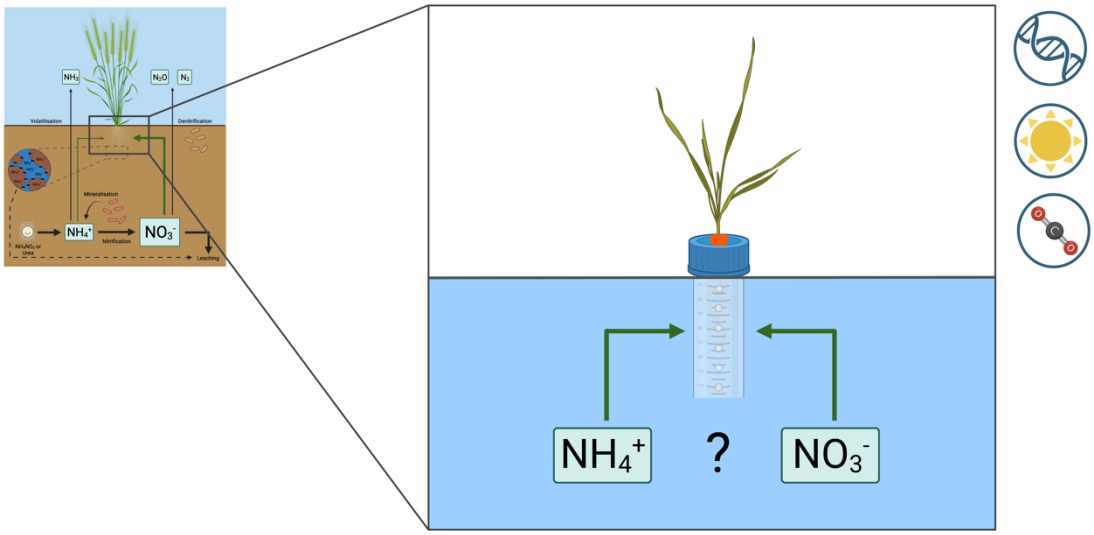


**Figure 5.1:** Conceptual diagram illustrating the simplified approach taken in this chapter to understand variation in innate N preference responses to high light and $CO_2$ across barley cultivars, with environmental preference constraints removed. Figure created in BioRender.

## 5.2 Materials and methods

### 5.2.1 Barley cultivar selection

Spring barley cultivars were provided by the James Hutton Institute and Syngenta. Cultivars included in Experiment 1 (initial N preference screen) were selected based on previous work carried out in the laboratory in addition to the transgenic *HvEPF1oe* barley line with significantly reduced stomatal density and carbon assimilation (Hughes et al., 2017) and its wild-type counterpart, Golden Promise. *HvEPF1oe* was chosen to assess whether reduced carbon assimilation would impact on plant preference. This selection was reduced to 8 cultivars in Experiment 2 (N preference under short-term high light) to allow increased replication and addition of a second environmental condition. Shortlisting was based on results from Experiment 1, spanning the N preference range observed. A total of 14 cultivars were selected for Experiment 3 (N preference under $eCO_2$), based on results obtained from the nitrification screen (Chapter 4) and results from Experiments 1 and 2, to include cultivars spanning a range of high, medium and low gross nitrification rate and nitrogen preference differences, to assess potential links between N preference and gross nitrification rate (Chapter 6). A full list of cultivars included in each experiment is listed in Table 5.1.

**Table 5.1:** Summary table of Spring Barley cultivars included in N preference experiments.

| Cultivar | Experiment 1 | Experiment 2 | Experiment 3 |
|---|---|---|---|
| **Annabell** | | | • |
| **Athos** | | | • |
| **B83** | • | • | |
| **Barke** | | | • |
| **Concerto** | • | | |
| **Derkado** | • | | • |
| **Diamant** | | | • |
| **Golden Promise** | • | • | • |
| ***HvEPF1oe*** | • | • | • |
| **Laureate** | • | • | • |
| **LG Diablo** | | | • |
| **Melius** | • | • | |
| **NFC Tipple** | • | • | • |
| **Optic** | • | | |
| **Shuffle** | • | | • |
| **Steffi** | | | • |
| **Troon** | • | | |
| **Waggon** | • | • | • |
| **Westminster** | • | • | • |

A total of 8 plants were included for each genotype in Experiment 1, with 3 exposed to $^{15}NH_4NO_3$, 3 to $NH_4{}^{15}NO_3$, and 3 to unlabelled control $NH_4NO_3$ at the time of labelling (see section 2.2.8). This was expanded to 4 plants under each labelling treatment and environmental condition for Experiments 2 and 3. Only a single control rep of 4 random cultivars (*Hordeum vulgare* cv Golden Promise, Melius, Westminster and the transgenic *HvEPF1oe* line) was included in Experiment 2 due to the small difference in control $^{15}N$ atom% values in Experiment 1, but this was increased to 1 control plant per labelling:$CO_2$ combination for all 14 cultivars in Experiment 3. Additional plant reps were included for redundancy where seed stocks allowed. Plants of all cultivars were included in each individual tank for all experiments, with a randomised list generated for each individual tank using the list function in R statistical software (v3.5.1; R Core Team 2018) with RStudio.

### 5.2.2 Seed sterilisation and germination

Spring barley seeds were sterilised and germinated as described in section **2.2.7.** Seedlings were germinated in petri dishes for 7-9 days before transferring to hydroponics tanks to ensure roots were long enough to reach the nutrient solution.

### 5.2.3 Hydroponics system

A simple deep-water culture hydroponics system was constructed based on the designs described by Conn et al., (2013) and modified for crop growth (Figure 5.2). Hydroponics tanks were constructed from 42 l storage boxes (B&M Retail Ltd.). A tap was fitted to each tank for easy drainage of nutrient solution (The Range). Lids were cut to size from ABS plastic (Eurocell) and a total of 35 28 mm holes drilled in 5 rows of 7 to hold a maximum of 35 plants. A total of 3 15 cm sections of 15 mm PVC pipe were secured vertically in each tank to support the ABS lid. Plants were held in modified 50 ml centrifuge tubes (Greiner) with the tube bottom cut off and 2 mm holes drilled up the sides to allow even nutrient flow to plant roots. A single 12 mm hole was drilled into tube lids, with plants secured in the lid with a foam earplug cut in half such that roots were contained within the tube and shoots remained above the lid. Small submersible aquarium pumps (Amazon UK) with a maximum flow rate of 300 l $hr^{-1}$ were placed at opposite ends of the tank to circulate nutrient solution.

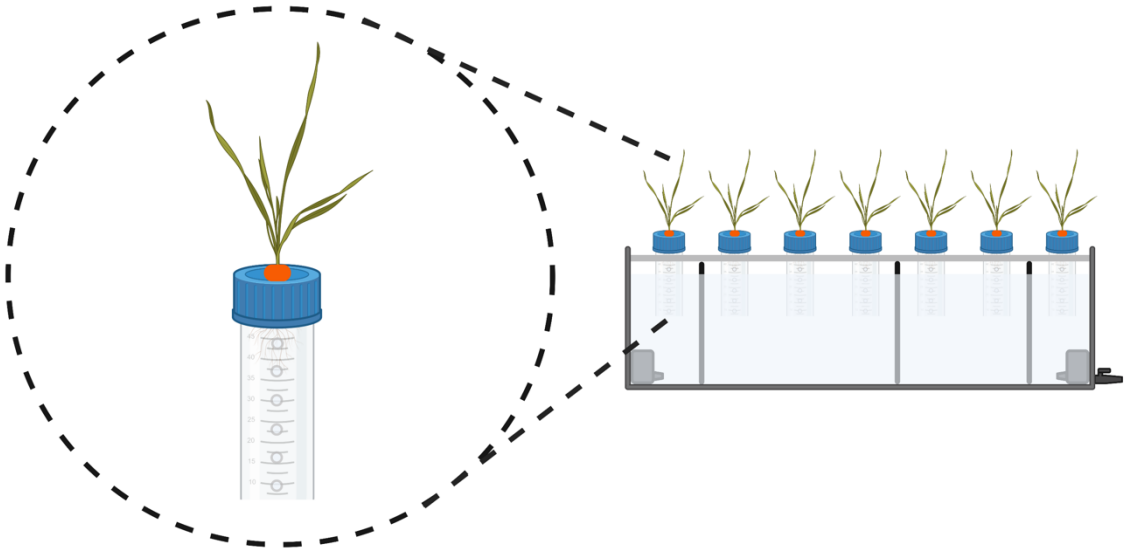

**Figure 5.2:** Schematic of deep-water culture hydroponics system designed for crop growth. Figure created in BioRender.

### 5.2.4 Nutrient solution

A modified Yoshida nutrient solution was used for all experiments, with a 1X concentration of N and 0.25X concentration of all other nutrients made up as described by Yoshida et al. (1976). Briefly, stock solutions of each of the 5 macronutrients were prepared as described in Table 5.2 by diluting with $dH_2O$ to a final volume of 1 l, and a single micronutrient stock solution prepared by dilution of the 7 micronutrients individually into 50 ml $dH_2O$ followed by combining and addition of 50 ml concentrated $H_2SO_4$ before making up to a final volume of 1 l with $dH_2O$. Separate $NH_4NO_3$ stock solutions were prepared for $^{15}N$-labelled solutions in the same way as for unlabelled $NH_4NO_3$, with 5 % of the $NH_4NO_3$ replaced with $^{15}NH_4NO_3$ or $NH_4{}^{15}NO_3$. Nutrient solution was prepared in a 150 l water butt (The Range) and contained the final macronutrient concentrations outlined in Table 5.3. Labelled solution was prepared using the $^{15}N$-enriched $NH_4NO_3$ stock solutions. Solution pH was adjusted to 5.5 when made and then daily using 4 M HCl and 4 M NaOH. Solution pH was measured with a Hanna Instruments portable pH meter. A volume of 30 l solution was made for each tank, and solution was replaced every 2 days to maintain equimolar $NH_4^+$ and $NO_3^-$ concentrations.

**Table 5.2:** Preparation of Yoshida nutrient stock solutions, adapted from Table 1. (Yoshida, 1976).

| Element | Reagent | Preparation (g/l $dH_2O$) |
|---|---|---|
| **Macronutrients** | | |
| N | $NH_4NO_3$ (with 5% $^{15}NH_4NO_3$ or $NH_4{}^{15}NO_3$ if enriched) | 91.4 |
| P | $NaH_2PO_4 \cdot 2H_2O$ | 40.3 |
| K | $K_2SO_4$ | 71.4 |
| Ca | $CaCl_2 \cdot 2H_2O$ | 117.4 |
| Mg | $MgSO_4$ | 158.3 |
| **Micronutrients** | | |
| Mn | $MnCl_2 \cdot 4H_2O$ | 1.5 |
| Mo | $(NH_4)_6 \cdot Mo_7O_{24} \cdot 4H_2O$ | 0.74 |
| B | $H_3BO_3$ | 0.93 |
| Zn | $ZnSO_4 \cdot 7H_2O$ | 0.035 |
| Cu | $CuSO_4 \cdot 5H_2O$ | 0.031 |
| Fe | $FeCl_3 \cdot 6H_2O$ | 7.7 |
| **NA** | Citric acid (monohydrate) | 11.9 |

**Table 5.3:** Composition of Yoshida nutrient solution.

| Element | Reagent | Final concentration of reagent (mM for macro, µM for micro) | Final concentration of element (ppm) |
|---|---|---|---|
| **Macronutrients** | | | |
| N | $NH_4NO_3$ | 1.43 | 40 |
| P | $NaH_2PO_4 \cdot 2H_2O$ | 0.08 | 10 |
| K | $K_2SO_4$ | 0.13 | 10 |
| Ca | $CaCl_2 \cdot 2H_2O$ | 0.25 | 10 |
| Mg | $MgSO_4$ | 0.41 | 10 |
| **Micronutrients** | | | |
| Mn | $MnCl_2 \cdot 4H_2O$ | 2.40 | 0.125 |
| Mo | $(NH_4)_6 \cdot Mo_7O_{24} \cdot 4H_2O$ | 0.02 | 0.0125 |
| B | $H_3BO_3$ | 4.72 | 0.05 |
| Zn | $ZnSO_4 \cdot 7H_2O$ | 0.04 | 0.0025 |
| Cu | $CuSO_4 \cdot 5H_2O$ | 0.06 | 0.0025 |
| Fe | $FeCl_3 \cdot 6H_2O$ | 10.45 | 0.5 |
| NA | Citric acid (monohydrate) | 17.68 | NA |

### 5.2.5 Plant growth and experimental conditions

In Experiment 1, plants were grown in a controlled greenhouse cubicle at the Arthur Willis Environment Centre, Sheffield, UK, set to the same conditions described in section **2.2.8**. In Experiments 2 and 3, plants were grown in Conviron controlled environment cabinets with the same temperature and day/night cycles as for Experiment 1 and a relative humidity of 60 %. A single cabinet was used for Experiment 2, with plants grown at a $CO_2$ concentration of 410 ppm and light levels of 300 μmol $m^{-2}$ $s^{-1}$ until the addition of labelled nutrient solution, where light intensity was increased to 600 μmol $m^{-2}$ $s^{-1}$ (512 μmol $m^{-2}$ $s^{-1}$ at canopy height) and half of the cabinet was shaded back to 300 μmol $m^{-2}$ $s^{-1}$ (187 μmol $m^{-2}$ $s^{-1}$ at canopy height) with a DIY shading tent (Figure 5.3) for a single photoperiod during the labelling period. Canopy level light intensity with and without shading was measured using a LI-COR LI-250A light meter (LI-COR Biosciences, Lincoln, NE, USA). In Experiment 3 a pair of Conviron cabinets were used, set to a light intensity of 300 μmol $m^{-2}$ $s^{-1}$ in both cabinets, and with one cabinet set to a $CO_2$ concentration of 410 ppm (ambient $CO_2$) and the other to 720 ppm (elevated $CO_2$).

**Figure 5.3:** Shading tent designed to implement high and ambient light intensity in Experiment 2.

Plants were grown for 17 days in Experiment 1 but this was reduced to 15 days for Experiments 2 and 3, with nutrient solution replaced every 2 days and $^{15}N$-enriched solution added for 24 h during the final nutrient solution replacement. A 5 % enriched $^{15}NH_4NO_3$ nutrient solution was added to half of the tanks and a 5 % enriched $NH_4{}^{15}NO_3$ solution to the other half. Plants of all cultivars studied were subjected to both enriched N forms. Roots of control plants were contained within unmodified 50 ml centrifuge tubes containing 50 ml unlabelled nutrient solution during the labelling period and placed back in the same position within hydroponics tanks. Roots did not come into contact with labelled nutrient solution. A summary of the screening method developed for determining N preference is displayed in Figure 5.4.

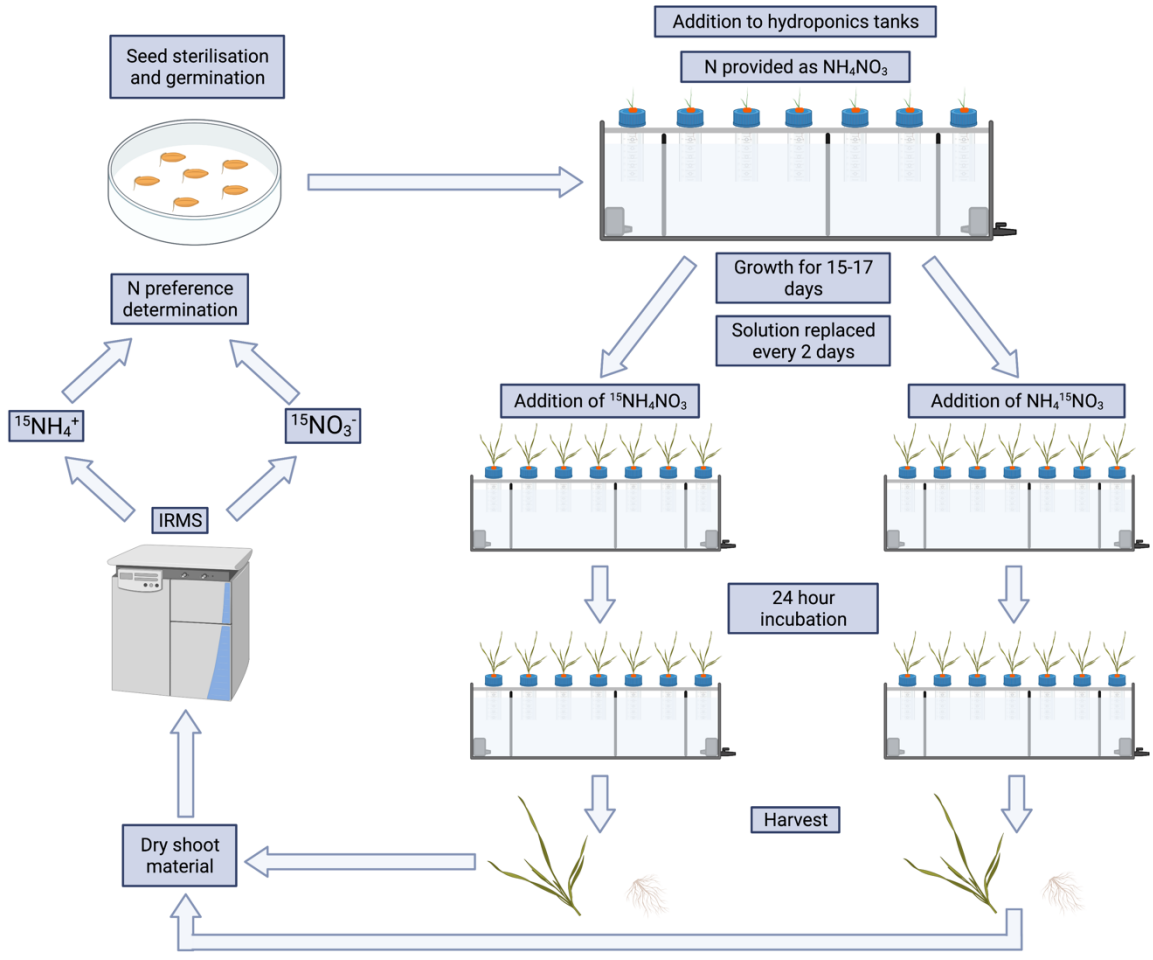


**Figure 5.4:** Overall workflow for N preference determination using deep water culture hydroponics and $^{15}N$ isotopic labelling. Figure created in BioRender.

### 5.2.6 Quantum yield measurement

Quantum yield (Φ) was measured in Experiment 2 only, using a portable Fluorpen FP 100. When taking measurements, the Fluorpen was clipped on to the youngest fully expanded leaf. Measurements were taken for each individual plant before imposing high light treatment and 24 h after imposing high light treatment.

### 5.2.7 Nutrient solution analysis

A total of 3 nutrient solution samples were taken from each hydroponics tank for each day during experiments, taken from opposite ends of the tank and the centre. On days where nutrient solution was replaced, samples were taken immediately before nutrient solution was replaced.

#### 5.2.7.1 Solution $NH_4^+$ and $NO_3^-$ concentration analysis

Solution $NH_4^+$ and $NO_3^-$ concentration was determined through the colourimetric methods described in **3.2.7.1** and **3.2.7.2** respectively, with $dH_2O$ used as the matrix when preparing serially diluted standards. Solution samples were diluted 10-fold in microtitre plates to ensure absorbance fell within the standard curve by adding 4 µl sample and 36 µl $dH_2O$ to each well. Sample $NH_4^+$ and $NO_3^-$ concentration was expressed in mM.

### 5.2.8 Harvest and plant biomass determination

Plants were harvested after being exposed to labelled nutrient solution for 24 h. Roots were blotted dry and plant shoots and roots separated and placed in envelopes. Shoot and root material was oven dried at 70°C for 72 h before weighing to determine dry shoot and root weight.

### 5.2.9 Sample preparation and IRMS analysis

The youngest fully expanded leaf from each plant was ground into a powder using a QIAGEN TissueLyser II and 2-4 mg powder weighed into 6x4 mm tin capsules (Sercon). Samples were analysed via IRMS using an elemental analyser connected to an ANCA GSL 20-20 Mass Spectrometer (Sercon PDZ Europa, Cheshire) to determine $^{15}N$ atom%.

### 5.2.10 Calculation of N preference

N preference was calculated for each cultivar under each environmental condition (Experiments 2 and 3) using the mean $^{15}N$ atom % values for $^{15}NH_4NO_3$ labelled plants and $NH_4{}^{15}NO_3$ labelled plants obtained via IRMS, using ***Equation 5.1***.

$$N\ preference = Mean\ ^{15}NO_3\ atom\ \% - Mean\ ^{15}NH_4\ atom\ \% \qquad \textbf{Equation 5.1}$$

The standard error of the mean (SEM) for each of the means used in ***Equation 5.1*** was propagated through the calculation to obtain a single 'propagated SEM' value for each N preference value using ***Equation 5.2***, where δQ = propagated SEM, δa = SEM for mean $^{15}NO_3$ atom %, and δb = SEM for mean $^{15}NH_4$ atom %. All N preference values are reported with propagated SEM.

$$\delta Q = \sqrt{(\delta a)^2 + (\delta b)^2} \qquad \textbf{Equation 5.2}$$

### 5.2.11 Data visualisation and statistical analysis

All graphs in this chapter were produced using GraphPad Prism version 9.4.1. All ANOVA analysis was performed using the Anova() function in R statistical software (v3.5.1; R Core Team 2018) with RStudio to perform Type II ANOVA tests. Prior to performing ANOVA, datasets were checked to ensure they met the assumptions of ANOVA through plotting of diagnostics using the autoplot function of the ggplot2 package. Datasets met the assumptions of homogeneity of variance and that data is drawn from a normal distribution except for biomass data from Experiments 1 and 2, which deviated slightly from a normal distribution. Transformation of this data did not improve the normal distribution, but ANOVA was considered robust against these deviations and so analysis was performed on natural, untransformed data. Tukey post-hoc tests were carried out using the HSD.test() function of the agricolae package in R, with different letters assigned to groups that significantly differed at the $p<0.05$ level.

To test for statistical significance of N preference values from 0, manual one-sample two-tailed *t*-tests were carried out and the calculated statistic looked up in a *t* table to identify significance

level. A significantly positive value indicated nitrate preference, a significantly negative value indicated ammonium preference, and a value not significantly different from 0 indicated no preference. For Experiments 2 and 3, independent samples *t*-tests were carried out to test for statistical significance between N preference values for the two environmental conditions within each cultivar.

## 5.3 Results

### 5.3.1 Experiment 1

#### 5.3.1.1 Solution $NH_4^+$ and $NO_3^-$ concentration

Solution ammonium concentration was consistently lower than nitrate concentration before solution replacement across all 4 tanks for the duration of the experiment except days 1-3 (Figure 5.5). Solution was replaced every other day on even-numbered days. Day 0 represents initial ammonium and nitrate concentration when first added to tanks. Nitrate concentration did not vary much from the expected 1.43 mM concentration, but from day 4 onwards ammonium concentration began to decrease from the expected 1.43 mM, with the difference between ammonium and nitrate concentration increasing over time (Figure 5.5).

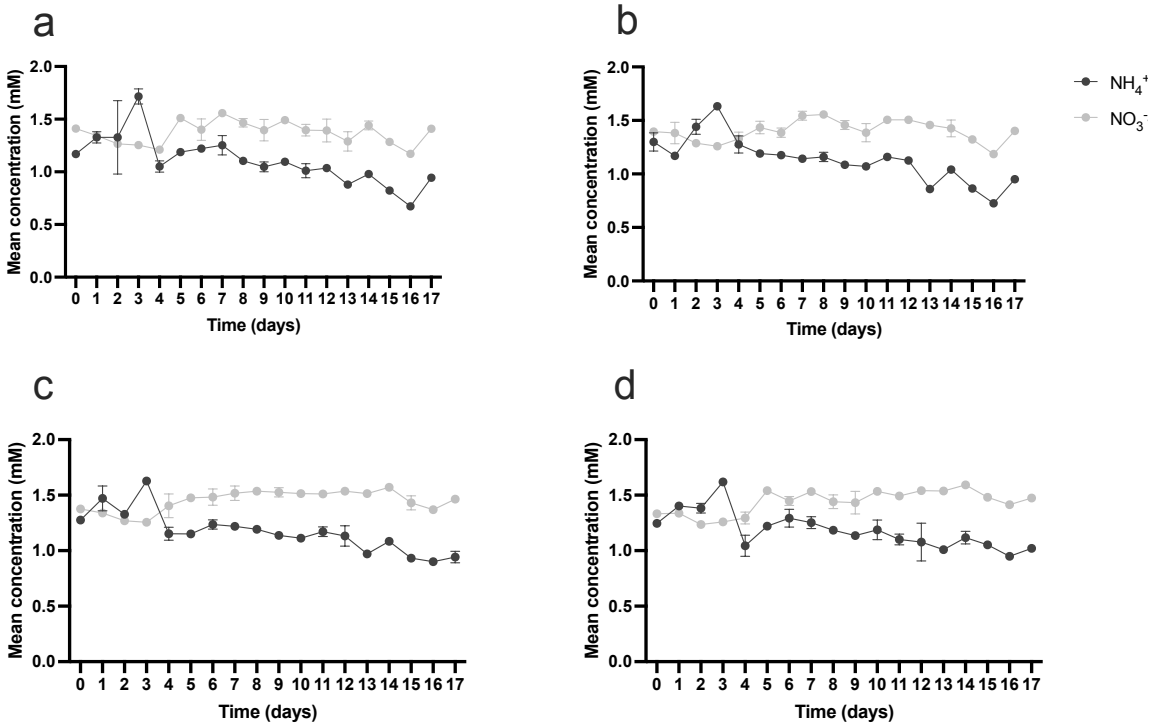


**Figure 5.5:** Solution $NH_4^+$ and $NO_3^-$ concentration for tanks 1-4 (**a-d** respectively) plotted against time for the duration of the experiment. Solution was replaced on even-numbered days. Mean±SEM is plotted, n=3.

#### 5.3.1.2 Plant biomass

Two-way ANOVA analysis revealed significant differences in shoot dry weight across cultivars ($F=3.4281$, $p<0.001$) and $^{15}N$ labelling treatments ($F=6.7133$, $p<0.01$), but no significant interaction between the two ($F=1.2150$, $p=0.2652$). Only data illustrating the main effects of these two factors is therefore displayed in Figure 5.6a and 5.6b for the cultivar and labelling treatment main effects respectively. Tukey post-hoc tests showed that most cultivars did not differ significantly, with Shuffle showing significantly higher shoot dry weight than NFC Tipple and the *HvEPF1oe* transgenic line, and *HvEPF1oe* showing significantly reduced shoot dry weight compared to several cultivars (Figure 5.6a). Tukey tests revealed a significant increase in shoot dry weight in plants that received the $^{15}NH_4^+$ labelling treatment compared to those that received the $^{15}NO_3^-$ treatment (Figure 5.6b). Plants that received the control treatment did not differ significantly compared to either $^{15}N$ labelling treatment.

Similar trends were observed for root dry weight, with a significant difference in root dry weight observed across genotypes ($F=2.3994$, $p<0.05$, two-way ANOVA) and labelling treatment ($F=4.6863$, $p<0.05$, two-way ANOVA). Again, no significant interaction was observed ($F=0.9425$, $p=0.5490$, two-way ANOVA) so only main effects are displayed for cultivar and labelling treatment in Figure 5.6c and 5.6d respectively. Tukey tests revealed reduced root dry weight in the *HvEPF1oe* line compared to Concerto and Shuffle (Figure 5.6c), and that plants that received the $^{15}NH_4^+$ labelling treatment showed a significantly higher root dry weight than those that received either the control or $^{15}NO_3^-$ treatment (Figure 5.6d).

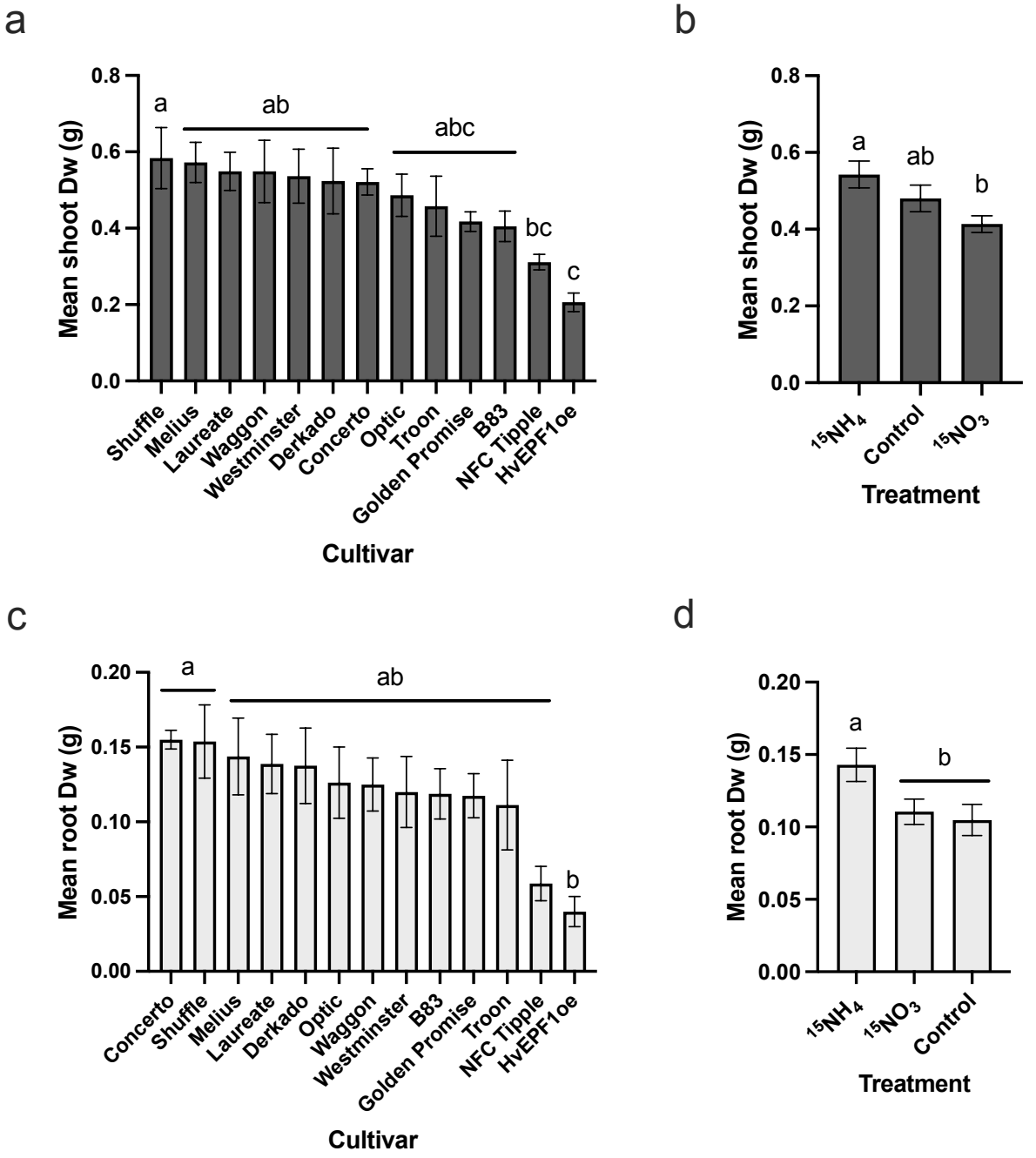


**Figure 5.6:** Plant shoot and root dry weight (Dw) after 17 days of growth in deep water culture hydroponics. Mean±SEM is displayed, significantly different groups are denoted with a different letter. For cultivar plots (**a.** and **c.** for shoot and root dry weight respectively), n=8 for all cultivars except *HvEPF1oe* (n=7). For labelling treatment plots (**b.** and **d.** for shoot and root dry weight respectively), n=77 for $^{15}NH_4^+$ and $^{15}NO_3^-$ treatments and n=25 for control treatment.

### 5.3.1.3 N preference

Statistical analysis using one-sample two-tailed *t*-tests revealed that most cultivars showed no significant preference for either ammonium or nitrate, with an N preference value not significantly different to 0 (red-coloured values, Figure 5.7). There were, however, both ammonium-preferring and nitrate-preferring cultivars identified; Waggon and Shuffle showed a significant positive N preference value indicating nitrate preference ($p<0.05$ and $p<0.01$ respectively), and the transgenic *HvEPF1oe* line showed significant preference at the $p<0.10$ level (green-coloured values, Figure 5.7). Laureate showed a significant negative N preference value indicating ammonium preference ($p<0.05$).

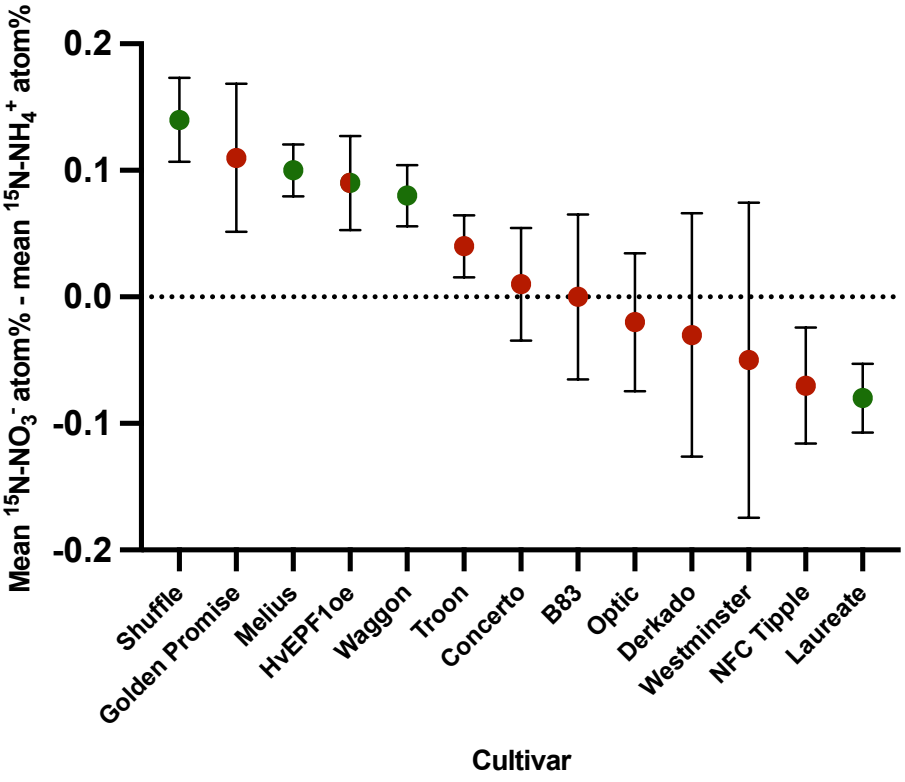


**Figure 5.7:** Variation in N preference in hydroponically grown spring barley under greenhouse conditions. Mean ± propagated SEM is displayed, n=6 for all cultivars except *HvEPF1oe*, where n=5. Points coloured in green are statistically significantly different from 0, points coloured in red are not ($p<0.05$, one-sample two-tailed *t*-test). Points coloured red and green are significantly different from 0 at the $p<0.10$ level.

### 5.3.2 Experiment 2

#### 5.3.2.1 Light intensity during high light treatment

A significant difference in light intensity was achieved between shaded and unshaded tanks using the shading tent ($F=476.91$, $p<0.0001$, one-way ANOVA). A Tukey post-hoc test revealed significantly higher light intensity in tanks 1 and 2 (high light) compared to tanks 3 and 4 (ambient light) as expected (Figure 5.8), with an average light intensity of 512±2 μmoles $m^{-2}$ $s^{-1}$ for hight light and 187±2 μmoles $m^{-2}$ $s^{-1}$ for ambient light. No significant differences were observed between tanks under the same light treatment.

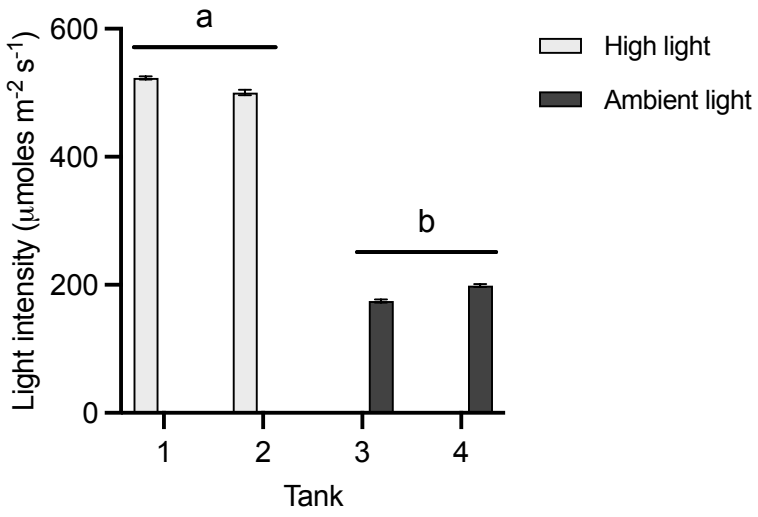


**Figure 5.8:** Light intensity at canopy height during high light treatment. Mean±SEM is plotted, n=33. Significantly different groups are denoted with different letters.

#### 5.3.2.2 Quantum yield

Quantum yield differed significantly between cultivar ($F=2.2142$, $p<0.05$, two-way ANOVA) and light treatment ($F=43.9515$, $p<0.001$, two-way ANOVA) but there was no significant interaction ($F=0.7343$, $p=0.6430$, two-way ANOVA) so only main effects are displayed in Figure 5.9. Tukey tests did not show a significant difference in grouping by cultivar (Figure 5.9a) but quantum yield was significantly reduced in plants exposed to high light treatment compared to those that remained at ambient light (Figure 5.9b).

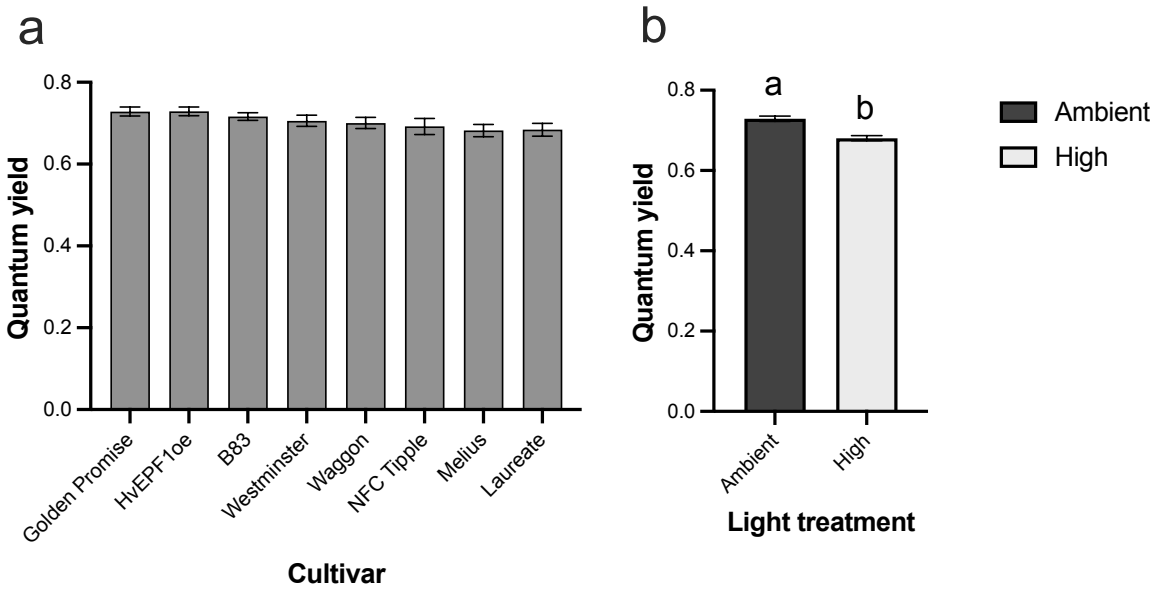


**Figure 5.9:** Quantum yield measurements of plants exposed to high light and those kept at ambient light intensity. **a.** Quantum yield cultivar main effect. Mean±SEM is plotted for each cultivar using data from both light conditions, n=16 for B83 and Westminster, n=15 for Golden Promise, Melius, NFC Tipple and Waggon, n=12 for Laureate and n=9 for *HvEPF1oe*. **b.** Quantum yield light treatment main effect. Mean±SEM is plotted for each light treatment using data from all cultivars, n=55 for ambient light and n=58 for high light. Significantly different groups are denoted with different letters.

### 5.3.2.3 Solution $NH_4^+$ and $NO_3^-$ concentration

Solution ammonium and nitrate concentration remained consistently similar throughout the experiment (Figure 5.10) with the exception of days 1-3 which saw increased nitrate concentration, particularly for tanks 1 and 2 (Figure 5.10a and 5.10b respectively). Both ammonium and nitrate remained close to the expected concentration of 1.43 mM for the duration of the experiment, even at times immediately before solution replacement (even-numbered days). Both ammonium and nitrate concentration remained similar at day 15 across all 4 tanks, suggesting concentration was not affected by imposing different light treatments.

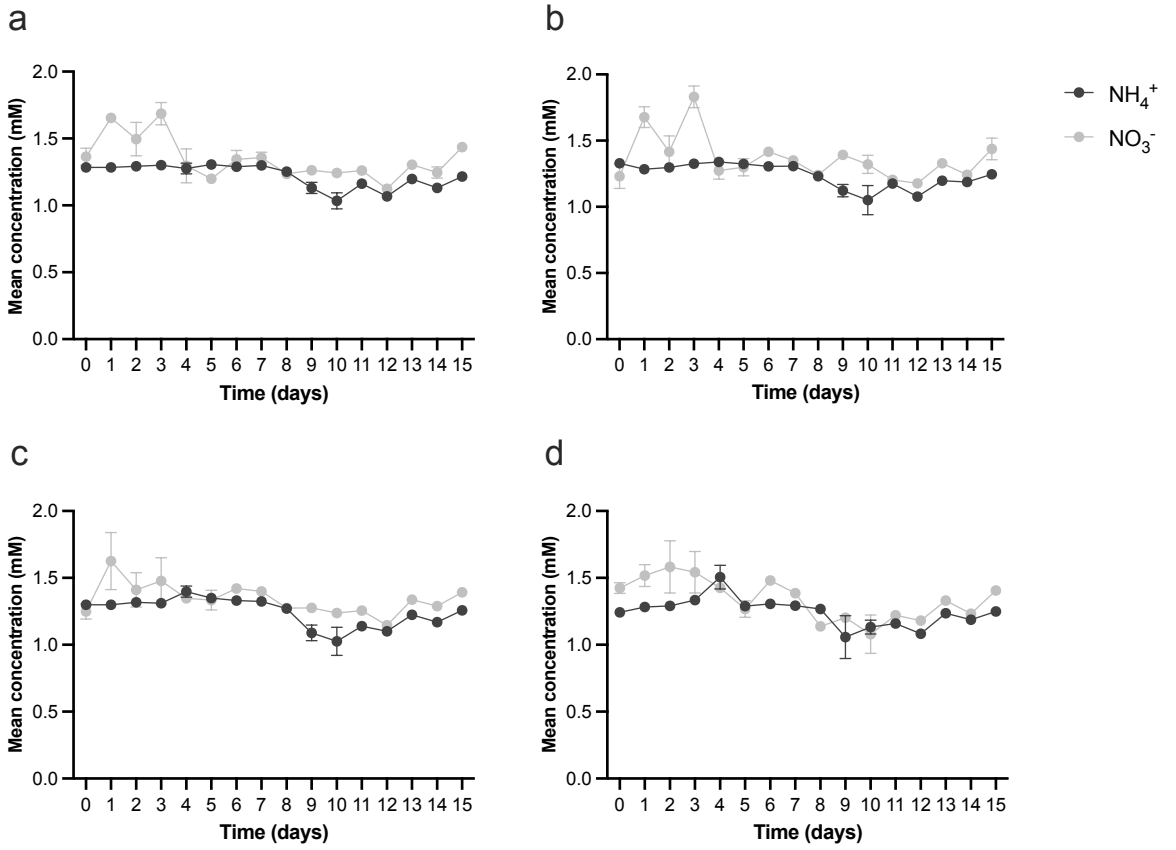


**Figure 5.10:** Solution $NH_4^+$ and $NO_3^-$ concentration for tanks 1 and 2 at high light 1-4 (**a** and **b** respectively) and tanks 3 and 4 at ambient light (**c** and **d** respectively) plotted against time. Solution was replaced on even-numbered days. Mean±SEM is plotted, n=3.

#### 5.3.2.4 Plant biomass

Three-way ANOVA analysis showed significant differences in shoot dry weight across cultivars ($F=7.8307$, $p<0.001$) and light treatments ($F=7.1653$, $p<0.01$), but no significant interaction between the two ($F=1.1440$, $p=0.3460$). Labelling treatment did not have a significant effect on shoot dry wright ($F=0.2852$, $p=0.7530$). Only data illustrating the main effects of cultivar and light treatment are therefore displayed in Figures 5.11a and 5.11b respectively. Tukey post-hoc tests showed that NFC Tipple showed significantly higher shoot dry weight compared to all other cultivars except Westminster and B83 (Figure 5.11a). Westminster showed significantly increased shoot dry weight compared to several cultivars, and both Melius and *HvEPF1oe* showed significantly reduced shoot dry weight compared to NFC Tipple, Westminster and B83. Tukey tests revealed a significant increase in shoot dry weight in plants exposed to high light treatment compared to those that remained at ambient light (Figure 5.11b). Root dry weight did not differ significantly across cultivars ($F=1.5239$, $p=0.1738$), light treatment ($F=1.2490$, $p=0.2676$) or labelling treatment ($F=0.5592$, $p=0.5743$). Root dry weight for each cultivar is shown in Figure 5.11c for completeness.

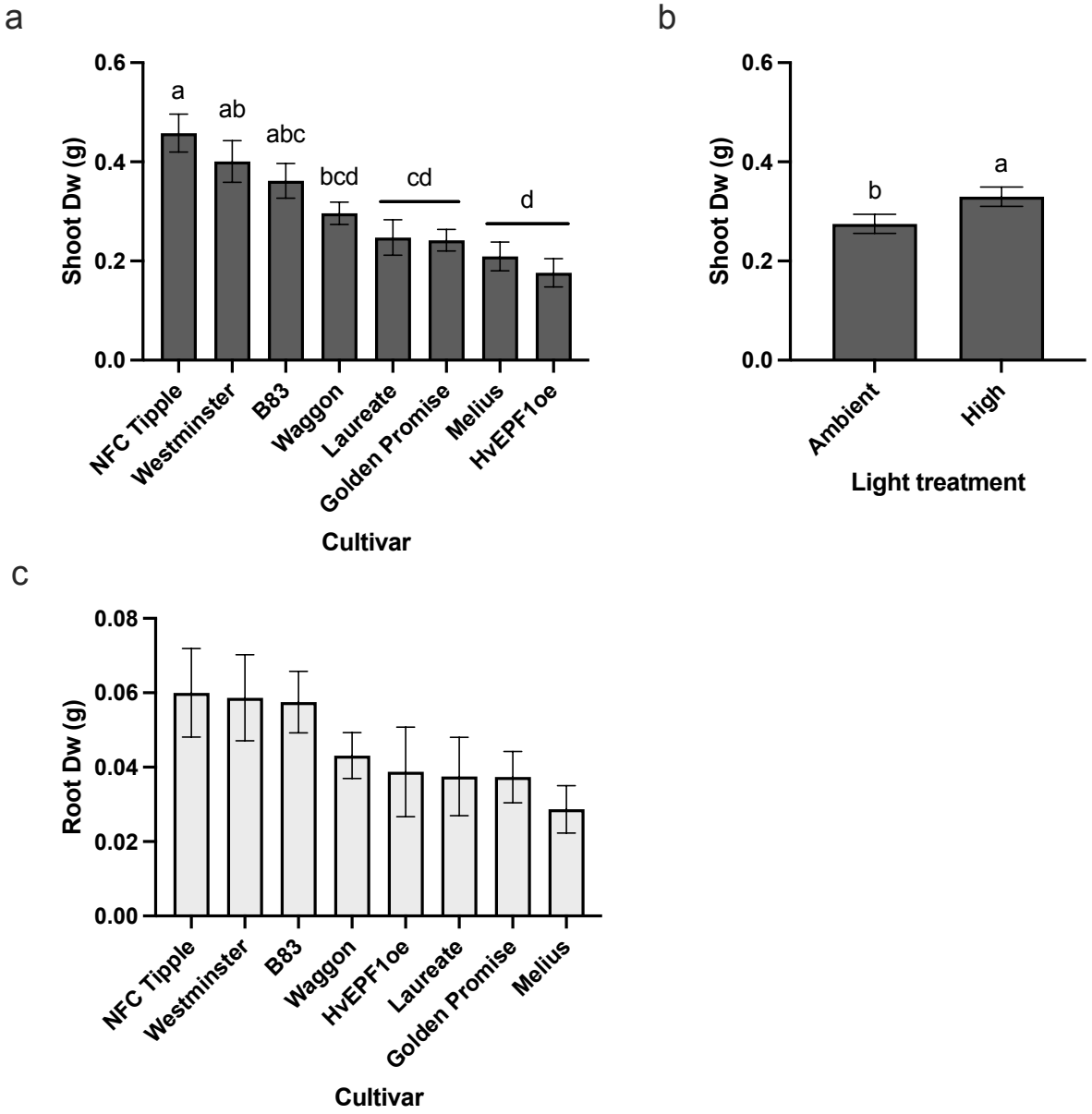


**Figure 5.11:** Plant shoot and root dry weight (Dw) after 15 days of growth in deep water culture hydroponics. Mean±SEM is displayed, significantly different groups are denoted with a different letter. For cultivar plots (**a.** and **c.** for shoot and root dry weight respectively), n=16 for B83 and Westminster, n=15 for Golden Promise, Melius, NFC Tipple and Waggon, n=12 for Laureate and n=9 for *HvEPF1oe*. For shoot dry weight plotted against light treatment (**b.**), n=55 for ambient light and n=58 for high light.

#### 5.3.2.5 N preference under varying light treatments

The majority of cultivars showed either no significant preference or ammonium preference at both ambient and high light conditions (Figure 5.12). One-sample two-tailed *t*-tests showed that Melius, NFC Tipple and Waggon all displayed significant ammonium preference under ambient light intensity (indicated with green circles, Figure 5.12) at the $p<0.05$ significance level. B83, Golden Promise and Laureate showed significant ammonium preference at the $p<0.10$ level (red and green circles, Figure 5.12). Westminster showed no significant preference even at the $p<0.10$ level (indicated with a red circle, Figure 5.12), but the transgenic *HvEPF1oe* line showed significant nitrate preference at the $p<0.10$ level (red and green circle, Figure 5.12). Only Golden Promise, Laureate and Melius showed significant ammonium preference at hight light at the $p<0.05$ level (indicated with green squares, Figure 5.12), but *HvEPF1oe*, Waggon and Westminster showed ammonium preference at the $p<0.10$ level (red and green squares, Figure 5.12). Both B83 and NFC Tipple did not show significant preference at high light (red squares, Figure 5.12).

Independent-samples *t*-tests revealed a significant shift towards increased ammonium preference only for *HvEPF1oe* ($p<0.05$) and Laureate ($p<0.01$) (Figure 5.12), but the same trend was observed for Waggon and Westminster, though this was not significant. Both NFC Tipple and B83 showed a slight decrease in ammonium preference at high light, with NFC Tipple significantly preferring ammonium under ambient light but showing no significant preference at high light. B83 was showed no significant preference at either light treatment at the $p<0.05$ level but showed significant ammonium preference under ambient light at the $p<0.10$ level. Melius remained ammonium-preferring at both light treatments.

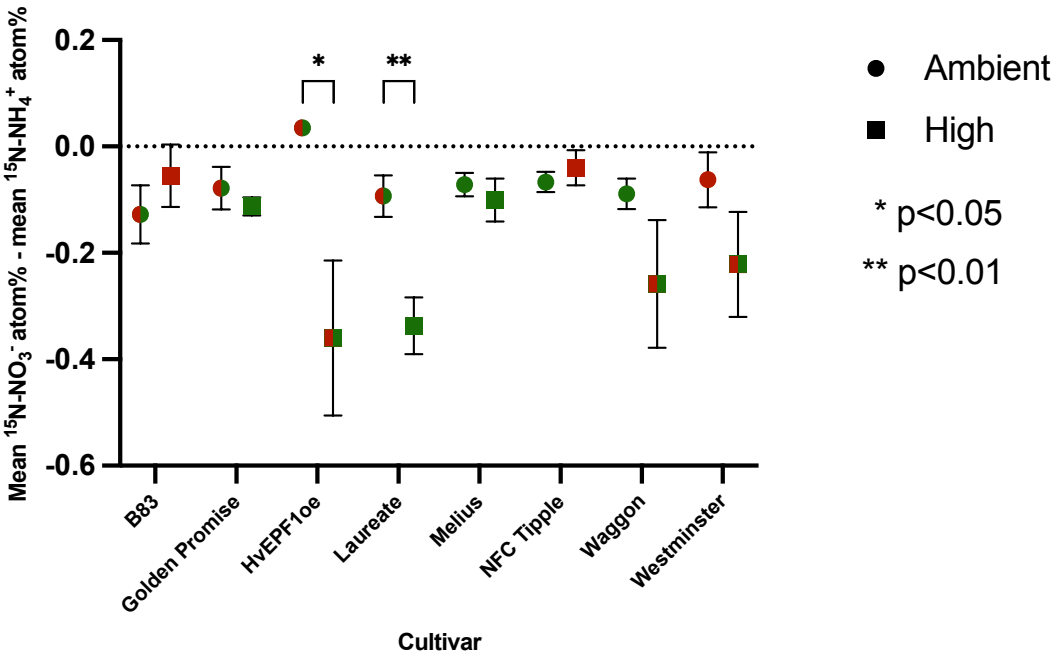


**Figure 5.12:** Variation in N preference in hydroponically grown spring barley under ambient and short-term high light treatment. Mean ± propagated SEM is displayed, n=8 for B83 and Waggon (high light), n=7 for Golden Promise, Melius, Waggon (high light) and Westminster, n=6 for Laureate (high light) and NFC Tipple, n=5 for Laureate (ambient light), and n=4 for *HvEPF1oe*. Circles indicate ambient light and squares high light treatment. Points coloured in green are statistically significantly different from 0, those in red are not ($p<0.05$, one-sample two-tailed *t*-test). Points coloured red and green are significantly different from 0 at the $p<0.10$ level. Differences in preference between light treatments within a cultivar are indicated with brackets and asterisks (independent-samples *t*-test).

### 5.3.3 Experiment 3

#### 5.3.3.1 Solution $NH_4^+$ and $NO_3^-$ concentration

Solution ammonium and nitrate concentration remained consistently similar across all tanks for the first 11-12 days (Figure 5.13) and close to the expected 1.43 mM, except tanks 2 and 4 (Figure 5.13b and 5.13b respectively) which showed lower nitrate concentration for the first 2-4 days. Solution nitrate concentration remained close to 1.43 mM until day 15, but concentration started to drop below this concentration at day 13 for tanks 1-4 (Figure 5.13a-d). This drop in ammonium concentration appeared to occur a day earlier at day 12 for tanks 5-8 (which were at $eCO_2$).

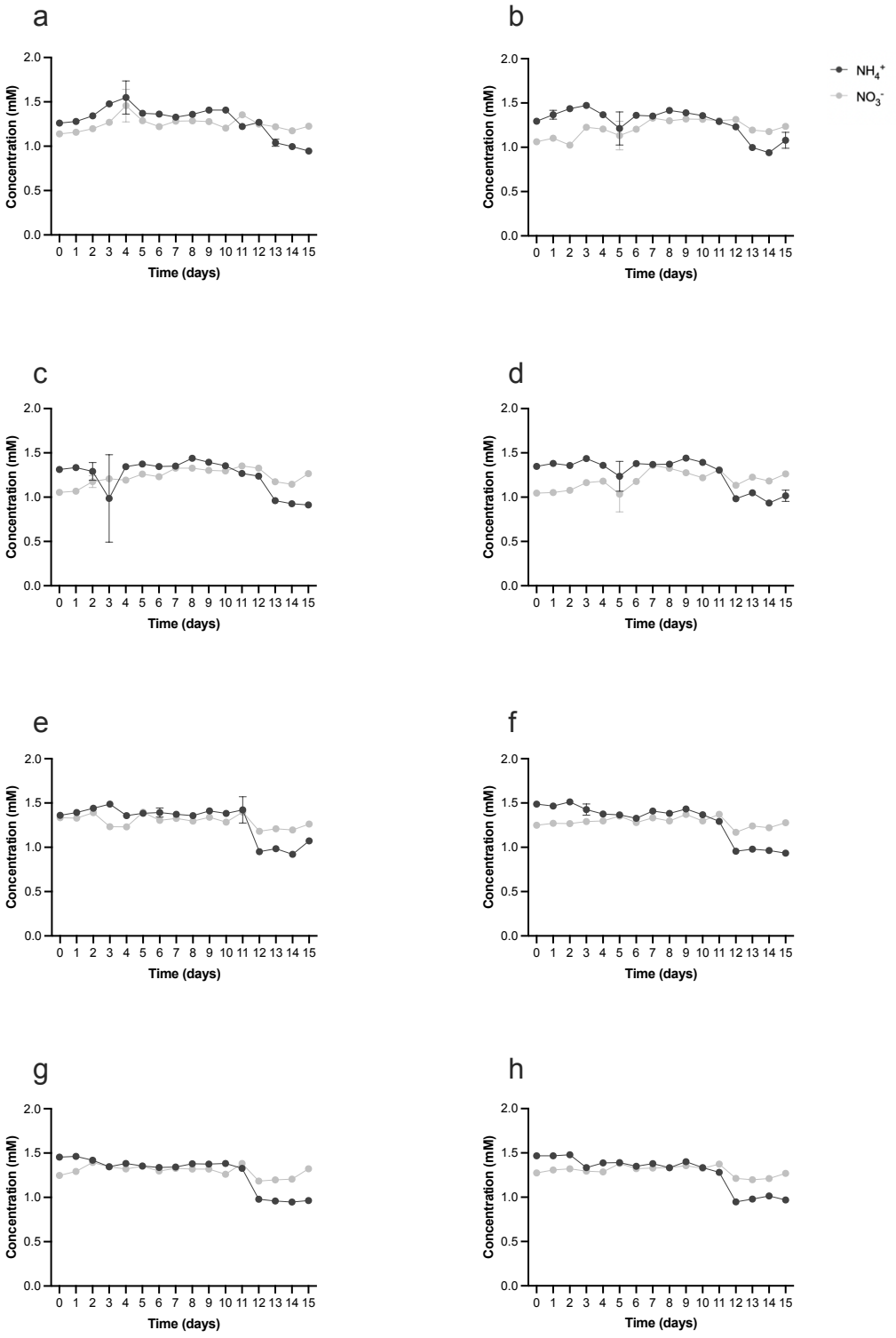


**Figure 5.13:** Solution $NH_4^+$ and $NO_3^-$ concentration for tanks 1-4 at ambient $CO_2$ (**a-d** respectively) and tanks 5-8 at elevated $CO_2$ (**e-f** respectively) plotted against time. Solution was replaced on even-numbered days. Mean±SEM is plotted, n=3.

#### 5.3.3.2 Plant biomass

Two-way ANOVA analysis revealed a significant interaction effect between cultivar and $CO_2$ treatment ($F=2.1778$, $p<0.05$) on shoot dry weight, shown in Figure 5.14a. With the exception of Golden Promise, Diamant and Steffi, shoot dry weight was increased in plants grown at $eCO_2$ compared to those grown at $aCO_2$. A significant interaction effect on shoot dry weight between cultivar and labelling treatment was also detected ($F=1.5951$, $p<0.05$), shown in Figure 5.14b. However, shoot dry weight did not appear to vary very much across labelling treatments for most cultivars except Shuffle which showed increased shoot dry weight in the $^{15}NO_3^-$ treatment, Steffi which showed increased shoot dry weight in the control treatment, and *HvEPF1oe* which showed increased shoot dry weight in the $^{15}NH_4^+$ treatment.

Root Dw varied significantly across cultivars ($F=13.0947$, $p<0.001$) and labelling treatment ($F=4.4560$, $p<0.05$), but there was no significant interaction between the two ($F=0.9889$, $p=0.4850$). Root dry weight did not vary significantly between the two $CO_2$ treatments ($F=2.2432$, $p=0.1360$). Main effects for cultivar and labelling treatment are shown in Figure 5.14c and 5.14d respectively. Root dry weight was highest in LG Diablo and lowest in Annabell, with all other cultivars falling somewhere in between (Figure 5.14c). Root dry weight was significantly higher in plants exposed to the $^{15}NH_4^+$ labelling treatment compared to the control treatment but did not differ significantly to plants exposed to the $^{15}NO_3^-$ labelling treatment (Figure 5.14d).

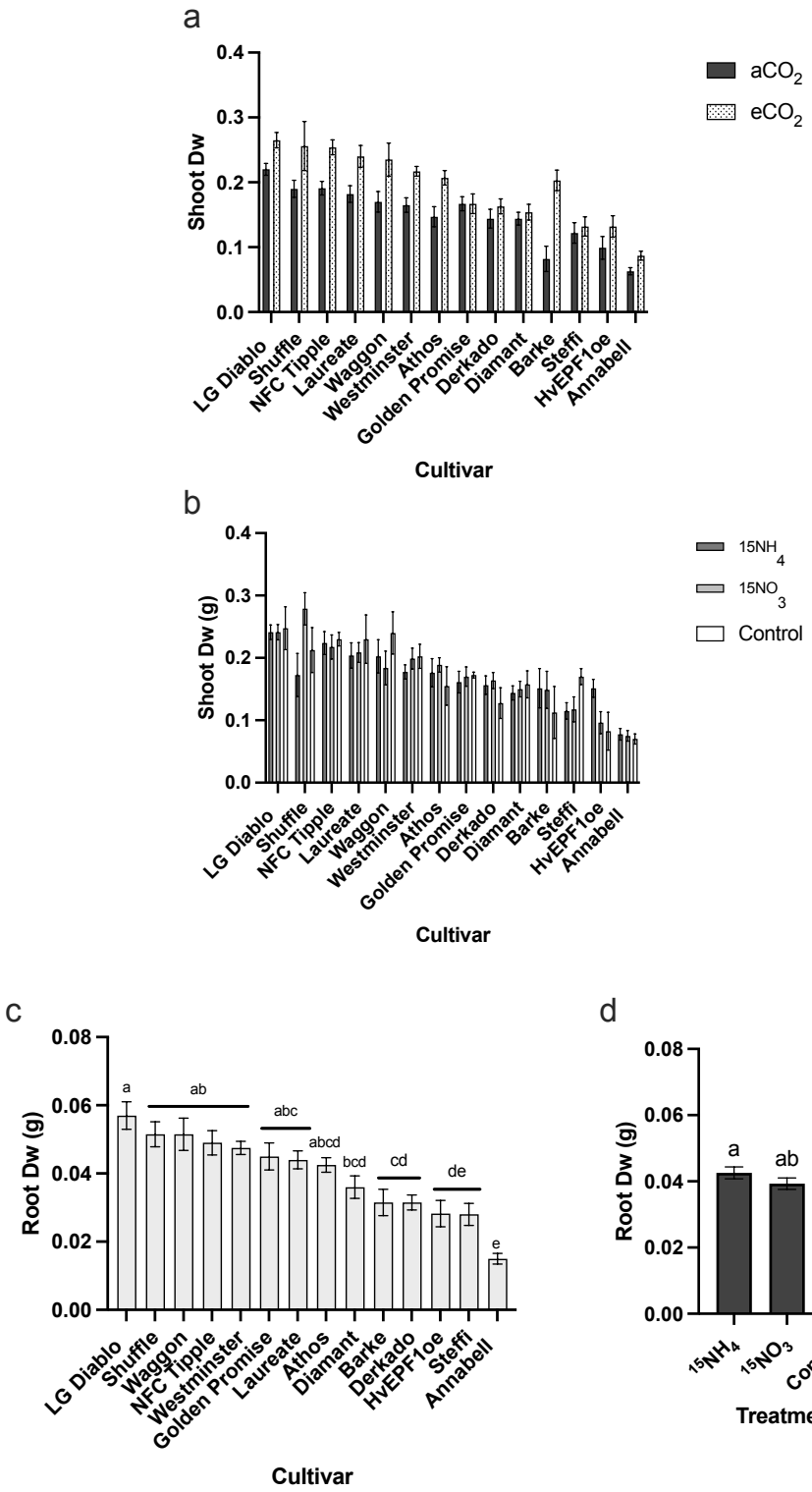


**Figure 5.14:** Plant shoot and root dry weight (Dw) after 15 days of growth in deep water culture hydroponics. Mean±SEM is displayed, significantly different groups are denoted with a different letter. **a.** Shoot dry weight plotted for each cultivar at ambient $CO_2$ (solid bars) and elevated $CO_2$ (dotted bars), n=10. **b.** Shoot dry weight plotted for each cultivar in each labelling treatment, n=8 for $^{15}NH_4^+$ (dark grey bars) and $^{15}NO_3^-$ (light grey bars), n=4 for control (white bars) treatment. **c.** Root dry weight plotted for each cultivar (all plants), n=20. **D.** Root dry weight plotted for each labelling treatment, n=8 for $^{15}NH_4^+$ and $^{15}NO_3^-$, n=4 for control treatment.

#### 5.3.3.3 N preference under varying $CO_2$ treatments

Similar to previous experiments, all cultivars either displayed no significant preference or $NH_4^+$ preference irrespective of $CO_2$ treatment (Figure 5.15). One-sample two-tailed *t*-tests showed that Athos, Diamant, *HvEPF1oe*, Golden Promise, LG Diablo, Steffi, NFC Tipple and Waggon significantly preferred ammonium under ambient $CO_2$ at the $p<0.05$ significance level (green open circles, Figure 5.15), and Annabell, Barke, Derkado, Laureate, Shuffle and Westminster showed no significant preference under ambient $CO_2$ at the $p<0.05$ significance level (red open circles, Figure 5.15). Cultivars appeared to show a range of preference responses to elevated $CO_2$, with Annabell and Laureate shifting from no significant preference under ambient $CO_2$ to becoming significantly ammonium-preferring under elevated $CO_2$. An independent samples *t*-test showed that this change was significant at the $p<0.10$ level for Annabell (Figure 5.15). Golden Promise significantly preferred ammonium under both $CO_2$ treatments, but preference shifted significantly in the direction of increased ammonium preference under elevated $CO_2$ ($p<0.01$, independent samples *t*-test). Athos, Steffi and NFC Tipple showed a different response to elevated $CO_2$, with preference shifting from significant ammonium preference at ambient $CO_2$ to no significant preference under elevated $CO_2$. This was significant at the $p<0.10$ level for NFC Tipple. Preference did not appear to change between the two $CO_2$ treatments for Barke, Derkado, Diamant, *HvEPF1oe*, LG Diablo, Shuffle, Waggon or Westminster.

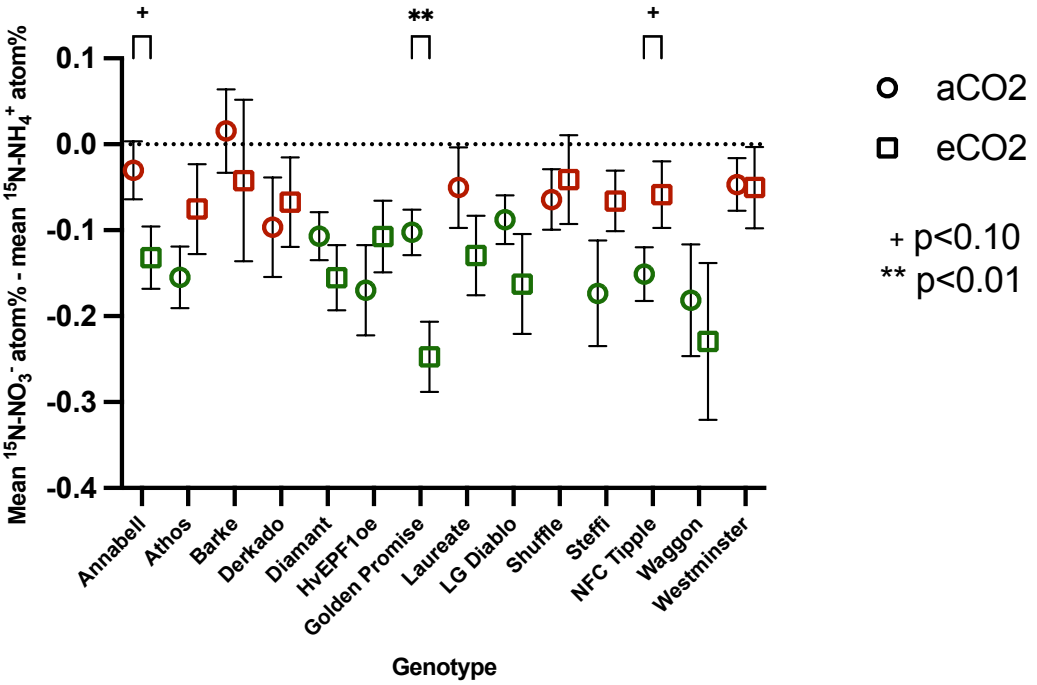


**Figure 5.15:** Variation in N preference in hydroponically grown spring barley under ambient $CO_2$ (circles) and elevated $CO_2$ (squares) treatment. Mean ± propagated SEM is displayed, n=8. Points coloured in green are statistically significantly different from 0, those in red are not ($p<0.05$, one-sample two-tailed *t*-test). Differences in preference between $CO_2$ treatments within a cultivar are indicated with brackets, with significance at the $p<0.01$ level indicated with ** and significance at the $p<0.10$ level indicated with + (independent-samples *t*-test).

## 5.4 Discussion

### 5.4.1 Innate N preference

The first experiment was set up to test whether the hydroponics system designed in this chapter (see section **5.2.3**) and the stable isotope approach described in sections **5.2.5** and **5.2.10** and Figure 5.4 could be used to measure what we have termed 'innate N preference', i.e. plant preference for ammonium or nitrate when environmental constraints are removed and plants are supplied with equal amounts of ammonium and nitrate (Figure 5.1, 5.5). Innate N preference was successfully determined for a total of 14 spring barley cultivars grown in a controlled greenhouse and allowed identification of both ammonium- and nitrate-preferring cultivars in addition to those that did not display significant N preference (Figure 5.7). Plant shoot and root dry weight varied significantly across cultivars as some favoured hydroponic growth more than others, most notably in the transgenic *HvEPF1oe* line, which showed significantly reduced shoot and root dry weight compared to several cultivars. This was not surprising given that *HvEPF1oe* has significantly reduced stomatal density and carbon assimilation (Hughes et al., 2017). Shoot and root dry weight also significantly varied between $^{15}NH_4^+$-labelled and $^{15}NO_3^-$-labelled plants (Figure 5.6b,d). This result is currently unexplained, given that plants were grown with identical supplies of nutrient throughout the experiment, with the only exception being the different N label, supplied only during the final 24 h of the experiment. A similar result was obtained for root dry weight in Experiment 3 (Figure 5.14d).

These results do not support the hypothesis that, in the absence of environmental factors known to drive N preference, plants revert to taking up more ammonium compared to nitrate. This suggests that there are additional cultivar-specific factors that determine the innate N preference, and plants do not simply revert to preferential uptake of ammonium because of the associated energetic cost benefit when presented with both N forms. Given that plants were grown in a controlled greenhouse without the presence of soil (and an associated microbiome) and with

equal ammonium and nitrate supply, these additional factors may be attributed to physiological plant responses that differ across cultivars.

Barley is considered an ammonium-sensitive species (Britto et al., 2001; Lewis et al., 1986), though to my knowledge variation in susceptibility to ammonium toxicity across barley cultivars has not been studied. Variation in ammonium toxicity has been observed across natural accessions of *Arabidopsis thaliana* (Sarasketa et al., 2014), suggesting the existence of intra-species variation in ammonium toxicity. One strategy to alleviate ammonium toxicity is to enhance ammonium assimilation, usually in the roots, requiring additional carbohydrate supply to plant roots (Finnemann & Schjoerring, 1999; Haynes & Goh, 1978; Kronzucker et al., 1998; Wang et al., 1993). Variation in susceptibility to ammonium toxicity could therefore in part explain the observed variation in N preference. Preference is also known to depend on photosynthesis and photorespiration, both of which generate reducing power used for nitrate reduction. Variation in photosynthetic performance and relative availability of reductant for nitrate reduction in leaves and carbohydrate supply to the roots for ammonium assimilation may also contribute to the observed variation in preference. Interestingly though, *HvEPF1oe* displayed significant nitrate preference at the $p<0.10$ level (Figure 5.7), despite having a reduced carbon assimilation phenotype. It is likely a combination of factors that contribute to the variation in N preference observed.

### 5.4.2 Barley N preference responses to changing environmental conditions

A major aim of this chapter was to identify sets of conditions where N preference differs with a cultivar. Downstream, this would allow establishment of a model system for dissecting the mechanisms underpinning variation in biological nitrification inhibition if the two traits are linked (see Chapter 6). In Experiments 2 and 3, plants were exposed to short-term high light and grown at elevated $CO_2$ respectively to identify conditions where preference differs within a cultivar, in addition to improving our understanding of the commonality of preference responses to environmental changes across a range of cultivars.

#### 5.4.2.1 N preference under short-term high light

There are conflicting reports in the literature of plant ammonium and nitrate uptake responses to increased light intensity. Zhu et al. (2000) found that ammonium-grown *Phaseolus vulgaris* plants were more sensitive to light stress than nitrate-grown plants. More recently, however, it has been shown that ammonium accounts for a larger amount of shoot N in *Brassica chinensis* after 25 days of growth under high light (Ma et al., 2016). The effect of high light on N uptake and preference in different barley cultivars remains poorly understood.

In this experiment, plants were grown for two weeks at ambient light in a fully controlled environment before imposing a high light treatment on half of the plants, achieved by increasing cabinet light intensity and placing a shading tent over half of the plants (Figure 5.3, 5.8). Contrary to Experiment 1, all plants exhibited ammonium preference or no preference irrespective of exposure to increased light intensity (Figure 5.12). Those that did not show significant N preference still displayed negative preference values, driven by increased $^{15}N$ detected in plants exposed to $^{15}NH_4^+$, suggesting these plants still took up more ammonium compared to nitrate. The only cultivar to show a positive preference value was *HvEPF1oe* under ambient light. Interestingly, *HvEPF1oe* showed the largest shift in N preference in response to short-term high light, with a shift from nitrate preference to strong ammonium preference under high light. Several other cultivars also showed increased ammonium preference under high light treatment supporting the results of Ma et al. (2016), though this was only significant for Laureate. A possible explanation for this shift in preference could be due to the imposed light stress. Quantum yield, a measure of photosynthetic efficiency, decreased significantly across all cultivars under high light (Figure 5.9) indicating a reduced capacity for photosynthesis, presumably due to a lack of photosynthetic machinery capable of dealing with the sudden excess light. In response to this, plants would require additional nitrogen to produce the necessary chlorophyll and proteins to adapt to the excess light. Reduced photosynthesis would lead to a smaller reductant pool available for nitrate reduction causing plants to switch to utilise ammonium, which does not require

reductant and has a lower associated photo-energetic cost (Raven, 1985). This idea is further supported by the large shift in preference of *HvEPF1oe*, which may have experienced increased light stress due to its reduced carbon assimilation and stomatal density. Shoot dry weight increased in response to high light across all cultivars (Figure 5.11b), possibly as a result of increased chlorophyll and protein production to adapt to high light.

Despite a significant reduction in quantum yield and increase in shoot dry weight for all cultivars under high light, not all displayed increased ammonium preference. Several cultivars appeared to show no change in preference under high light, and NFC Tipple took up slightly more nitrate under high light, though not enough to significantly alter preference (Figure 5.12). This suggests that while all cultivars took up additional N to support adaptation to high light, not all cultivars acquired the additional necessary N as ammonium and the increase in ammonium preference is not a universal response across barley cultivars as hypothesised. Further work is required to identify other factors involved in determining the preference response of a particular cultivar to light stress.

#### 5.4.2.2 N preference under elevated atmospheric $CO_2$

The effect of elevated $CO_2$ on N uptake and preference is better understood, with several studies reporting reduced relative growth rate under nitrate nutrition compared to ammonium nutrition (Bloom, 2015; Bloom et al., 2002, 2012), attributed to reduced availability of photosynthetic reductant for nitrate reduction due to increased demand for carbon fixation and reduced rates of photorespiration. It is less clear how crops such as barley will respond to elevated $CO_2$, and whether responses are universal across cultivars.

In this study, no barley cultivars significantly preferred nitrate under either ambient or elevated $CO_2$ (Figure 5.15), in line with the results from Experiment 2. Cultivars could again be put into 3 groups, with several barley cultivars showing increased ammonium preference when grown under elevated $CO_2$, particularly Golden Promise and Annabell, as expected based on the work of Bloom et al. (2002, 2012). In contrast to this, a second group of cultivars appeared not to change

N preference in response to elevated $CO_2$. Yet another group showed reduced ammonium preference under $eCO_2$, even being significant at the $p<0.10$ level for NFC Tipple. Shoot dry weight increased in many, but not all, cultivars grown under elevated $CO_2$ (Figure 5.14a), though this appears not to be related to the preference response. Clearly, the preference response to elevated $CO_2$ is cultivar-specific, at least under the conditions of the experiment, and may have important implications for the production of climate-ready crops.

### 5.4.3 Conclusion and future work

The results from this chapter indicate that barley plants, when environmental constraints that drive N preference in natural environments are removed, overall tend to revert to an innate preference for ammonium over nitrate, likely because of the reduced photo-energetic cost in a system where both forms are available. Preference appeared to be shifted more towards increased nitrate uptake in Experiment 1 compared to Experiments 2 and 3. However, this experiment was carried out in a controlled greenhouse during summer and therefore plants experienced much higher light intensities compared to experiments 2 and 3, which were carried out in a controlled growth cabinet with regulated light. It is possible that due to this high light, $CO_2$ was limiting for photosynthesis during the first experiment, meaning additional reductant was available for nitrate reduction and assimilation. In the later experiments, light intensity was not as high and $CO_2$ may not have been as limiting for photosynthesis, with most available reductant used to fix carbon and therefore less available for nitrate reduction.

In contrast, N preference responses to changes in environmental conditions appear to be cultivar-specific, suggesting that a genetic component at least in part determines plant preference, which is revealed when environment is held constant. The term ‘preference’ reflects this, and therefore should not be replaced with the term ‘plasticity’, but the two should be distinguished and included together when discussing this phenomenon.

It is important to recognise that despite hydroponics being a logical starting point for N preference research (Chalk & Smith, 2021), the work carried out in this chapter was performed

in a completely artificial system that is not representative of an agricultural soil, and it is likely that nitrate preference would be more prominent in a soil system given that barley is generally considered to be a nitrate-preferring species. Future work should focus on understanding barley N preference and interactions with changing environment in a soil system to see whether cultivar-specific responses hold true. Screening N preference in soil using the $^{15}N$ labelling approach taken here is difficult, mainly due to the complication of nitrification. For plants treated with $^{15}NH_4^+$ it would be impossible to distinguish in the plant whether any $^{15}N$ present in the plant had come from the applied $^{15}NH_4^+$ or from $^{15}NO_3^-$ produced by nitrification that was subsequently taken up by the plant. This issue has been addressed before with the addition of a nitrification inhibitor (Huangfu et al., 2016), though one could argue that this is no longer an accurate representation of the system, and this could provide additional complications if trying to understand interactions between N preference and soil nitrogen cycling. Future research should therefore also focus on the development of alternative measures of preference to better take into account the complexity of the system.

# Chapter 6: General discussion

Detailed discussion sections were presented in each of the results chapters. The purpose of this chapter was therefore to collectively present the important findings of the thesis both alone and together, to explain the results in a wider context and propose future directions for the work.

An understanding of the scope of variation in traits such as BNI activity and ability to alter denitrifier community structure and activity could pave the way for increased NUE, reduced N losses and reduced environmental pollution through nitrate leaching and emission of $N_2O$ (Skiba et al., 2011; Subbarao et al., 2015) (Summarised in Figure 1.2). The key to drawing meaningful links between such traits and potential related genes/genomic regions is high-throughput screening of sufficient germplasm to detect potential variation in traits. This is not trivial, and while recent advancements in genetic technologies mean we now have access to vast amounts of genetic data, there has been a distinct lag in scaling up of phenotyping technologies that would allow meaningful links between phenotype and genotype to be made (Ortiz et al., 2018). This is a particular issue when studying processes sensitive to changes in WFPS and soil oxygen content, such as nitrification (an aerobic process) and denitrification (an anaerobic process), and a contributing factor to the difficulty of screening for these traits in a high-throughput manner (Subbarao et al., 2015). Systematic screening of crops of agronomic importance for BNI activity and ability to promote $N_2O$ reduction has been proposed as the initial research focus to accelerate the development of BNI as an N loss and $N_2O$ emission mitigation strategy (de Klein et al., 2022).

The tension tables described in Chapter 2 were designed as a means to automate the current standard practice of watering to weight, holding soil at a specific aerobic or anaerobic WFPS range more accurately than by watering to weight, allowing high-throughput screening of nitrification and denitrification processes in soil. After proof of concept that the tension tables could hold WFPS at a consistent set point (section **3.3.1**), the relationship between soil WFPS and reservoir height was characterised for 3 bulk densities of a sandy loam soil, allowing bulk density/reservoir

height combinations to be identified (section **3.3.3**) that would allow maintenance of largely aerobic or anaerobic conditions for screening of nitrification and denitrification.

The system was scaled up to facilitate screening of a panel of 200 spring barley varieties for variation in BNI activity and ability to alter denitrification rates, and while WFPS was held sufficiently aerobic (below 60 %) in all soil microcosms during the nitrification screen and sufficiently anaerobic (above 70 %) in all soil microcosms in the denitrification screen, several issues arose during these experiments (discussed in Chapters 3 and 4) that meant WFPS varied significantly across blocks. This meant that WFPS had to be included as a covariate in subsequent ANCOVA analysis in order for nitrification and denitrification rates to be compared across cultivar. Nevertheless, the tension tables performed largely as designed and allowed sufficient control of WFPS to generate aerobic WFPS (<60 %) for nitrification screening and anaerobic WFPS (>70 %) for denitrification screening. To my knowledge, this is the first application of tension table technology to large-scale plant growth and phenotyping experiments, and with further refinements it could be a powerful tool to study processes dependent on soil WFPS and oxygen content in a high-throughput manner.

BNI activity has the potential to improve agronomic NUE and reduce N losses and $N_2O$ emissions (see Figure 1.2b), but the first step to exploit this trait (as with any other trait) in any future breeding programs is to identify if sufficient variation exists in germplasm. Barley is an important staple crop (discussed in section **1.6**) but to date variation in BNI activity in barley germplasm has not been identified. In Chapter 3 I observed significant variation in gross nitrification rate across a panel of 200 modern spring barley varieties with an 8-fold difference in GNR across barley cultivars (Figure 3.1), demonstrating, to my knowledge, for the first time that variation exists in the ability of barley germplasm to alter soil nitrification. Gross nitrification rate was measured in this experiment, and while this is not a direct measure of BNI activity, such as the bioluminescent *Nitrosomonas europaea* assay (Iizumi et al., 1998; Subbarao et al., 2006a) it does indicate that germplasm is responsible for the variation observed since the same soil type, bulk

density, WFPS and growth conditions were used throughout. Moreover, since GNR takes into account other transformation processes (Drury et al., 2007; de Klein et al., 2022), it is likely that inhibition is due to a direct effect on nitrification. It was not possible to determine from these results whether the mechanism of BNI is through enhanced plant competition for ammonium in cultivars with low nitrification rate, root exudation, or a combination of the two, but a logical next step for this work is to collect exudates from these cultivars and add them to soil. If the same differences in GNR are observed, then it could be concluded that root exudation is responsible. Subsequent metabolomics analysis of these root exudates with contrasting BNI activity could lead to the identification of novel BNI compounds.

The large number of cultivars selected for this experiment were chosen based on available genetic information and will allow downstream GWAS analysis to be performed to assess whether BNI activity is linked to any genomic regions which could provide future breeding targets and shed light on the nature of the observed BNI activity. It will also be important to characterise the nitrifier communities and their activity. I would hypothesise that cultivars displaying increased BNI activity will correlate with reduced nitrifier activity, which could be assessed through qPCR analysis of *amoA* mRNA transcript abundance. An assessment of nitrifier community structure through 16S rRNA sequence analysis would shed light on the relative contribution of bacterial and archaeal nitrifiers to nitrification in this system. Soil samples were taken during this experiment which will allow such analysis to be performed.

In Chapter 4 I utilised the same tension table system to screen barley germplasm at anaerobic WFPS (>70 %) for variation in $N_2O$ emission rate, $N_2$ emission rate, total denitrification rate and the ratio of incomplete to total denitrification. However, no significant effect of cultivar on soil $N_2O$ emissions or denitrification rates was observed. These results do not support previous unpublished work by Tim Daniell, Tim George and colleagues at the James Hutton Institute where a significant effect of barley cultivar on $N_2O$ emissions was observed in a smaller scale experiment. However, the screening experiment in this chapter held WFPS constantly anaerobic

for the duration of the experiment, whereas WFPS was fluctuated between aerobic and anaerobic conditions in the aforementioned study. This suggests that barley plants are having little effect on total denitrification rate but may be driving variation in $N_2O$ emissions through alteration of $N_2O$ reductase activity or through the alteration of denitrifier community structure. In my study, the conditions favoured complete denitrification (reflected in overall relatively low ratios of incomplete to total denitrification) because the system was maintained in an anaerobic state, which may have masked any variation across cultivar in affecting $N_2O$ reductase activity. Performing another screen under fluctuating WFPS could help to resolve this.

In Chapter 5, I successfully designed a method based on the hydroponics system described by Conn et al. (2013) and the Wang & Macko (2011) stable isotope approach for measuring N preference for screening of 'innate N preference', the preference for ammonium or nitrate when both forms are supplied equally, and all other environmental constraints are removed. It is commonly thought that environment is the major driver of N preference (Houlton et al., 2007; Harrison, et al., 2007; Chalk & Smith, 2021), largely driven by rates of nitrification which is in turn affected by the various environmental and biotic factors discussed throughout this thesis. This has led to suggestions that the term 'N preference' is an anachronism, and that perhaps 'N plasticity' may be a more suitable term (Chalk & Smith, 2021). In this chapter I showed for the first time in barley that germplasm does not show a common innate N preference, as is suggested would be the case if indeed environment was the sole driver of N preference. Moreover, I demonstrated for the first time in barley that N preference is altered under both short-term high light and growth at elevated $CO_2$. Significant shifts in N preference moved almost exclusively towards increased ammonium preference for both conditions, though responses were cultivar-specific. The results from the $eCO_2$ experiment are to my knowledge the first report of a direct effect of $eCO_2$ on plant N preference, and for those that showed altered preference at $eCO_2$, my results support previous research that has demonstrated previously that shoot nitrate assimilation is inhibited under $eCO_2$ due to a lack of reducing power from photosynthesis and

photorespiration, which is inhibited by the presence of additional $CO_2$ (Bloom, 2015; Bloom et al., 2002, 2012; Cousins & Bloom, 2004; Searles & Bloom, 2003).

Interestingly, several cultivars displayed increased nitrate preference under elevated $CO_2$ with the strongest response in NFC Tipple, though this was only significant at the $p<0.10$ level. Nevertheless, it is clear that under the conditions of the experiments performed in this study that both innate N preference and preference responses are cultivar-specific and not driven solely by environment, and this has several implications. Further research is needed to understand the nature of these cultivar-specific responses, but variation in N preference in barley germplasm provides scope for future selection of more ammonium-preferring cultivars that would presumably reduce N losses and $N_2O$ emissions in much the same way as a cultivar with high BNI activity would (Figure 1.2b). Additionally, these results have implications for the appropriate terminology when investigating this phenomenon. The term 'N plasticity', as suggested by Chalk & Smith (2021), is a suitable term to use when describing plant N uptake responses to environment but, unlike 'preference', it does not capture the influence of genetics on this trait (this is by design since genetics were thought to only play a small role in the determination of plant N uptake responses). I would therefore encourage the continued use of the term N preference as I have done throughout this thesis, as a more suitable term to describe both genetic and environmental components of plant N preference responses.

It is important to remember that these experiments were performed in hydroponics. This allows fine control of ammonium and nitrate concentrations and removes other factors affecting N preference and therefore is a logical starting point for N preference research (Chalk & Smith, 2021). Nevertheless, it does not reflect a soil system and it is possible that these responses may be masked when other edaphic and environmental factors are introduced. Future work should assess preference of these barley cultivars in soil, though this remains a challenge in N preference research and a robust method has yet to be developed. Using the methods described in this thesis to assess N preference in a soil system would be difficult, because subsequent IRMS analysis of

plant shoot material would not be able to differentiate $^{15}N$ signal from ammonium taken up by plants and $^{15}NH_4^+$ that has been nitrified to $^{15}NO_3^-$ and then taken up by the plant, and therefore could not provide an accurate measure of preference. Synthetic nitrification inhibitors have been added to tackle this (Huangfu et al., 2016), but this is not ideal since nitrification occurs at high rates in most agricultural systems and should not be inhibited if preference is to be determined in a true 'real world' system.

Results from Chapters 3 and 5 have demonstrated that variation in both BNI activity and nitrogen preference exists in barley germplasm, each of which could further goals to reduce N losses from barley cultivation and improve agronomic NUE. One could predict that an ammonium-preferring plant would show increased BNI activity compared to a nitrate-preferring plant as it would confer a selective advantage to compete with nitrifiers for ammonium. It is widely recognised in nitrogen preference research that soil nitrification (and denitrification) determine the dominant N form in a given system and therefore are major drivers of N preference (reviewed in Chalk & Smith, 2021). This is reinforced by studies that have shown that plants display ammonium preference in wetter, anaerobic soils and nitrate preference in drier, aerobic soils (Houlton et al., 2007, Wang & Macko, 2011). This would suggest that there may be a link between plant nitrogen preference and BNI activity. Despite this, no studies to date have directly assessed links between plant N preference and BNI activity, except in a modelling study of nitrification inhibition effects on primary productivity in the Lamto savanna (Boudsocq et al., 2009). BNI release from roots has been hypothesised to be linked to ammonium uptake and assimilation driving proton pump ATPase activity and transport of BNIs out of roots via voltage-dependent anion channels (Subbarao et al., 2015; Zhu et al., 2012).

The $eCO_2$ preference experiment performed in Chapter 5 was designed such that a comparison between preference and BNI activity could be performed. Cultivars included in this experiment were chosen based on variation in N preference from previous experiments in Chapter 5 and variation in BNI activity, based on results from the screen carried out in chapter 3. Scatter plots

were drawn to assess the linear relationship between N preference at ambient $CO_2$ (using results from Experiment 3, Chapter 5) and $log_{10}$ estimated marginal mean gross nitrification rate (Chapter 3) for 12 cultivars where data for both variables was available (Figure 6.1a, b). A Pearson correlation coefficient was computed in Microsoft Excel to statistically assess this linear relationship between N preference and GNR. A positive relationship was observed between the two variables, though this was not significant ($r_{(10)}$=0.05, p=0.87). This trend became stronger if Barke was excluded, which appears to be an outlier ($r_{(9)}$=0.46, p=0.15). This is interesting given that Barke showed the lowest GNR in the screening experiment carried out in Chapter 3 (Figure 3.1), and reassessment of Barke N preference may be necessary to confirm its apparent nitrate preference. Inclusion of further cultivars in this analysis once N preference data is available will help to further understand the strength of this relationship. Nevertheless, these results suggest a potential link between N preference and BNI activity, with increased ammonium preference i.e. more negative values linked to reduced gross nitrification rate and therefore increased BNI activity.

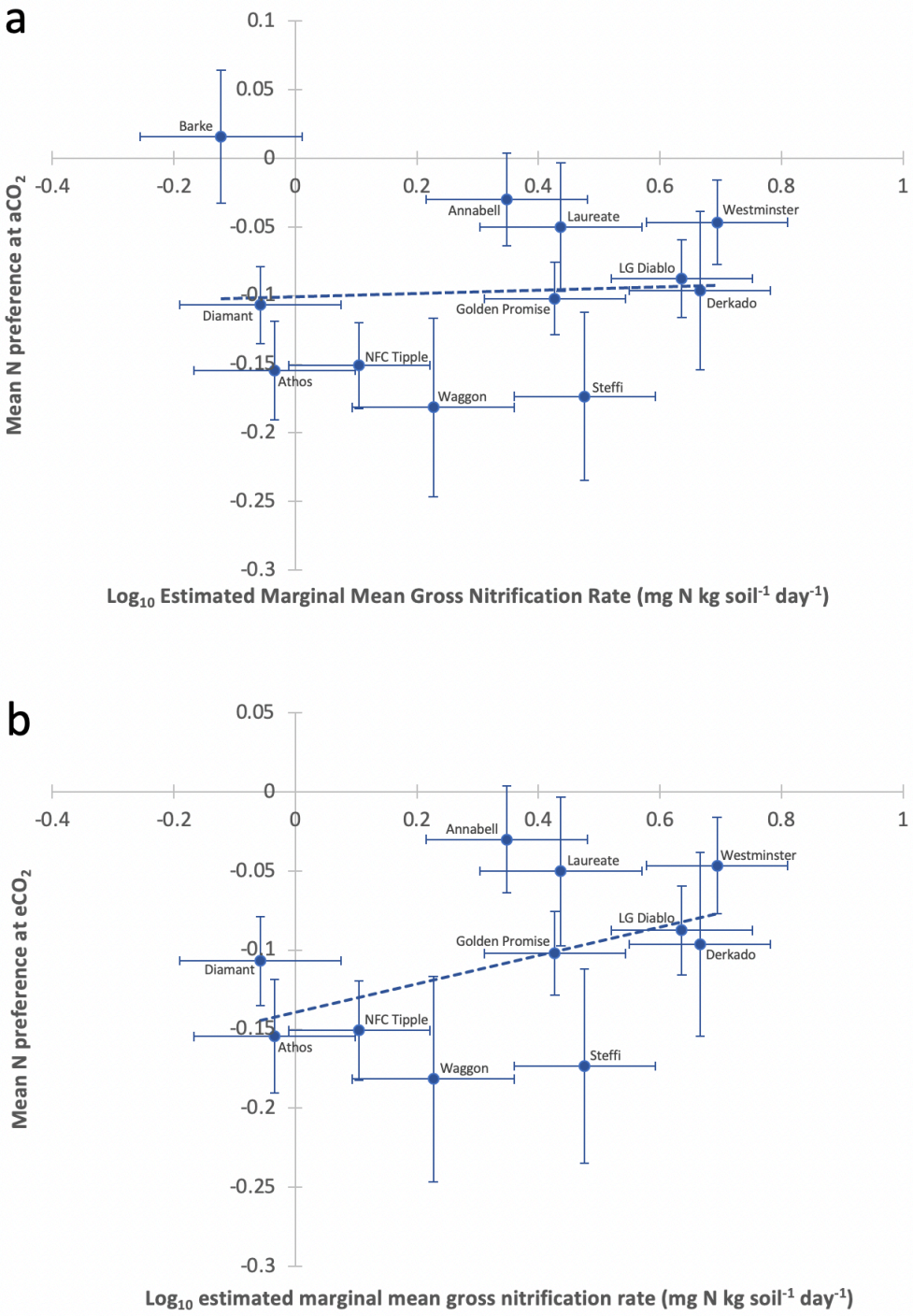


**Figure 6.1:** Scatter plots revealing correlation between mean N preference at $aCO_2$ and mean $log_{10}$ estimated marginal mean gross nitrification rate (mg N kg soil$^{-1}$ day$^{-1}$) for **a** 12 cultivars for which N preference and GNR data is available, and **b** for the same 12 cultivars with Barke omitted. Vertical error bars indicate ± propagated SEM for N preference, horizontal error bars indicate ± estimated SEM for $log_{10}$ estimated marginal mean gross nitrification rate (mg N kg soil$^{-1}$ day$^{-1}$). The dashed line indicates the line of best fit, and each data point is labelled with the corresponding cultivar name. Graphs were produced in Microsoft Excel.

To my knowledge, this is the first report of a direct comparison of plant N preference and BNI activity and provides evidence to support a major initial hypothesis of my thesis that ammonium-preferring plants may show increased BNI activity. Moreover, it is possible that increased ammonium uptake is in itself a BNI mechanism, both through increased competition with nitrifiers for ammonium and by increasing BNI release through increased proton pump ATPase activity, as suggested by Subbarao et al. (2015) and Zhu et al. (2012). Further research is required with additional barley cultivars to assess the extent to which this relationship exists, and it is possible that this relationship will strengthen or weaken if N preference is measured in soil. Determination of plant N preference in soil will help to further our understanding of the extent to which N preference and BNI activity are linked in a soil setting.

The establishment that N preference and BNI may be linked, in addition to the identification of environmental conditions that drive alteration of N preference within select cultivars (see sections **5.3.2.5** and **5.3.3.3**), may allow N preference to be used as a model system to further understand the nature of observed BNI activity in barley. Comparison of root exudates from a single cultivar of barley that shifts N preference in response to changes in environmental conditions, for example Golden Promise grown at ambient and elevated atmospheric $CO_2$ (see Figure 5.15) through metabolomics may allow identification of potential BNI compounds, the release of which is promoted by imposing conditions that drive increased ammonium preference. This would allow identification of BNI compounds without the complication of comparing root exudates of genetically distinct germplasm.

Correlation analysis was also performed to assess the linear relationship between N preference and $N_2O/(N_2+N_2O)$ ratio (Figure 6.2), however Pearson correlation analysis revealed no significant relationship ($r_{(10)}=0.10$, $p=0.76$). This was not entirely surprising given that no significant variation was observed across cultivars in $N_2O/(N_2+N_2O)$ ratio or any of the calculated denitrification rates (see section **4.3.1**).

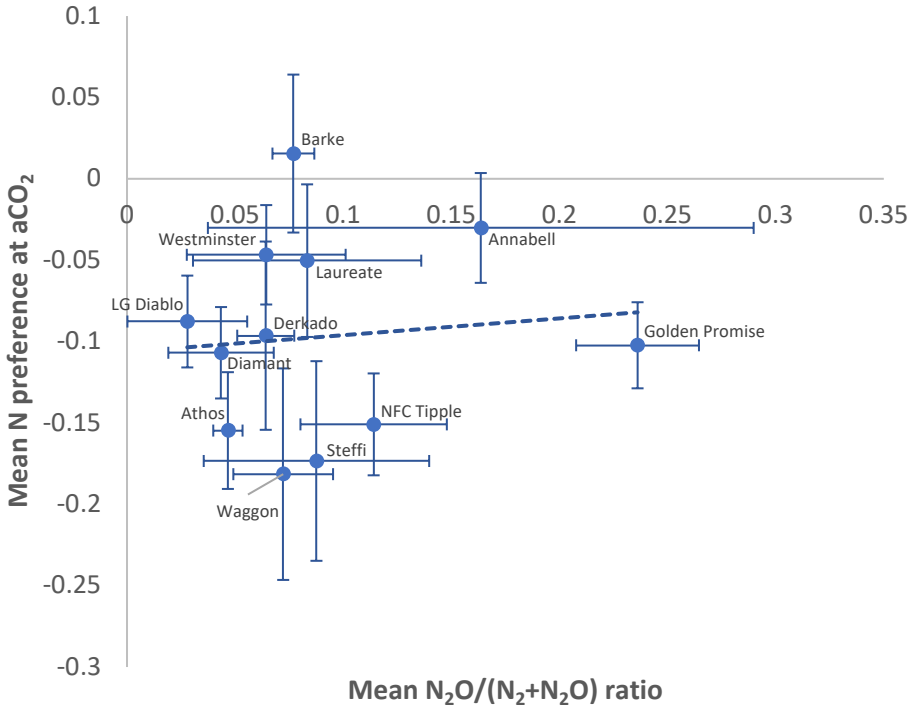


**Figure 6.2:** Scatter plot between mean N preference at $aCO_2$ and mean $N_2O/(N_2+N_2O)$ ratio for 12 cultivars for which N preference and $N_2O/(N_2+N_2O)$ ratio data is available. Vertical error bars indicate ± propagated SEM for N preference, horizontal error bars indicate ± SEM for $N_2O/(N_2+N_2O)$ ratio. The dashed line indicates the line of best fit, and each data point is labelled with the corresponding cultivar name. Graph was produced in Microsoft Excel.

Similarly, no significant linear relationship was observed between GNR and $N_2O/(N_2+N_2O)$ ratio ($r_{(156)}$=-0.14, p=0.09), though a scatter plot shows a weak negative correlation (Figure 6.3). However, if significant variation is observed in a future denitrification screening experiment under fluctuating WFPS conditions, it will be important to repeat this analysis because variation in nitrification rate (occurring under aerobic conditions) driven by BNI will likely affect nitrate availability and therefore the amount of substrate available for denitrification, which could translate to variation in $N_2O$ emissions.

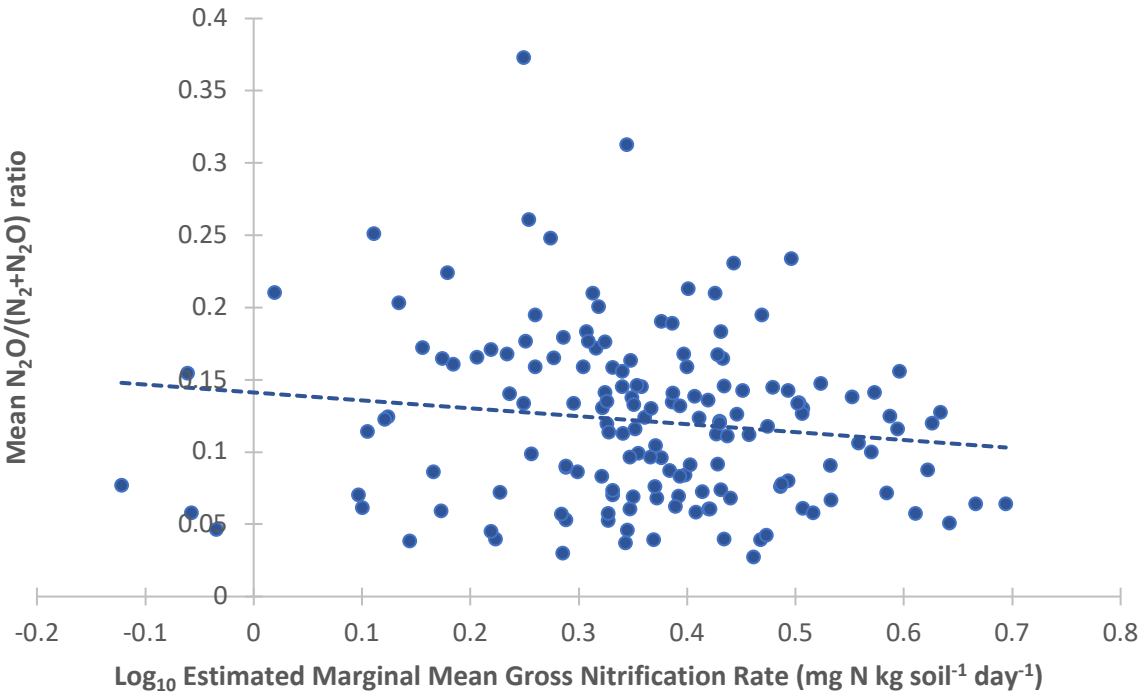


**Figure 6.3:** Scatter plot between mean $N_2O/(N_2+N_2O)$ ratio and mean $log_{10}$ estimated marginal mean gross nitrification rate (mg N kg $soil^{-1}$ $day^{-1}$) for 158 cultivars for which $N_2O/(N_2+N_2O)$ ratio and GNR data is available. The dashed line indicates the line of best fit. Error bars are omitted for clarity. Graph was produced in Microsoft Excel.

The results from this thesis have advanced our understanding of variation in N preference and BNI activity in barley germplasm and represent a first step towards improving agronomic NUE in barley cultivation through selection for increased ammonium preference and/or BNI activity (summarised in Figure 6.4). BNI activity and ammonium preference both have the potential to suppress nitrification and associated losses and the two may in fact be inherently linked (Figure 6.1 and 6.4). Variation in BNI activity and N preference and their potential interaction suggests that selecting for cultivars with increased ammonium preference may also select for enhanced BNI activity. Moreover, if selected cultivars show a shift towards increased ammonium preference under elevated $CO_2$ as observed for several barley cultivars in this thesis, selection for these traits may allow for selection of crops adapted to a future elevated atmospheric $CO_2$ climate.

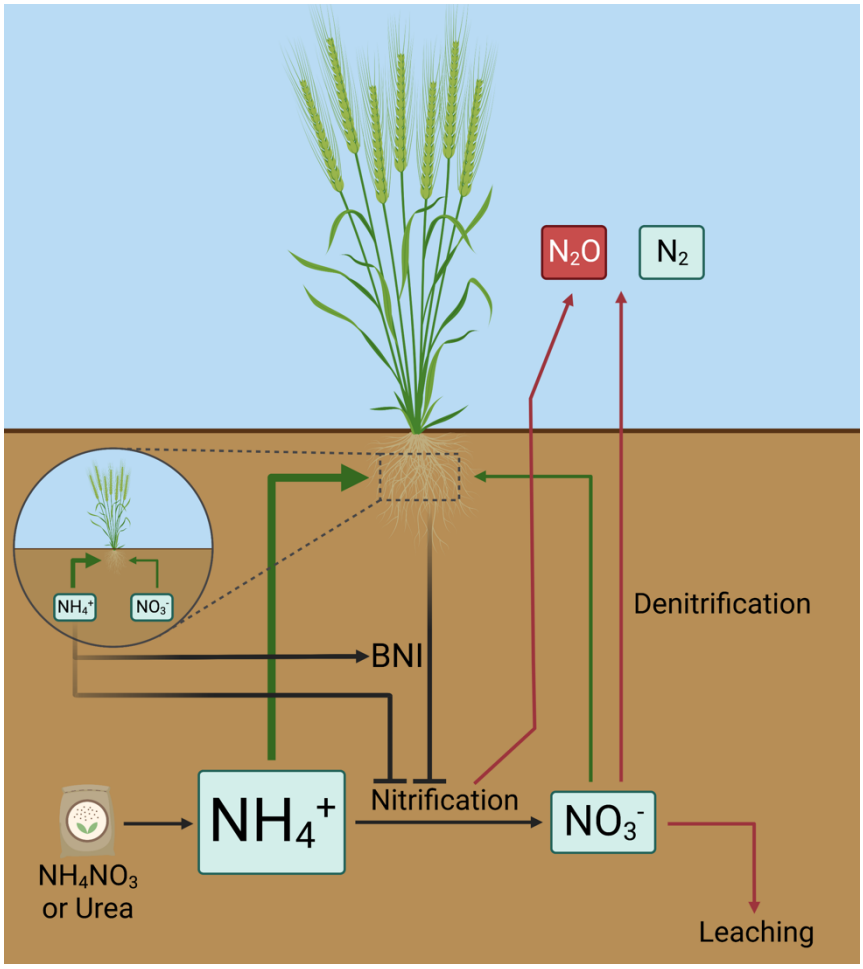


**Figure 6.4:** Conceptual summary diagram of hypothesised shifts in $NH_4^+$ and $NO_3^-$ pools, N preference and flux through major N pathways when plants exhibit BNI activity, shown to be variable in spring barley. Increased barley $NH_4^+$ preference may correlate with BNI activity and act as a BNI mechanism through stimulation of BNI release and increased competition with nitrifiers. Figure created in BioRender.

# References


Abalos, D., Jeffery, S., Sanz-Cobena, A., Guardia, G., & Vallejo, A. (2014). Meta-analysis of the effect of urease and nitrification inhibitors on crop productivity and nitrogen use efficiency. *Agriculture, Ecosystems and Environment* **189**, 136–144. https://doi.org/10.1016/j.agee.2014.03.036

Ali, A., Tucker, T. C., Thompson, T. L., & Salim, M. (2001). Effects of salinity and mixed ammonium and nitrate nutrition on the growth and nitrogen utilization of barley. *Journal of Agronomy and Crop Science* **186**(4), 223–228. https://doi.org/10.1046/j.1439-037X.2001.00471.x

Allery, T. (2019). Do arbuscular mycorrhizas modify the rhizospheric C balance to reduce soil N2O emissions? *The University of Sheffield*.

Allison, S. M., & Prosser, J. I. (1993). Ammonia oxidation at low pH by attached populations of nitrifying bacteria. *Soil Biology and Biochemistry* **25**(7), 935-941.

Anderson, I. C., Poth, M., Homstead, J., & Burdige, D. (1993). A Comparison of NO and $N_20$ Production by the Autotrophic Nitrifier Nitrosomonas europaea and the Heterotrophic Nitrifier Alcaligenes faecalis. *Applied and environmental microbiology* **59**(11), 3525-3533.

Arp, D. J., Sayavedra-Soto, L. A., & Hommes, N. G. (2002). Molecular biology and biochemistry of ammonia oxidation by Nitrosomonas europaea. *Archives of Microbiology* **178**(4), 250–255. https://doi.org/10.1007/s00203-002-0452-0

Ashton, I. W., Miller, A. E., Bowman, W. D., & Suding, K. N. (2008). Nitrogen preferences and plant-soil feedbacks as influenced by neighbors in the alpine tundra. *Oecologia* **156**(3), 625–636. https://doi.org/10.1007/s00442-008-1006-1

Azam, F., Müller, C., Weiske, A., Benckiser, G., & Ottow, J. C. G. (2002). Nitrification and denitrification as sources of atmospheric nitrous oxide - Role of oxidizable carbon and

applied nitrogen. *Biology and Fertility of Soils* **35**(1), 54–61. https://doi.org/10.1007/s00374-001-0441-5

Baer, S. E., Connelly, T. L., Sipler, R. E., Yager, P. L., & Bronk, D. A. (2014). Effect of temperature on rates of ammonium uptake and nitrification in the western coastal Arctic during winter, spring, and summer. *Global Biogeochemical Cycles* **28**(12), 1455–1466. https://doi.org/10.1002/2013GB004765

Baethgen, W. E., & Alley, M. M. (1989). A manual colorimetric procedure for measuring ammonium nitrogen in soil and plant kjeldahl digests. *Communications in Soil Science and Plant Analysis* **20**(9–10), 961–969. https://doi.org/10.1080/00103628909368129

Baggs, E., & Philippot, L. (2010). Microbial terrestrial pathways to Nitrous Oxide. In K. Smith (Ed.), *Nitrous Oxide and Climate Change*. Routledge. https://doi.org/10.4324/9781849775113

Baker, L. (2019). Identifying the biological nitrification inhibition ability of barley root exudates. *The University of Sheffield.*

Bakken, L. R. (1988). Denitrification under different cultivated plants: effects of soil moisture tension, nitrate concentration, and photosynthetic activity. *Biology and Fertility of Soils* **6**, 271-278

Bakken, L. R., Bergaust, L., Liu, B., & Frostegård, Å. (2012). Regulation of denitrification at the cellular level: A clue to the understanding of $N_2O$ emissions from soils. *Philosophical Transactions of the Royal Society B: Biological Sciences*, **367**(1593), 1226–1234. https://doi.org/10.1098/rstb.2011.0321

Ball, B. C., & Hunter, R. (1988). The Determination of Water Release Characteristics of Soil Cores at Low Suctions. *Geoderma* **43**, 195-212.

Bardgett, R. D., Streeter, T. C., & Bol, R. (2003). Soil microbes compete effectively with plants for organic-nitrogen inputs to temperate grasslands. *Ecology* **84**(5), 1277–1287. https://doi.org/10.1890/0012-9658(2003)084[1277:SMCEWP]2.0.CO;2

Barraclough, D. (1988). Studying mineralisation/immobilization turnover in field experiments: The use of nitrogen-15 and simple mathematical analysis. *Nitrogen efficiency in agricultural soils,* 409–417. Elsevier Applied Sciences.

Barraclough, D. (1991). The use of mean pool abundances to interpret $^{15}N$ tracer experiments. *Plant and Soil* **131**, 89-96.

Barraclough, D. (1995). $^{15}N$ isotope dilution techniques to study soil nitrogen transformations and plant uptake. *Fertilizer Research* **42**, 185-192.

Barraclough, D., Geens, E. L., Davies, G. P., & Maggs, J. M. (1985). Fate of fertilizer nitrogen. *Journal of Soil Science* **36**(4), 593–603. https://doi.org/10.1111/j.1365-2389.1985.tb00361.x

Barraclough, D., & Smith, M. J. (1987). The estimation of mineralization, immobilization and nitrification in nitrogen-15 field experiments using computer simulation. *Journal of Soil Science* **38**(3), 519–530. https://doi.org/10.1111/j.1365-2389.1987.tb02287.x

Bassirirad, H., Griffin, K. L., Strain, B. R., & Reynolds, J. F. (1996). Effects of $CO_2$ enrichment on root $^{15}NH_4^+$ uptake kinetics and growth in seedlings of loblolly and ponderosa pine. *Tree Physiology* **16**, 957-962

Bassirirad, H., Reynolds, J. F., Virginia, R. A., & Brunelle, M. H. (1997). Growth and root $NO_3^-$ and $PO_4^{3-}$ uptake capacity of three desert species in response to atmospheric $CO_2$ enrichment. *Australian Journal of Plant Physiology* **24**(3), 353–358. https://doi.org/10.1071/PP96109

Bateman, E. J., & Baggs, E. M. (2005). Contributions of nitrification and denitrification to $N_2O$ emissions from soils at different water-filled pore space. *Biology and Fertility of Soils* **41**(6), 379–388. https://doi.org/10.1007/s00374-005-0858-3

Benckiser, G., Christ, E., Herbert, T., Weiske, A., Blome, J., & Hardt, M. (2013). The nitrification inhibitor 3,4-dimethylpyrazole-phosphat (DMPP) - quantification and effects on soil metabolism. *Plant and Soil* **371**(1–2), 257–266. https://doi.org/10.1007/s11104-013-1664-6

Bergaust, L., Mao, Y., Bakken, L. R., & Frostegård, Å. (2010). Denitrification response patterns during the transition to anoxic respiration and posttranscriptional effects of suboptimal pH on nitrogen oxide reductase in *Paracoccus denitrificans*. *Applied and Environmental Microbiology* **76**(19), 6387–6396. https://doi.org/10.1128/AEM.00608-10

Berks, B. C., Ferguson, S. J., Moir, J. W. B., & Richardson, D. J. (1995). Enzymes and associated electron transport systems that catalyse the respiratory reduction of nitrogen oxides and oxyanions. *Biochimica et Biophysics Acta* **1232**, 97-173.

Bertin, C., Yang, X., & Weston, L. A. (2003). The role of root exudates and allelochemicals in the rhizosphere. *Plant and Soil* **256**, 67-83.

Bloom, A. J. (2015). The increasing importance of distinguishing among plant nitrogen sources. In *Current Opinion in Plant Biology* **25**, 10–16. Elsevier Ltd. https://doi.org/10.1016/j.pbi.2015.03.002

Bloom, A. J., Rubio Asensio, J. S., Randall, L., Rachmilevitch, S., Cousins, A. B., & Carlisle, E. A. (2012). $CO_2$ enrichment inhibits shoot nitrate assimilation in $C_3$ but not $C_4$ plants and slows growth under nitrate in $C_3$ plants. *Ecology* **93**(2), 355–367. https://doi.org/10.1890/11-0485.1

Bloom, A. J., Smart, D. R., Nguyen, D. T., & Searles, P. S. (2002). Nitrogen assimilation and growth of wheat under elevated carbon dioxide. *Proceedings of the National Academy of Sciences of the United States of America* **99**(3), 1730-1735.

Bloom, A. J., Sukrapanna, S. S., & Warner, R. L. (1992). Root respiration associated with ammonium and nitrate absorption and assimilation by Barley. *Plant Physiology* **99**, 1294-1301.

Boudsocq, S., Lata, J. C., Mathieu, J., Abbadie, L., & Barot, S. (2009). Modelling approach to analyse the effects of nitrification inhibition on primary production. *Functional Ecology* **23**(1), 220–230. https://doi.org/10.1111/j.1365-2435.2008.01476.x

Boudsocq, S., Niboyet, A., Lata, J. C., Raynaud, X., Loeuille, N., Mathieu, J., Blouin, M., Abbadie, L., & Barot, S. (2012). Plant preference for ammonium versus nitrate: A neglected determinant of

ecosystem functioning? *American Naturalist* **180**(1), 60–69. https://doi.org/10.1086/665997

Bouwman, A. F., Beusen, A. H. W., Griffioen, J., van Groenigen, J. W., Hefting, M. M., Oenema, O., van Puijenbroek, P. J. T. M., Seitzinger, S., Slomp, C. P., & Stehfest, E. (2013). Global trends and uncertainties in terrestrial denitrification and $N_2O$ emissions. *Philosophical Transactions of the Royal Society B: Biological Sciences* **368**(1621). https://doi.org/10.1098/rstb.2013.0112

Bozal-Leorri, A., Corrochano-Monsalve, M., Arregui, L. M., Aparicio-Tejo, P. M., & González-Murua, C. (2021). Biological and synthetic approaches to inhibiting nitrification in non-tilled Mediterranean soils. *Chemical and Biological Technologies in Agriculture* **8**(1). https://doi.org/10.1186/s40538-021-00250-7

Brady, N. C., & Weil, R. R. (1999). *The nature and properties of soils.* (12th ed.). Prentice Hall Publishers.

Breidenbach, B., Pump, J., & Dumont, M. G. (2016). Microbial community structure in the rhizosphere of rice plants. *Frontiers in Microbiology* **6**. https://doi.org/10.3389/fmicb.2015.01537

Brenzinger, K., Dörsch, P., & Braker, G. (2015). pH-driven shifts in overall and transcriptionally active denitrifiers control gaseous product stoichiometry in growth experiments with extracted bacteria from soil. *Frontiers in Microbiology* **6**. https://doi.org/10.3389/fmicb.2015.00961

Britto, D. T., & Kronzucker, H. J. (2002). $NH_4^+$ toxicity in higher plants: A critical review. *Journal of Plant Physiology* **159**(6), 567–584. https://doi.org/10.1078/0176-1617-0774

Britto, D. T., & Kronzucker, H. J. (2005). Nitrogen acquisition, PEP carboxylase, and cellular pH homeostasis: New views on old paradigms. *Plant, Cell and Environment* **28**(11), 1396–1409). Blackwell Publishing Ltd. https://doi.org/10.1111/j.1365-3040.2005.01372.x

Britto, D. T., & Kronzucker, H. J. (2013). Ecological significance and complexity of N-source preference in plants. *Annals of Botany* **112**(6), 957–963. https://doi.org/10.1093/aob/mct157

Britto, D. T., Siddiqi, M. Y., Glass, A. D. M., & Kronzucker, H. J. (2001). Futile transmembrane $NH_4^+$ cycling: A cellular hypothesis to explain ammonium toxicity in plants. *Proceedings of the National Academy of Sciences of the United States of America* **98**(7), 4255–4258. https://doi.org/10.1073/pnas.061034698

Brooks, P. D., Stark, J. M., McInteer, B. B., & Preston, T. (1989). Diffusion Method To Prepare Soil Extracts For Automated Nitrogen-15 Analysis. *Soil Science Society of America Journal* **53**(6), 1707–1711. https://doi.org/10.2136/sssaj1989.03615995005300060016x

Burton, S. A. Q., & Prosser, J. I. (2001). Autotrophic Ammonia Oxidation at Low pH through Urea Hydrolysis. *Applied and Environmental Microbiology* **67**(7), 2952–2957. https://doi.org/10.1128/AEM.67.7.2952-2957.2001

Cameron, K. C., & Di, H. J. (2002). The use of a nitrification inhibitor, dicyandiamide (DCD), to decrease nitrate leaching and nitrous oxide emissions in a simulated grazed and irrigated grassland. *Soil Use and Management* **18**(4), 395–403. https://doi.org/10.1079/sum2002151

Capdevila-Cortada, M. (2019). Electrifying the Haber–Bosch. *Nature Catalysis* **2**(12), 1055–1055. https://doi.org/10.1038/s41929-019-0414-4

Caranto, J. D., & Lancaster, K. M. (2017). Nitric oxide is an obligate bacterial nitrification intermediate produced by hydroxylamine oxidoreductase. *Proceedings of the National Academy of Sciences of the United States of America* **114**(31), 8217–8222. https://doi.org/10.1073/pnas.1704504114

Carpenter, S. R., Caraco, N. F., Correll, D. L., Howarth, R. W., Sharpley, A. N., & Smith, V. H. (1998). Nonpoint pollution of surface waters with phosphorus and nitrogen. *Ecological Applications* **8**(3), 559–568. https://doi.org/10.1890/1051-0761(1998)008[0559:NPOSWW]2.0.CO;2

Chalk, P., & Smith, C. (2021). On inorganic N uptake by vascular plants: Can $^{15}N$ tracer techniques resolve the $NH_4^+$ versus $NO_3^-$ "preference" conundrum? *European Journal of Soil Science* **72**(4), 1762–1779). https://doi.org/10.1111/ejss.13069

Chapin, S., Moilanen, L., & Kielland, K. (1993). Preferential use of organic nitrogen for growth by a non-mycorrhizal arctic sedge. *Nature* **361**, 150–153.

Chen, X. P., Zhu, Y. G., Xia, Y., Shen, J. P., & He, J. Z. (2008). Ammonia-oxidizing archaea: Important players in paddy rhizosphere soil? *Environmental Microbiology* **10**(8), 1978–1987. https://doi.org/10.1111/j.1462-2920.2008.01613.x

Chen, X., Zhang, L. M., Shen, J. P., Xu, Z., & He, J. Z. (2010). Soil type determines the abundance and community structure of ammonia-oxidizing bacteria and archaea in flooded paddy soils. *Journal of Soils and Sediments* **10**(8), 1510–1516. https://doi.org/10.1007/s11368-010-0256-9

Chicano, T. M., Dietrich, L., de Almeida, N. M., Akram, M., Hartmann, E., Leidreiter, F., Leopoldus, D., Mueller, M., Sánchez, R., Nuijten, G. H. L., Reimann, J., Seifert, K. A., Schlichting, I., van Niftrik, L., Jetten, M. S. M., Dietl, A., Kartal, B., Parey, K., & Barends, T. R. M. (2021). Structural and functional characterization of the intracellular filament-forming nitrite oxidoreductase multiprotein complex. *Nature Microbiology* **6**(9), 1129–1139. https://doi.org/10.1038/s41564-021-00934-8

Cicerone, R. J. (1987). Changes in Stratospheric Ozone. *Science* **237**(4810), 35–42.

Clayton, H., Mctaggart, I. P., Parker, · J, Swan, · L, Smith, K. A., & Smith, · K A. (1997). Nitrous oxide emissions from fertilised grassland: A 2-year study of the effects of N fertiliser form and environmental conditions. *Biology and Fertiity ofl Soils* **25**, 252-260.

Clement, C. R. (1966). A simple and reliable tension table. *Journal of Soil Science* **17**(1), 133–135. https://doi.org/10.1111/j.1365-2389.1966.tb01460.x

Conn, S. J., Hocking, B., Dayod, M., Xu, B., Athman, A., Henderson, S., Aukett, L., Conn, V., Shearer, M. K., Fuentes, S., Tyerman, S. D., & Gilliham, M. (2013). Protocol: Optimising hydroponic growth systems for nutritional and physiological analysis of Arabidopsis thaliana and other plants. *Plant Methods* **9**(1). https://doi.org/10.1186/1746-4811-9-4

Cousins, A. B., & Bloom, A. J. (2004). Oxygen consumption during leaf nitrate assimilation in a $C_3$ and $C_4$ plant: The role of mitochondrial respiration. *Plant, Cell and Environment* **27**(12), 1537–1545. https://doi.org/10.1111/j.1365-3040.2004.01257.x

Cui, C., Mei, H., Liu, Y., Zhang, H., & Zheng, Y. (2017). Genetic diversity, population structure, and linkage disequilibrium of an association-mapping panel revealed by genome-wide SNP markers in sesame. *Frontiers in Plant Science* **8**. https://doi.org/10.3389/fpls.2017.01189

Dai, Y., Di, H. J., Cameron, K. C., & He, J. Z. (2013). Effects of nitrogen application rate and a nitrification inhibitor dicyandiamide on ammonia oxidizers and $N_2O$ emissions in a grazed pasture soil. *Science of the Total Environment* **465**, 125–135. https://doi.org/10.1016/j.scitotenv.2012.08.091

Davies, D. M., & Williams, P. J. (1995). The Effect of the Nitrification Inhibitor Dicyandiamide on Nitrate Leaching and Ammonia Volatilization: A UK Nitrate Sensitive Areas Perspective. *Journal of Environmental Management* **45**, 263-272.

Dayan, F. E., Rimando, A. M., Pan, Z., Baerson, S. R., Gimsing, A. L., & Duke, S. O. (2010). Sorgoleone. *Phytochemistry* **71**(10), 1032–1039. https://doi.org/10.1016/j.phytochem.2010.03.011

de Klein, C. A. M., Bowatte, S., Simon, P. L., Arango, J., Cardenas, L. M., Chadwick, D. R., Pijlman, J., Rees, R. M., Richards, K. G., Subbarao, G. v., & Whitehead, D. (2022). Accelerating the development of biological nitrification inhibition as a viable nitrous oxide mitigation

strategy in grazed livestock systems. *Biology and Fertility of Soils* **58**(3), 235–240. https://doi.org/10.1007/s00374-022-01631-2

Devkota, K. P., Pasuquin, E., Elmido-Mabilangan, A., Dikitanan, R., Singleton, G. R., Stuart, A. M., Vithoonjit, D., Vidiyangkura, L., Pustika, A. B., Afriani, R., Listyowati, C. L., Keerthisena, R. S. K., Kieu, N. T., Malabayabas, A. J., Hu, R., Pan, J., & Beebout, S. E. J. (2019). Economic and environmental indicators of sustainable rice cultivation: A comparison across intensive irrigated rice cropping systems in six Asian countries. *Ecological Indicators* **105**, 199–214. https://doi.org/10.1016/j.ecolind.2019.05.029

Di, H. J., Cameron, K. C., Shen, J. P., Winefield, C. S., O'Callaghan, M., Bowatte, S., & He, J. Z. (2009). Nitrification driven by bacteria and not archaea in nitrogen-rich grassland soils. *Nature Geoscience* **2**(9), 621–624. https://doi.org/10.1038/ngeo613

Dinnes, D. L., Karlen, D. L., Jaynes, D. B., Kaspar, T. C., Hatfield, J. L., Colvin, T. S., & Cambardella, C. A. (2002). Nitrogen Management Strategies to Reduce Nitrate Leaching in Tile-Drained Midwestern Soils. *Agronomy Journal* **94**(1), 153–171. https://doi.org/10.2134/agronj2002.1530

Djaman, K., Mel, V. C., Diop, L., Sow, A., El-Namaky, R., Manneh, B., Saito, K., Futakuchi, K., & Irmak, S. (2018). Effects of alternate wetting and drying irrigation regime and nitrogen fertilizer on yield and nitrogen use efficiency of irrigated rice in the Sahel. *Water* **10**. https://doi.org/10.3390/w10060711

Dong, N. Q., & Lin, H. X. (2020). Higher yield with less nitrogen fertilizer. *Nature Plants* **6**(9), 1078–1079. https://doi.org/10.1038/s41477-020-00763-3

Drury, C., Hart, S., & Yang, X. (2007). Nitrification techniques for soils. In: Soil Sampling and Methods of Analysis. https://www.researchgate.net/publication/305371878

Duxbury, J. M., Bouldin, D. R., Terry, R. E., & Tate, R. L. (1982). Emissions of nitrous oxide from soils. *Nature* **298**(5873), 462–464. https://doi.org/10.1038/298462a0

EEA. (2010). Annual European Union greenhouse gas inventory 1990-2008 and inventory report 2010. EPA technical report 6/2010.

Engels, C., & Marschner, H. (1995). Plant uptake and utilisation of nitrogen. *Nitrogen Fertilisation in the Environment.*, 41–81. Marcel Dekker, Inc.

Enwall, K., Philippot, L., & Hallin, S. (2005). Activity and composition of the denitrifying bacterial community respond differently to long-term fertilization. *Applied and Environmental Microbiology* **71**(12), 8335–8343. https://doi.org/10.1128/AEM.71.12.8335-8343.2005

Faeflen, S. J., Li, S., Xin, X., Wright, A. L., & Jiang, X. (2016). Autotrophic and Heterotrophic Nitrification in a Highly Acidic Subtropical Pine Forest Soil. *Pedosphere* **26**(6), 904–910). https://doi.org/10.1016/S1002-0160(15)60095-9

FAOSTAT (2019). http://www.fao.org/faostat/en/#data/EF?visualise

Fillery, I. R. P. (2007). Plant-based manipulation of nitrification in soil: A new approach to managing N loss? *Plant and Soil* **294**(1–2), 1–4). https://doi.org/10.1007/s11104-007-9263-z

Finnemann, J., & Schjoerring, J. K. (1999). Translocation of $NH_4^+$ in oilseed rape plants in relation to glutamine synthetase isogene expression and activity. *Physiologia Plantarum* **105**(3), 469–477.

Finzi, A. C., & Berthrong, S. T. (2005). The uptake of amino acids by microbes and trees in three cold-temperate forests. *Ecology* **86**(12), 3345–3353. https://doi.org/10.1890/04-1460

Firestone, M. K., & Davidson, E. A. (1989). Microbiological basis of NO and $N_2O$ production and consumption in soil. *Exchange of trace gases between terrestrial ecosystems and the atmosphere*, 7–21.

Firestone, M. K., Smith, M. S., Firestone, R. B., & Tiedje, J. M. (1979). The Influence of Nitrate, Nitrite, and Oxygen on the Composition of the Gaseous Products of Denitrification in Soil. *Soil Science*

*Society of America Journal* **43**(6), 1140–1144. https://doi.org/10.2136/sssaj1979.03615995004300060016x

Fischer, R. A. (1993). Irrigated spring wheat and timing and amount of nitrogen fertilizer. II. Physiology of grain yield response. *Field Crops Research* **33**, 57-80.

Forster, P., Ramaswamy, V., Artaxo, P., Berntsen, T., Betts, R., Fahey, D. W., Haywood, J., Lean, J., Lowe, D. C., Myhre, G., Nganga, J., Prinn, R., Raga, G., Schulz, M., & von Dorland, R. (2007). Changes in atmospheric constituents and in radiative forcing. In: Solomon, S., Qin, D., Manning, M., Chen, Z., Marquis, M., Averyt, K. B., Tignor, M., Miller, H. L. (Eds.), Climate change 2007: the physical science basis. Contribution of working group I t. *Cambridge University Press*, 129–234. https://doi.org/10.1103/PhysRevB.77.220407

Galloway, J. N., Dentener, F. J., Capone, D. G., Boyer, E. W., Howarth, R. W., Seitzinger, S. P., Asner, G. P., Cleveland, C. C., Green, P. A., Holland, E. A., Karl, D. M., Michaels, A. F., Porter, J. H., Townsend, A. R., & Vorosmarty, C. J. (2004). Nitrogen cycles: past, present, and future. *Biogeochemistry* **70**, 153-206.

Garcia-Ruiz, R., Pattinson, S. N., & Whitton, B. A. (1998). Nitrous oxide production in the river swale-ouse, North-east England. *Water Research* **33**(5), 1231-1237.

Gaskell, J. F., Blackmer, A. M., & Bremner, J. M. (1981). Comparison of Effects of Nitrate, Nitrite, and Nitric Oxide on Reduction of Nitrous Oxide to Dinitrogen by Soil Microorganisms. *Soil Science Society of America Journal* **45**(6), 1124–1127. https://doi.org/10.2136/sssaj1981.03615995004500060022x

Gerendás, J., Zhu, Z., Bendixen, R., Ratcliffe, R. G., & Sattelmacher, B. (1997). Physiological and biochemical processes related to ammonium toxicity in higher plants. *Journal of Plant Nutrition and Soil Science* **160**(3), 239–251. https://doi.org/10.1002/jpln.19971600218

Gilch, S., Meyer, O., & Schmidt, I. (2009). A soluble form of ammonia monooxygenase in Nitrosomonas europaea. *Biological Chemistry* **390**(9), 863–873. https://doi.org/10.1515/BC.2009.085

Giles, M. E., Daniell, T. J., & Baggs, E. M. (2017). Compound driven differences in $N_2$ and $N_2O$ emission from soil; the role of substrate use efficiency and the microbial community. *Soil Biology and Biochemistry* **106**, 90–98.

Giles, M., Morley, N., Baggs, E. M., & Daniell, T. J. (2012). Soil nitrate reducing processes - Drivers, mechanisms for spatial variation, and significance for nitrous oxide production. *Frontiers in Microbiology* **3**, 1–16. https://doi.org/10.3389/fmicb.2012.00407

Giltrap, D. L., Singh, J., Saggar, S., & Zaman, M. (2010). A preliminary study to model the effects of a nitrification inhibitor on nitrous oxide emissions from urine-amended pasture. *Agriculture, Ecosystems and Environment* **136**(3–4), 310–317. https://doi.org/10.1016/j.agee.2009.08.007

Glass, A. D. M. (2003). Nitrogen Use Efficiency of Crop Plants: Physiological Constraints upon Nitrogen Absorption. *Critical Reviews in Plant Sciences* **22**(5), 453–470). https://doi.org/10.1080/07352680390243512

González-Cabaleiro, R., Curtis, T. P., & Ofiţeru, I. D. (2019). Bioenergetics analysis of ammonia-oxidizing bacteria and the estimation of their maximum growth yield. *Water Research* **154**, 238–245. https://doi.org/10.1016/j.watres.2019.01.054

Gopalakrishnan, S., Watanabe, T., Pearse, S. J., Ito, O., Hossain, Z. A. K. M., & Subbarao, G. v. (2009). Biological nitrification inhibition by *Brachiaria humidicola* roots varies with soil type and inhibits nitrifying bacteria, but not other major soil microorganisms. *Soil Science and Plant Nutrition* **55**(5), 725–733. https://doi.org/10.1111/j.1747-0765.2009.00398.x

Goreau, T. J., Kaplan, W. A., Wofsy, S. C., McElroy, M. B., Valois, F. W., & Watson, S. W. (1980). Production of $NO_2^-$ and $N_2O$ by Nitrifying Bacteria at Reduced Concentrations of Oxygen. *Applied and Environmental Microbiology* **40**(3), 526–532.

Graf, D. R. H., Jones, C. M., & Hallin, S. (2014). Intergenomic comparisons highlight modularity of the denitrification pathway and underpin the importance of community structure for $N_2O$ emissions. *PLoS ONE* **9**(12). https://doi.org/10.1371/journal.pone.0114118

Granier, C., Aguirrezabal, L., Chenu, K., Cookson, S. J., Dauzat, M., Hamard, P., Thioux, J. J., Rolland, G., Bouchier-Combaud, S., Lebaudy, A., Muller, B., Simonneau, T., & Tardieu, F. (2006). PHENOPSIS, an automated platform for reproducible phenotyping of plant responses to soil water deficit in *Arabidopsis thaliana* permitted the identification of an accession with low sensitivity to soil water deficit. *New Phytologist* **169**(3), 623–635. https://doi.org/10.1111/j.1469-8137.2005.01609.x

Grundmann, G. L., Renault, P., Rosso, L., & Bardin, R. (1995). Differential Effects of Soil Water Content and Temperature on Nitrification and Aeration. *Soil Science Society of America Journal* **59**(5), 1342–1349. https://doi.org/10.2136/sssaj1995.03615995005900050021x

Gubry-Rangin, C., Nicol, G. W., & Prosser, J. I. (2010). Archaea rather than bacteria control nitrification in two agricultural acidic soils. *FEMS Microbiology Ecology* **74**(3), 566–574. https://doi.org/10.1111/j.1574-6941.2010.00971.x

Harrison, K. A., Bol, R., & Bardgett, R. D. (2007). Preferences for uptake of different nitrogen forms by co-existing plant species and soil microbes. *Ecology* **88**(4), 989–999. https://doi.org/10.1890/06-1018

Hayatsu, M., Tago, K., & Saito, M. (2008). Various players in the nitrogen cycle: Diversity and functions of the microorganisms involved in nitrification and denitrification. *Soil Science and Plant Nutrition* **54**(1), 33–45. https://doi.org/10.1111/j.1747-0765.2007.00195.x

Haynes, R. J., & Goh, K. M. (1978). Ammonium and nitrate nutrition of plants. *Biological Reviews* **53**(4), 465–510. https://doi.org/10.1111/j.1469-185x.1978.tb00862.x

Henry, H. A. L., & Jefferies, R. L. (2003). Plant amino acid uptake, soluble N turnover and microbial N capture in soils of a grazed Arctic salt marsh. *Journal of Ecology* **91**(4), 627–636. https://doi.org/10.1046/j.1365-2745.2003.00791.x

Henry, S., Texier, S., Hallet, S., Bru, D., Dambreville, C., Chèneby, D., Bizouard, F., Germon, J. C., & Philippot, L. (2008). Disentangling the rhizosphere effect on nitrate reducers and denitrifiers: Insight into the role of root exudates. *Environmental Microbiology* **10**(11), 3082–3092. https://doi.org/10.1111/j.1462-2920.2008.01599.x

Hernandez, D., & Rowe, J. J. (1987). Oxygen Regulation of Nitrate Uptake in Denitrifying Pseudomonas aeruginosa. *Applied and Environmental Microbiology* **53**(4), 745-750.

Herold, M. B., Baggs, E. M., & Daniell, T. J. (2012). Fungal and bacterial denitrification are differently affected by long-term pH amendment and cultivation of arable soil. *Soil Biology and Biochemistry* **54**, 25–35. https://doi.org/10.1016/j.soilbio.2012.04.031

Herold, M. B., Giles, M. E., Alexander, C. J., Baggs, E. M., & Daniell, T. J. (2018). Variable response of *nirK* and *nirS* containing denitrifier communities to long-term pH manipulation and cultivation. *FEMS Microbiology Letters* **365**(7). https://doi.org/10.1093/femsle/fny035

Hirsch, P. R., Miller, A. J., & Dennis, P. G. (2013). Do Root Exudates Exert More Influence on Rhizosphere Bacterial Community Structure Than Other Rhizodeposits? *Molecular Microbial Ecology of the Rhizosphere*, 229–242. https://doi.org/10.1002/9781118297674.ch22

*Hoorman (2016). Role of Soil Bacteria | Ohioline*.

Houlton, B. Z., Sigman, D. M., Schuur, E. A. G., & Hedin, L. O. (2007). A climate-driven switch in plant nitrogen acquisition within tropical forest communities*. Proceedings for the National Academy of Sciences of the United States of America* **104**(21), 8902-8906.

Hu, H. W., Macdonald, C. A., Trivedi, P., Anderson, I. C., Zheng, Y., Holmes, B., Bodrossy, L., Wang, J. T., He, J. Z., & Singh, B. K. (2016). Effects of climate warming and elevated $CO_2$ on autotrophic nitrification and nitrifiers in dryland ecosystems. *Soil Biology and Biochemistry* **92**, 1–15. https://doi.org/10.1016/j.soilbio.2015.09.008

Hu, L., Dong, Z., Wang, Z., Xiao, L., & Zhu, B. (2022). The contributions of ammonia oxidizing bacteria and archaea to nitrification-dependent $N_2O$ emission in alkaline and neutral purple soils. *Scientific Reports* **12**(1). https://doi.org/10.1038/s41598-022-23084-1

Huangfu, C., Li, H., Chen, X., Liu, H., Wang, H., & Yang, D. (2016). Response of an invasive plant, *Flaveria bidentis*, to nitrogen addition: a test of form-preference uptake. *Biological Invasions* **18**(11), 3365–3380. https://doi.org/10.1007/s10530-016-1231-1

Hughes, J., Hepworth, C., Dutton, C., Dunn, J. A., Hunt, L., Stephens, J., Waugh, R., Cameron, D. D., & Gray, J. E. (2017). Reducing stomatal density in barley improves drought tolerance without impacting on yield. *Plant Physiology* **174**(2), 776–787. https://doi.org/10.1104/pp.16.01844

Iizumi, T., Mizumoto, M., & Nakamura, K. (1998). A Bioluminescence Assay Using *Nitrosomonas europaea* for Rapid and Sensitive Detection of Nitrification Inhibitors. Applied and Environmental Microbiology 64(10), 3656-3662.

Jarvis, S. C., Stockdale, E. A., Shepherd, M. A., & Powlson, D. S. (1996). Nitrogen Mineralization in Temperate Agricultural Soils: Processes and Measurement. *Advances in Agronomy* **57,** 187–235. https://doi.org/10.1016/S0065-2113(08)60925-6

Jia, Z., & Conrad, R. (2009). Bacteria rather than Archaea dominate microbial ammonia oxidation in an agricultural soil. *Environmental Microbiology* **11**(7), 1658–1671. https://doi.org/10.1111/j.1462-2920.2009.01891.x

Jones, C. M., Graf, D. R. H., Bru, D., Philippot, L., & Hallin, S. (2013). The unaccounted yet abundant nitrous oxide-reducing microbial community: A potential nitrous oxide sink. *ISME Journal* **7**(2), 417–426. https://doi.org/10.1038/ismej.2012.125

Kanter, D., Mauzerall, D. L., Ravishankara, A. R., Daniel, J. S., Portmann, R. W., Grabiel, P. M., Moomaw, W. R., & Galloway, J. N. (2013). A post-Kyoto partner: Considering the stratospheric ozone regime as a tool to manage nitrous oxide. In *Proceedings of the National Academy of Sciences of the United States of America* **110**(12), 4451–4457. https://doi.org/10.1073/pnas.1222231110

Kielland, K. (1994). Amino Acid Absorption by Arctic Plants: Implications for Plant Nutrition and Nitrogen Cycling. *Ecology*,**75**(8), 2373-2383. https://doi.org/10.2307/1940891

Kirk, G. J. D. (2001). Plant-mediated processes to acquire nutrients: nitrogen uptake by rice plants. *Plant and Soil* **232**, 129-134.

Kirk, G. J. D., & Kronzucker, H. J. (2005). The potential for nitrification and nitrate uptake in the rhizosphere of wetland plants: A modelling study. *Annals of Botany* **96**(4), 639–646. https://doi.org/10.1093/aob/mci216

Kirkby, E. A. (1968). Influence of ammonium and nitrate nutrition on the cation-anion balance and nitrogen and carbohydrate metabolism of white mustard plants grown in dilute nutrient solutions. *Soil Science* **105**(3), 133–141.

Klemedtsson, L., Svensson, B. H., & Rosswall, T. (1987). Dinitrogen and nitrous oxide produced by denitrification and nitrification in soil with and without barley plants. *Plant and Soil* **99**, 303-319.

Knowles (1982). Denitrification. *Microbiological Reviews,* 43-70.

Kodama, O., Miyakawa, J., Akatsuka, T., & Kiyosawa, S. (1992). Sakuranetin, a flavanone phytoalexin from ultraviolet-irradiated rice leaves*. Phytochemistry* **31**(11), 3807-3809.

Kronzucker, H. J., Schjoerring, J. K., Enter, Y., Kirk, G. J. D., Yaeesh Siddiqi, M., & Glass, A. D. M. (1998). Dynamic interactions between root influx and long-distance N translocation in rice: Insights into feedback processes. *Plant and Cell Physiology* **39**(12), 1287–1293. https://doi.org/10.1093/oxfordjournals.pcp.a029332

Kurimoto, K., Day, D. A., Lambers, H., & Noguchi, K. (2004). Effect of respiratory homeostasis on plant growth in cultivars of wheat and rice. *Plant, Cell and Environment* **27**(7), 853–862. https://doi.org/10.1111/j.1365-3040.2004.01191.x

Kuzyakov and Domanski (2000). Carbon input by plants into the soil. Review. *Journal of Plant Nutrition and Soil Science* **163**, 421-431.

Lam, S. K., Suter, H., Mosier, A. R., & Chen, D. (2017). Using nitrification inhibitors to mitigate agricultural $N_2O$ emission: a double-edged sword? *Global Change Biology* **23**(2), 485–489. https://doi.org/10.1111/gcb.13338

Lan, T., Suter, H., Liu, R., Yuan, S., & Chen, D. (2018). Effects of nitrification inhibitors on gross N nitrification rate, ammonia oxidizers, and $N_2O$ production under different temperatures in two pasture soils. *Environmental Science and Pollution Research* **25**(28), 28344–28354. https://doi.org/10.1007/s11356-018-2873-6

Langarica-Fuentes, A., Manrubia, M., Giles, M. E., Mitchell, S., & Daniell, T. J. (2018). Effect of model root exudate on denitrifier community dynamics and activity at different water-filled pore space levels in a fertilised soil. *Soil Biology and Biochemistry* **120**, 70–79. https://doi.org/10.1016/j.soilbio.2018.01.034

Larsen, K. S., Andresen, L. C., Beier, C., Jonasson, S., Albert, K. R., Ambus, P., Arndal, M. F., Carter, M. S., Christensen, S., Holmstrup, M., Ibrom, A., Kongstad, J., van der Linden, L., Maraldo, K., Michelsen, A., Mikkelsen, T. N., Pilegaard, K., Priemé, A., Ro-Poulsen, H., … Stevnbak, K. (2011). Reduced N cycling in response to elevated $CO_2$, warming, and drought in a Danish heathland: Synthesizing results of the CLIMAITE project after two years of treatments.

*Global Change Biology* **17**(5), 1884–1899. https://doi.org/10.1111/j.1365-2486.2010.02351.x

Leininger, S., Urich, T., Schloter, M., Schwark, L., Qi, J., Nicol, G. W., Prosser, J. I., Schuster, S. C., & Schleper, C. (2006). Archaea predominate among ammonia-oxidizing prokaryotes in soils. *Nature* **442**(7104), 806–809. https://doi.org/10.1038/nature04983

Lewis, O. A. M. (1992). *Plants and nitrogen.* Cambridge University Press.

Lewis, O. A. M., & Chadwick, S. (1983). An $^{15}N$ investigation into nitrogen assimilation in hydroponically-grown barley (*Hordeum vulgare* L. cv. Clipper) in response to nitrate and ammonium nutrition. *New Phytologist* **95**(4), 635–646. https://doi.org/10.1111/j.1469-8137.1983.tb03527.x

Lewis, O. A. M., Soares, M. I. M., & Lips, S. H. (1986). A photosynthetic and N investigation of the differential growth response of barley to nitrate, ammonium and nitrate + ammonium nutrition. In H. Lambers, J. J. Neeteson, & I. Stulen (Eds.), *Fundamental, Ecological and Agricultural Aspects of Nitrogen Metabolism in Higher Plants,* 295–300.

Li, G., Dong, G., Li, B., Li, Q., Kronzucker, H. J., & Shi, W. (2012). Isolation and characterization of a novel ammonium overly sensitive mutant, *amos2*, in *Arabidopsis thaliana*. *Planta* **235**(2), 239–252. https://doi.org/10.1007/s00425-011-1504-y

Li, Y., Chapman, S. J., Nicol, G. W., & Yao, H. (2018). Nitrification and nitrifiers in acidic soils. *Soil Biology and Biochemistry* **116**, 290–301. https://doi.org/10.1016/j.soilbio.2017.10.023

Li, Y. L., Fan, X. R., & Shen, Q. R. (2008). The relationship between rhizosphere nitrification and nitrogen-use efficiency in rice plants. *Plant, Cell and Environment* **31**(1), 73–85. https://doi.org/10.1111/j.1365-3040.2007.01737.x

Lipson, D. A., & Monson, R. K. (1998). Plant-microbe competition for soil amino acids in the alpine tundra: effects of freeze-thaw and dry-rewet events. *Oecologica* **113**, 406-414

Liu, B., Mørkved, P. T., Frostegård, Å., & Bakken, L. R. (2010). Denitrification gene pools, transcription and kinetics of NO, N 2O and N2 production as affected by soil pH. *FEMS Microbiology Ecology* **72**(3), 407–417. https://doi.org/10.1111/j.1574-6941.2010.00856.x

Liu, R., Suter, H., He, J., Hayden, H., & Chen, D. (2015). Influence of temperature and moisture on the relative contributions of heterotrophic and autotrophic nitrification to gross nitrification in an acid cropping soil. *Journal of Soils and Sediments* **15**(11), 2304–2309. https://doi.org/10.1007/s11368-015-1170-y

Lu, Y., Zhang, X., Jiang, J., Kronzucker, H. J., Shen, W., & Shi, W. (2019). Effects of the biological nitrification inhibitor 1,9-decanediol on nitrification and ammonia oxidizers in three agricultural soils. *Soil Biology and Biochemistry* **129**, 48–59. https://doi.org/10.1016/j.soilbio.2018.11.008

Ma, L., Jiang, X., Liu, G., Yao, L., Liu, W., Pan, Y., & Zuo, Y. (2020). Environmental Factors and Microbial Diversity and Abundance Jointly Regulate Soil Nitrogen and Carbon Biogeochemical Processes in Tibetan Wetlands. *Environmental Science and Technology* **54**(6), 3267–3277. https://doi.org/10.1021/acs.est.9b06716

Ma, Q., Cao, X., Wu, L., Mi, W., & Feng, Y. (2016). Light intensity affects the uptake and metabolism of glycine by pakchoi (*Brassica chinensis* L.). *Scientific Reports* **6**. https://doi.org/10.1038/srep21200

Magalhães, J. R., Machado, A. T., & Huber, D. M. (1995). Similarities in response of maize genotypes to water logging and ammonium toxicity. *Journal of Plant Nutrition* **18**(11), 2339–2346. https://doi.org/10.1080/01904169509365069

Mahmood, R., Yaseen, M., Ali, A., Iqbal, J., Sarwar, M., & Hussain, S. (2011). Effect of rate and application depth matrix-I calcium carbide based formulation on growth, yield and nitrogen uptake of wheat. *African Journal of Agricultural Research* **6**(30), 6363–6368. https://doi.org/10.5897/AJAR11.1420

Mahmood, T., Ali, · R, Malik, K. A., Shamsi, · S R A, & Shamsi, S. R. A. (1997). Denitrification with and without maize plants (*Zea mays* L.) under irrigated field conditions. *Biology and Fertility of Soils* **24**, 323-328.

Mahmud, K., Panday, D., Mergoum, A., & Missaoui, A. (2021). Nitrogen losses and potential mitigation strategies for a sustainable agroecosystem. *Sustainability* **13**(4), 1–23. https://doi.org/10.3390/su13042400

Marschner, H. (2008). *Mineral nutrition of higher plants.* (2nd ed.). Academic Press.

Ming, H., Zhang, H., Chen, Q., Wang, Y., Su, J., Zhao, X., & Fan, J. (2020). Abundance and community structure of ammonium monooxygenase (*amoA*) genes in the wet season of liaohe estuary sediments. *Continental Shelf Research* **209**. https://doi.org/10.1016/j.csr.2020.104253

Miranda, K. M., Espey, M. G., & Wink, D. A. (2001). A rapid, simple spectrophotometric method for simultaneous detection of nitrate and nitrite. *Nitric Oxide - Biology and Chemistry* **5**(1), 62–71. https://doi.org/10.1006/niox.2000.0319

Morley, N., & Baggs, E. M. (2010). Carbon and oxygen controls on $N_2O$ and $N_2$ production during nitrate reduction. *Soil Biology and Biochemistry* **42**(10), 1864–1871. https://doi.org/10.1016/j.soilbio.2010.07.008

Morley, N., Baggs, E. M., Dorsch, P., & Bakken, L. (2008). Production of NO, $N_2O$ and $N_2$ by extracted soil bacteria, regulation by $NO_2$, $N_2O$ and $O_2$ concentrations. *FEMS Microbiology Ecology* **65**(1), 102–112. https://doi.org/10.1111/j.1574-6941.2008.00495.x

Morley, N. J., Richardson, D. J., & Baggs, E. M. (2014). Substrate induced denitrification over or underestimates shifts in soil $N_2/N_2O$ ratios. *PLoS ONE* **9**(9). https://doi.org/10.1371/journal.pone.0108144

Nasholm, T., Ekblad, A., Nordin, R., Giesler, M., HÖgberg, M., & HÖgberg, P. (1998). Boreal forest plants take up organic nitrogen. *Nature* **392**, 914-916.

Newton, A. C., Flavell, A. J., George, T. S., Leat, P., Mullholland, B., Ramsay, L., Revoredo-Giha, C., Russell, J., Steffenson, B. J., Swanston, J. S., Thomas, W. T. B., Waugh, R., White, P. J., & Bingham, I. J. (2011). Crops that feed the world 4. Barley: a resilient crop? Strengths and weaknesses in the context of food security. *Food Security* **3**(2), 141–178. https://doi.org/10.1007/s12571-011-0126-3

Nguyen, C. (2003). Rhizodeposition of organic C by plants: mechanisms and controls. *Agronomie* **23**(5–6), 375–396. https://doi.org/10.1051/agro:2003011

Niboyet, A., le Roux, X., Dijkstra, P., Hungate, B. A., Barthes, L., Blankinship, J. C., Brown, J. R., Field, C. B., & Leadley, P. W. (2011). Testing interactive effects of global environmental changes on soil nitrogen cycling. *Ecosphere* **2**(5). https://doi.org/10.1890/ES10-00148.1

Nordin, A., Högberg, P., & Näsholm, T. (2001). Soil nitrogen form and plant nitrogen uptake along a boreal forest productivity gradient. *Oecologia* **129**(1), 125–132. https://doi.org/10.1007/s004420100698

Nordin, A., Schmidt, I. K., & Shaver, G. R. (2004). Nitrogen uptake by arctic soil microbes and plants in relation to soil nitrogen supply. *Ecology* **85**(4), 955–962. https://doi.org/10.1890/03-0084

Norton, J. M., Alzerreca, J. J., Suwa, Y. & Klotz, M. G. (2002). Diversity of ammonia monooxygenase operon in autotrophic ammonia-oxidising bacteria. *Archives of Microbiology* **177**, 139-149. DOI 10.1007/s00203-001-0369-z

Norton, J., & Ouyang, Y. (2019). Controls and adaptive management of nitrification in agricultural soils. *Frontiers in Microbiology* **10.** https://doi.org/10.3389/fmicb.2019.01931

O'connor, A. (2018). *SPICe Briefing Paper SPICe. Brewing and distilling in Scotland-economic facts and figures*.

Offre, P., Prosser, J. I., & Nicol, G. W. (2009). Growth of ammonia-oxidizing archaea in soil microcosms is inhibited by acetylene. *FEMS Microbiology Ecology* **70**(1), 99–108. https://doi.org/10.1111/j.1574-6941.2009.00725.x

Ohte, N., Tokuchi', N., & Suzukib, M. (1997). An in situ lysimeter experiment on soil moisture influence on inorganic nitrogen discharge from forest soil Nitrogen cycling plays an important role in the hydrobiochemical phenomena in forest ecosystems. Many forest ecologists have extensively investigated to evaluate the. *Journal of Hydrology* **195**.

Onley, J. R., Ahsan, S., Sanford, R. A., & Löffler, F. E. (2018). Denitrification by *Anaeromyxobacter dehalogenans*, a common soil bacterium lacking the nitrite reductase genes *nirS* and *nirK*. *Applied and Environmental Microbiology* **84**(4). https://doi.org/10.1128/AEM.01985-17

Ortiz, D., Litvin, A. G., & Salas Fernandez, M. G. (2018). A cost-effective and customizable automated irrigation system for precise high-throughput phenotyping in drought stress studies. *PLoS ONE* **13**(6). https://doi.org/10.1371/journal.pone.0198546

Osborne, B. B., Baron, J. S., & Wallenstein, M. D. (2016). Moisture and temperature controls on nitrification differ among ammonia oxidizer communities from three alpine soil habitats. *Frontiers of Earth Science* **10**(1), 1–12. https://doi.org/10.1007/s11707-015-0556-x

Ouyang, Y., Norton, J. M., & Stark, J. M. (2017). Ammonium availability and temperature control contributions of ammonia oxidizing bacteria and archaea to nitrification in an agricultural soil. *Soil Biology and Biochemistry* **113**, 161–172. https://doi.org/10.1016/j.soilbio.2017.06.010

Overthrow, R. (2005). Nitrogen management in spring malting barley for optimum yield and quality. *HGCA Project Report 367.*

Patel, M. C. S. V., Lal, M., Patel, R. N. S. V., & Patel, S. Y. S. V. (2019). *Role of polymer coated fertilizers (PCFS) an advance technology for improving nutrient use efficiency and crop productivity: A review Publication and Project Review Recognition View project Resource conservation*

*technologies for sustainable development of agriculture View project*. https://www.researchgate.net/publication/338187675

Payne, W. (1981). The status of nitric oxide and nitrous oxide as intermediates in denitrification. C.C. Delwiche (Ed.), Denitrification, Nitrification and Atmospheric Nitrous Oxide, Wiley, New York, 85-103.

Peng, S., Buresh, R. J., Huang, J., Zhong, X., Zou, Y., Yang, J., Wang, G., Liu, Y., Hu, R., Tang, Q., Cui, K., Zhang, F., & Dobermann, A. (2010). Improving nitrogen fertilization in rice by site-specific N management. A review. *Agronomy for Sustainable Development* **30**(3), 649–656). https://doi.org/10.1051/agro/2010002

Pérez-Lucas, G., Vela, N., Aatik, A. el, & Navarro, S. (2019). Environmental Risk of Groundwater Pollution by Pesticide Leaching through the Soil Profile. www.intechopen.com

Pervin, S. (2022). Understanding the Interaction of Rice (*Oryza sativa* L.) with Soil Nitrification and Microbial Community in Paddy Soil*. The University of Sheffield.*

Philippot, L. (2002). Denitrifying genes in bacterial and Archaeal genomes. *Biochimica et Biophysica Acta* **1577**, 355-376.

Philippot, L., Raaijmakers, J. M., Lemanceau, P., & van der Putten, W. H. (2013). Going back to the roots: The microbial ecology of the rhizosphere. *Nature Reviews Microbiology* **11**(11), 789–799. https://doi.org/10.1038/nrmicro3109

Power, J., & Prasad, R. (1997). Nitrification inhibitors for agriculture, health, and the environment. *Advances in Agronomy* **54**.

Puttanna, K., Nanje Gowda, N. M., & Rao, E. V. S. P. (1999). Effect of concentration, temperature, moisture, liming and organic matter on the efficacy of the nitrification inhibitors benzotriazole, o-nitrophenol, m-nitroaniline and dicyandiamide. *Nutrient Cycling in Agroecosystems* **54**.

Qin, R., Su, C., Liu, W., Tang, L., Li, X., Deng, X., Wang, A., & Chen, Z. (2020). Effects of exposure to polyether sulfone microplastic on the nitrifying process and microbial community structure in aerobic granular sludge. *Bioresource Technology* **302**. https://doi.org/10.1016/j.biortech.2020.122827

Raab, T. K., Lipson, D. A., & Monson, R. K. (1999). Soil amino acid utilization among species of the *Cyperaceae*: Plant and soil processes. *Ecology* **80**(7), 2408–2419. https://doi.org/10.1890/0012-9658(1999)080[2408:SAAUAS]2.0.CO;2

Rani, S., Koh, H. W., Rhee, S. K., Fujitani, H., & Park, S. J. (2017). Detection and Diversity of the Nitrite Oxidoreductase Alpha Subunit (*nxrA*) Gene of *Nitrospina* in Marine Sediments. *Microbial Ecology* **73**(1), 111–122. https://doi.org/10.1007/s00248-016-0897-3

Raun, W. R., & Johnson, G. v. (1999). Improving nitrogen use efficiency for cereal production. In *Agronomy Journal* **91**(3), 357–363). American Society of Agronomy. https://doi.org/10.2134/agronj1999.00021962009100030001x

Raven, J. A. (1985). TANSLEY REVIEW No. 2: Regulation of pH and generation of osmolarity in vascular plants: a cost-benefit analysis in relation to efficiency of use of energy, nitrogen and water. *New Phytologist* **101**(1), 25–77. https://doi.org/10.1111/j.1469-8137.1985.tb02816.x

Ravishankara, A. R., Daniel, J. S., & Portmann, R. W. (2009). Nitrous oxide ($N_2O$): The dominant Ozone-depleting substance emitted in the 21st Century. *Science* **326**(5949), 123–125.

R Core team (2016). R: A language and environment for statistical computing. R Foundation for statistical computing: Vienna, Austria. https://www.R-project.org/

Richardson, D. J. (2000). SGM SPECIAL LECTURE 1999 Fleming Lecture Bacterial respiration : a flexible process for a changing environment. *Microbiology* **146**.

Robertson, G. P., & Groffman, P. M. (2006). Nitrogen transformations. In *Soil Microbiology, Ecology and Biochemistry: Third Edition*, 341–364. Elsevier. https://doi.org/10.1016/b978-0-12-415955-6.00014-1

Romano, N., Hopmans, J. W., & Dane, J. (2002). *Suction table*. https://www.researchgate.net/publication/288937037

Rychel, K., Meurer, K. H. E., Börjesson, G., Strömgren, M., Getahun, G. T., Kirchmann, H., & Kätterer, T. (2020). Deep N fertilizer placement mitigated $N_2O$ emissions in a Swedish field trial with cereals. *Nutrient Cycling in Agroecosystems* **118**(2), 133–148. https://doi.org/10.1007/s10705-020-10089-3

Sadhukhan, R., Jatav, H. S., Sen, S., Sharma, L. D., Rajput, V. D., Thangjam, R., Devedee, A. K., Singh, S. K., Gorovtsov, A., Choudhury, S., & Patra, K. (2022). Biological nitrification inhibition for sustainable crop production. In *Plant Perspectives to Global Climate Changes*, 135–150. Elsevier. https://doi.org/10.1016/B978-0-323-85665-2.00007-8

Sahrawat, K. L., & Keeney, D. R. (1985). Perspectives for research on development of nitrification inhibitors. *Communications in Soil Science and Plant Analysis* **16**(5), 517–524. https://doi.org/10.1080/00103628509367624

Salsac, L., Chaillou, S., Morot-Gaudry, J. F., Lesaint, C., & Jolivoe, E. (1987). Nitrate and ammonium nutrition in plants. *Plant Physiology and Biochemistry* **25**, 805–812.

Sarasketa, A., González-Moro, M. B., González-Murua, C., & Marino, D. (2014). Exploring ammonium tolerance in a large panel of Arabidopsis thaliana natural accessions. *Journal of Experimental Botany* **65**(20), 6023–6033. https://doi.org/10.1093/jxb/eru342

Schauss, K., Focks, A., Leininger, S., Kotzerke, A., Heuer, H., Thiele-Bruhn, S., Sharma, S., Wilke, B. M., Matthies, M., Smalla, K., Munch, J. C., Amelung, W., Kaupenjohann, M., Schloter, M., & Schleper, C. (2009). Dynamics and functional relevance of ammonia-oxidizing archaea in

two agricultural soils. *Environmental Microbiology* **11**(2), 446–456. https://doi.org/10.1111/j.1462-2920.2008.01783.x

Schimel, J. P., & Chapin, F. S. (1996). Tundra Plant Uptake of Amino Acid and $NH_4^+$ Nitrogen in Situ: Plants Complete Well for Amino Acid N. *Ecology* **77**(7), 2142–2147. https://doi.org/10.2307/2265708

Schwarzer, Ch., & Haselwandter, K. (1991). Enzymatic degradation of the nitrification inhibitor dicyandiamide by a soil bacterium. *Soil Biology and Biochemistry* **23**, 309–310.

Scotch Whisky Association (2017). The Economic Impact of Scotch Whisky Production in the UK. http://www.scotch-whisky.org.uk/news-publications/publications/documents/the-economic-impact-of-scotch-whisky-production-in-the- uk/#.W6NcU2hKi71

Searles, P. S., & Bloom, A. J. (2003). Nitrate photo-assimilation in tomato leaves under short-term exposure to elevated carbon dioxide and low oxygen. *Plant, Cell and Environment* **26**(8), 1247–1255. https://doi.org/10.1046/j.1365-3040.2003.01047.x

Senbayram, M., Budai, A., Bol, R., Chadwick, D., Marton, L., Gündogan, R., & Wu, D. (2019). Soil $NO_3^-$ level and $O_2$ availability are key factors in controlling $N_2O$ reduction to $N_2$ following long-term liming of an acidic sandy soil. *Soil Biology and Biochemistry* **132**, 165–173. https://doi.org/10.1016/j.soilbio.2019.02.009

Sexstone, A. J., Revsbech, N. P., Parkin, T. B., & Tiedje, J. M. (1985). Direct Measurement of Oxygen Profiles and Denitrification Rates in Soil Aggregates. *Soil Science Society of America Journal* **49**, 645-651.

Shaw, M. R., & Harte, J. (2001). Response of nitrogen cycling to simulated climate change: Differential responses along a subalpine ecotone. *Global Change Biology* **7**(2), 193–210. https://doi.org/10.1046/j.1365-2486.2001.00390.x

Shi-Wei, G., Yi, Z., Ying-Xu, G., Yong, L., & Qi-Rong, S. (2007). New Insights into the Nitrogen Form Effect on Photosynthesis and Photorespiration . *Pedosphere* **17**(5).

Šimek, M., & Cooper, J. E. (2002). The influence of soil pH on denitrification: Progress towards the understanding of this interaction over the last 50 years. *European Journal of Soil Science* **53**(3), 345–354. https://doi.org/10.1046/j.1365-2389.2002.00461.x

Skiba, M. W., George, T. S., Baggs, E. M., & Daniell, T. J. (2011). Plant influence on nitrification. *Biochemical Society Transactions* **39**(1), 275–278. https://doi.org/10.1042/BST0390275

Skiba, U., Jones, S. K., Dragosits, U., Drewer, J., Fowler, D., Rees, R. M., Pappa, V. A., Cardenas, L., Chadwick, D., Yamulki, S., & Manning, A. J. (2012). UK emissions of the greenhouse gas nitrous oxide. In *Philosophical Transactions of the Royal Society B: Biological Sciences* **367**(1593), 1175–1185). https://doi.org/10.1098/rstb.2011.0356

Slangen, J., & Kerkhoff, P. (1984). Nitrification inhibitors in agriculture and horticulture: A literature review.

Smart, D. R., & Bloom, A. J. (2001). Wheat leaves emit nitrous oxide during nitrate assimilation. *Proceedings for the National Academy of Sciences of the United States of America* **98**(14), 7875-7878.

Smil, V. (1999). Nitrogen in crop production: An account of global flows. *Global Biogeochemical Cycles* **13**(2), 647–662. https://doi.org/10.1029/1999GB900015

Smith, K. A. (1990). Greenhouse gas fluxes between land surfaces and the atmosphere. *Progress in Physical Geography: Earth and Environment* **14**(3), 349–372. https://doi.org/10.1177/030913339001400304

Smith, K., & Arah, J. (1990). Losses of nitrogen by denitrification and emissions of nitrogen oxides from soils. *Proceedings of the Fertiliser Society* **299**.

Soler-Jofra, A., Pérez, J., & van Loosdrecht, M. C. M. (2021). Hydroxylamine and the nitrogen cycle: A review. *Water Research* **190**. https://doi.org/10.1016/j.watres.2020.116723

Stakman, W. D., Valk, G. A., & van der Harst, G. G. (1969). Determination of soil moisture retention curves, I. Sandbox apparatus range pF 0-2.7. *Publications of the Institute for Land and Water Management Research.*

Stevens, R. J., Laughlin, R. J., Burns, L. C., Arah, J. R. M., & Hood, R. C. (1997). Measuring the contributions of nitrification and denitrification to the flux of nitrous oxide from soil. *Soil Biology and* **Biochemistry** 29(2), 139-151.

Streeter, T. C., Bol, R., & Bardgett, R. D. (2000). Amino acids as a nitrogen source in temperate upland grasslands: The use of dual labelled $^{13}C$, $^{15}N$ glycine to test for direct uptake by dominant grasses. *Rapid Communications in Mass Spectrometry* **14**(15), 1351–1355. https://doi.org/10.1002/1097-0231(20000815)14:15<1351::AID-RCM23>3.0.CO;2-9

Subbarao, G., Ito, O., Sahrawat, K., Berry, W., Nakahara, K., Ishikawa, T., Watanabe, T., Suenaga, K., Rondon, M., & Rao, I. (2006b). Scope and strategies for regulation of nitrification in agricultural systems - Challenges and opportunities. *Critical Reviews in Plant Sciences* **25**(4), 303-335. https://doi.org/10.1080/07352680600794232

Subbarao, G. v., Ishikawa, T., Ito, O., Nakahara, K., Wang, H. Y., & Berry, W. L. (2006a). A bioluminescence assay to detect nitrification inhibitors released from plant roots: A case study with *Brachiaria humidicola*. *Plant and Soil* **288**(1–2), 101–112. https://doi.org/10.1007/s11104-006-9094-3

Subbarao, G. v, Nakahara, K., Ishikawa, T., Ono, H., Yoshida, M., Yoshihashi, T., Zhu, Y., Zakir, H. A. K. M., Deshpande, S. P., Hash, C. T., & Sahrawat, K. L. (2013b). Biological nitrification inhibition (BNI) activity in sorghum and its characterization. *Plant and Soil* **366**(1), 243–259.

Subbarao, G. v., Rao, I. M., Nakahara, K., Sahrawat, K. L., Ando, Y., & Kawashima, T. (2013a). Potential for biological nitrification inhibition to reduce nitrification and $N_2O$ emissions in

pasture crop-livestock systems. *Animal* **7**(2), 322–332. https://doi.org/10.1017/s1751731113000761

Subbarao, G. v., Rondon, M., Ito, O., Ishikawa, T., Rao, I. M., Nakahara, K., Lascano, C., & Berry, W. L. (2007). Biological nitrification inhibition (BNI) - Is it a widespread phenomenon? *Plant and Soil* **294**(1–2), 5–18. https://doi.org/10.1007/s11104-006-9159-3

Sun, H., Zhang, H., Powlson, D., Min, J., & Shi, W. (2015). Rice production, nitrous oxide emission and ammonia volatilization as impacted by the nitrification inhibitor 2-chloro-6-(trichloromethyl)-pyridine. *Field Crops Research* **173**, 1–7. https://doi.org/10.1016/j.fcr.2014.12.012

Sun, L., Lu, Y., Yu, F., Kronzucker, H. J., & Shi, W. (2016). Biological nitrification inhibition by rice root exudates and its relationship with nitrogen-use efficiency. *New Phytologist* **212**(3), 646–656. https://doi.org/10.1111/nph.14057

Tan, X., Shao, D., & Gu, W. (2018). Effects of temperature and soil moisture on gross nitrification and denitrification rates of a Chinese lowland paddy field soil. *Paddy and Water Environment* **16**(4), 687–698. https://doi.org/10.1007/s10333-018-0660-0

Tesfamariam, T., Yoshinaga, H., Deshpande, S. P., Srinivasa Rao, P., Sahrawat, K. L., Ando, Y., Nakahara, K., Hash, C. T., & Subbarao, G. v. (2014). Biological nitrification inhibition in sorghum: The role of sorgoleone production. *Plant and Soil* **379**(1–2), 325–335. https://doi.org/10.1007/s11104-014-2075-z

Teske, A., Alm, E., Regan, J. M., Toze, S., Rittmann, B. E., & Stahl, D. A. (1994). Evolutionary Relationships among Ammonia-and Nitrite-Oxidizing Bacteria. *Journal of Bacteriology* 176(21).

van Beusichem, M. L., Kirkby, E. A., & Baas, R. (1988). Influence of Nitrate and Ammonium Nutrition on the Uptake, Assimilation, and Distribution of Nutrients in *Ricinus communis*. *Plant Physiology* **86**, 914-921.

Venter, J. C., Remington, K., Heidelberg, J. F., Halpern, A. L., Rusch, D., Eisen, J. A., Wu, D., Paulsen, I., Nelson, K. E., Nelson, W., Fouts, D. E., Levy, S., Knap, A. H., Lomas, M. W., Nealson, K., White, O., Peterson, J., Hoffman, J., Parsons, R., …Smith, H. O. (2004). Environmental Genome Shotgun Sequencing of the Sargasso Sea. *Science* **304**(5667), 66–74. https://doi.org/10.1126/science.1093857

Vitousek, P. M., & Howarth, R. W. (1991). Nitrogen limitation on land and in the sea: How can it occur? *Biogeochemistry* **13**.

Wang, M. Y., Siddiqi, M. Y., Ruth, T. J., & Glass, A. D. M. (1993). Ammonium Uptake by Rice Roots. 1. Fluxes and Subcellular Distribution of $^{13}NH_4^+$. *Plant Physiology* **103**, 1249-1258.

Wang, L., & Macko, S. A. (2011). Constrained preferences in nitrogen uptake across plant species and environments. *Plant, Cell and Environment* **34**(3), 525–534. https://doi.org/10.1111/j.1365-3040.2010.02260.x

Wang, M., Pendall, E., Fang, C., Li, B., & Nie, M. (2018a). A global perspective on agroecosystem nitrogen cycles after returning crop residue. *Agriculture, Ecosystems and Environment* **266**, 49-54. https://doi.org/10.1016/j.agee.2018.07.019

Wang, M., Wu, Y., Zhu, J., Wang, C., Zhu, Y., & Tian, Q. (2018b). The New Developments Made in the Autotrophic and Heterotrophic Ammonia Oxidation. *IOP Conference Series: Earth and Environmental Science* **178**(1). https://doi.org/10.1088/1755-1315/178/1/012016

Wang, Q., Zhang, L. M., Shen, J. P., Du, S., Han, L. L., & He, J. Z. (2016). Effects of dicyandiamide and acetylene on $N_2O$ emissions and ammonia oxidizers in a fluvo-aquic soil applied with urea. *Environmental Science and Pollution Research* **23**(22), 23023–23033. https://doi.org/10.1007/s11356-016-7519-y

Ward, B. B. (2013). Nitrification. In *Encyclopedia of Ecology*, 351–358. Elsevier. https://doi.org/10.1016/B978-0-12-409548-9.00697-7

Webb, J., Ellis, S., Harrison, R., & Thorman, & R. (2004). Measurement of N fluxes and soil N in two arable soils in the UK. *Plant and Soil* **260**.

Weier, K. L., Doran, J. W., Power, J. F., & Walters, D. T. (1993). Denitrification and the Dinitrogen/Nitrous Oxide Ratio as Affected by Soil Water, Available Carbon, and Nitrate. *Soil Science Society of America Journal* **57**(1), 66–72. https://doi.org/10.2136/sssaj1993.03615995005700010013x

Weigelt, A., Bol, R., & Bardgett, R. D. (2005). Preferential uptake of soil nitrogen forms by grassland plant species. *Oecologia* **142**(4), 627–635. https://doi.org/10.1007/s00442-004-1765-2

Weigelt, A., King, R., Bol, R., & Bardgett, R. D. (2003). Inter-specific variability in organic nitrogen uptake of three temperate grassland species. *Journal of Plant Nutrition and Soil Science* **166**(5), 606–611. https://doi.org/10.1002/jpln.200320322

White, C. S. (1988). Nitrification Inhibition by Monoterpenoids: Theoretical Mode of Action Based on Molecular Structures. *Ecology* **69**(5), 1631-1633.

White, C. S. (1991). The Role of Monoterpenes in Soil Nitrogen Cycling Processes in Ponderosa Pine: Results from Laboratory Bioassays and Field Studies. *Biogeochemistry* **12**(1), 43-68.

Whittaker, M., Bergmann, D., Arciero, D., & Hooper, A. B. (2000). Electron transfer during the oxidation of ammonia by the chemolithotrophic bacterium *Nitrosomonas europaea*. *Biochimica et Biophysica Acta* **1459**, 346-355.

Woodward, E. E., Edwards, T. M., Givens, C. E., Kolpin, D. W., & Hladik, M. L. (2021). Widespread Use of the Nitrification Inhibitor Nitrapyrin: Assessing Benefits and Costs to Agriculture, Ecosystems, and Environmental Health. *Environmental Science and Technology* **55**(3), 1345–1353. https://doi.org/10.1021/acs.est.0c05732

Wright, C. L., Schatteman, A., Crombie, A. T., Murrell, J. C., & Lehtovirta-Morley, L. E. (2020). Inhibition of Ammonia Monooxygenase from Ammonia-Oxidizing Archaea by Linear and

Aromatic Alkynes. *Applied and Environmental Microbiology* **86**(9). https://doi.org/10.1128/AEM

Wu, L., Yuan, S., Huang, L., Sun, F., Zhu, G., Li, G., Fahad, S., Peng, S., & Wang, F. (2016). Physiological mechanisms underlying the high-grain yield and high-nitrogen use efficiency of elite rice varieties under a low rate of nitrogen application in China. *Frontiers in Plant Science* **7**. https://doi.org/10.3389/fpls.2016.01024

Xia, W., Zhang, C., Zeng, X., Feng, Y., Weng, J., Lin, X., Zhu, J., Xiong, Z., Xu, J., Cai, Z., & Jia, Z. (2011). Autotrophic growth of nitrifying community in an agricultural soil. *ISME Journal* **5**(7), 1226–1236. https://doi.org/10.1038/ismej.2011.5

Xie, W.-M., Xie, W.-M., Ma, Y., Li, S.-J., Sh, W.-M., Zhang, H.-L., Fang, F., Meng, H., Wang, G.-X., & Zhang, L.-M. (2019). Nitrogen Leaching Loss Estimation from Paddy Soil in the Taihu Lake Region of China by a Newly Developed Simple Model. *Journal of Agronomy Research* **2**(3), 19–30. https://doi.org/10.14302/issn.2639-3166.jar-19-3097

Yoshida, S., Forno, D. A., Cock, J. H., & Gomez, K. A. (1976). *Laboratory Manual for Physiological Studies of Rice*.

Zerihun, A., & Bassirirad, H. (2001). Interspecies variation in nitrogen uptake kinetic responses of temperate forest species to elevated $CO_2$: Potential causes and consequences. *Global Change Biology* **7**(2), 211–222. https://doi.org/10.1046/j.1365-2486.2001.00384.x

Zhang, Z., Gao, S., & Chu, C. (2020). Improvement of nutrient use efficiency in rice: current toolbox and future perspectives. *Theoretical and Applied Genetics* **133**(5), 1365-1384. https://doi.org/10.1007/s00122-019-03527-6

Zhu, Y., Zeng, H., Shen, Q., Ishikawa, T., & Subbarao, G. V. (2012). Interplay among $NH_4^+$ uptake, rhizosphere pH and plasma membrane $H^+$-ATPase determine the release of BNIs in sorghum roots – possible mechanisms and underlying hypothesis. *Plant and Soil* **358**(1–2), 131–141. https://doi.org/10.1007/s11104-012-1151-5

Zhu, Z., Gerendas, J., Bendixen, R., Schinner, K., Tabrizi, H., Sattelmacher, B., & Hansen, U. P. (2000). Different tolerance to light stress in $NO_3^-$- and $NH_4^+$-grown *Phaseolus vulgaris* L. *Plant Biology* **2**(5), 558–570. https://doi.org/10.1055/s-2000-7498

Zumft, W. G. (1997). Cell Biology and Molecular Basis of Denitrification. *Microbiology and Molecular Biology* **Reviews** 61(4).

# Appendix

**Appendix A.1:** Detailed schematic for building tension table ladder circuits. Elbow and T connectors are shown in black, porous pipe is shown in blue. Dashed blue lines indicate porous pipe sections cut to fit individual tables depending where the hole was drilled into the acrylic wall of the tank.

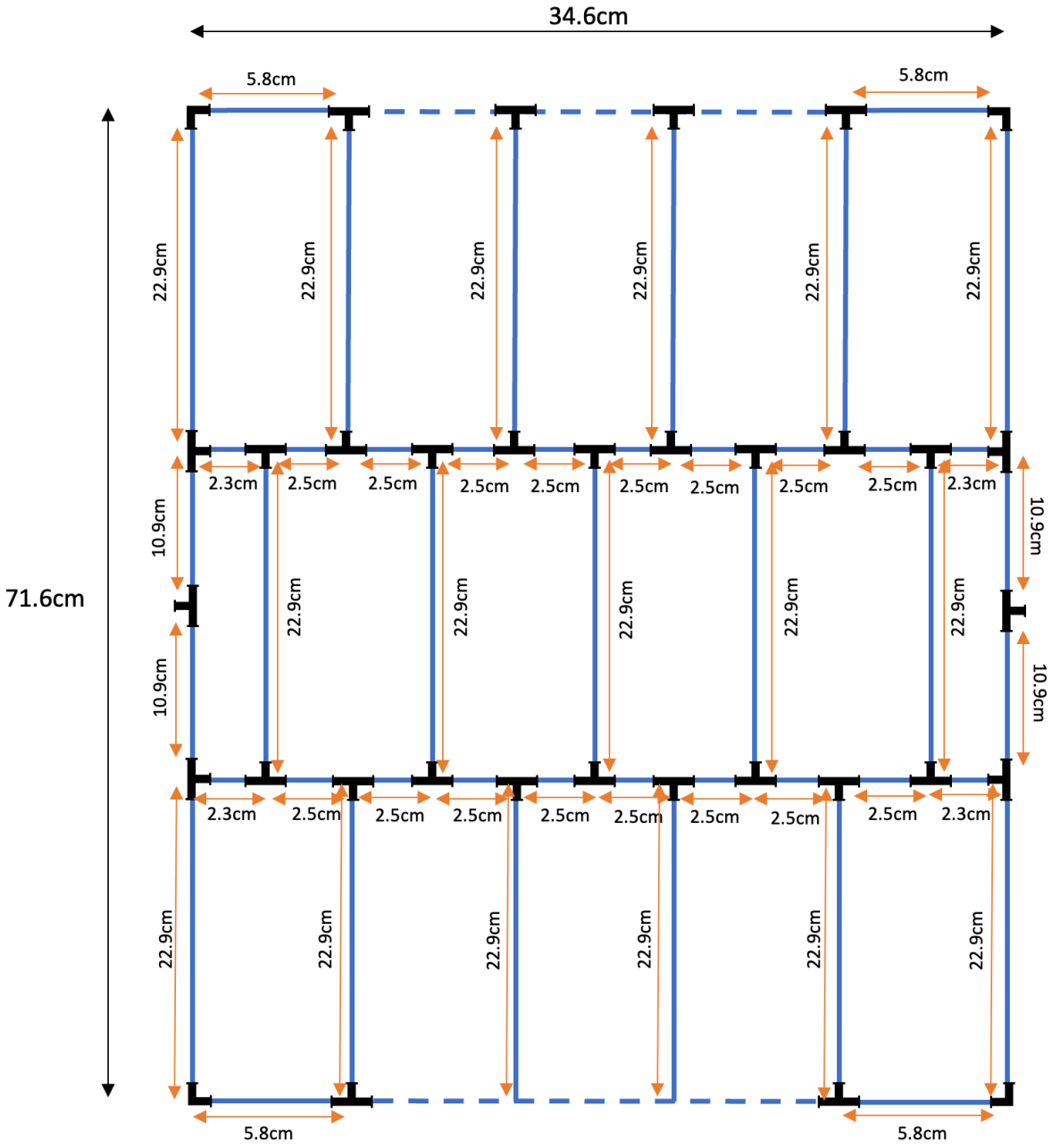

**Appendix table A.1:** Overview of the 200 barley cultivars included in Chapters 3 and 4, their assigned number code, cultivar name and whether they were supplied by the James Hutton Institute (JHI) or Syngenta (Syn).

| Number code | Cultivar name | Source of seed |
|---|---|---|
| 1 | Alabama | JHI |
| 2 | Alexis | JHI |
| 3 | Alliot | JHI |
| 4 | Aluminium | JHI |
| 5 | Anais | JHI |
| 6 | Annabell | JHI |
| 7 | Apex | JHI |
| 8 | Appaloosa | JHI |
| 9 | Aramir | JHI |
| 10 | Armelle | JHI |
| 11 | Arvo | JHI |
| 12 | Athos | JHI |
| 13 | Atlas | JHI |
| 14 | Avec | JHI |
| 15 | B83 | JHI |
| 16 | Balder | JHI |
| 17 | Balga | JHI |
| 18 | Barke | JHI |
| 19 | Baronesse | JHI |
| 20 | Beatrix | JHI |
| 21 | Beka | JHI |
| 22 | Berenice | JHI |
| 23 | Berwick | JHI |
| 24 | Binder Abed | JHI |
| 25 | Blenheim | JHI |
| 26 | Bonus | JHI |
| 27 | Braemar | JHI |
| 28 | Brazil | JHI |
| 29 | Bulle | Syn |

| Number code | Cultivar name | Source of seed |
|---|---|---|
| 30 | Camargue | JHI |
| 31 | Campala | JHI |
| 32 | Carlsberg | JHI |
| 33 | Caromia | Syn |
| 34 | Cellar | JHI |
| 35 | Centurion | JHI |
| 36 | Century | JHI |
| 37 | Chad | JHI |
| 38 | Chalice | JHI |
| 39 | Chariot | JHI |
| 40 | Chaser | JHI |
| 41 | Chevalier Tystofte 2 | JHI |
| 42 | Chieftain | JHI |
| 43 | Chime | JHI |
| 44 | Claret | JHI |
| 45 | Class | JHI |
| 46 | Cocktail | JHI |
| 47 | Colada | JHI |
| 48 | Concerto | JHI |
| 49 | Cooper | JHI |
| 50 | Corniche | JHI |
| 51 | Crusader | JHI |
| 52 | Deba Abed | JHI |
| 53 | Decanter | JHI |
| 54 | Derkado | JHI |
| 55 | Diamant | JHI |
| 56 | Digger | JHI |
| 57 | Dioptric | JHI |
| 58 | Domen | JHI |
| 59 | Doyen | JHI |
| 60 | Dragoon | Syn |
| 61 | Drum | JHI |
| 62 | Egmont | JHI |

| Number code | Cultivar name | Source of seed |
|---|---|---|
| 63 | Emir | JHI |
| 64 | Fairing | JHI |
| 65 | Fairytale | JHI |
| 66 | Freja | JHI |
| 67 | Georgie | JHI |
| 68 | Gitane | JHI |
| 69 | Golden Promise | JHI |
| 70 | Golf | JHI |
| 71 | Gull | JHI |
| 72 | Hannchen | JHI |
| 73 | Hart | JHI |
| 74 | Hellas | JHI |
| 75 | Heron | JHI |
| 76 | Imidis | JHI |
| 77 | Isabella | JHI |
| 78 | Isaria | JHI |
| 79 | Kassima | JHI |
| 80 | Klaxon | JHI |
| 81 | Koral | JHI |
| 82 | Krona | JHI |
| 83 | Krystal | JHI |
| 84 | KWS Irina | JHI |
| 85 | KWS Sassy | JHI |
| 86 | Kym | JHI |
| 87 | Landlord | JHI |
| 88 | Latrobe | Syn |
| 89 | Laureate | Syn |
| 90 | LG Diablo | JHI |
| 91 | Livet | JHI |
| 92 | Macaw | JHI |
| 93 | Maja | JHI |
| 94 | Maresi | JHI |
| 95 | Maris Mink | JHI |

| Number code | Cultivar name | Source of seed |
|---|---|---|
| 96 | Marthe | JHI |
| 97 | Maypole | JHI |
| 98 | Melius | Syn |
| 99 | Meltan | JHI |
| 100 | Mickle | Syn |
| 101 | Midas | JHI |
| 102 | Natasha | JHI |
| 103 | NFC Tipple | JHI |
| 104 | Novello | JHI |
| 105 | Optic | JHI |
| 106 | Ovation | JHI |
| 107 | Overture | JHI |
| 108 | Pallas | JHI |
| 109 | Pewter | JHI |
| 110 | Pilote | Syn |
| 111 | Pitcher | JHI |
| 112 | Poker | JHI |
| 113 | Potter | JHI |
| 114 | Power | JHI |
| 115 | Prague | JHI |
| 116 | Prestige | JHI |
| 117 | Prisma | JHI |
| 118 | Proctor | JHI |
| 119 | Propino | Syn/JHI |
| 120 | Publican | JHI |
| 121 | Quench | JHI |
| 122 | Rainbow | JHI |
| 123 | Reggae | JHI |
| 124 | Renata | JHI |
| 125 | RGT Asteroid | JHI |
| 126 | RGT Planet | JHI |
| 127 | Riviera | JHI |
| 128 | Rummy | JHI |

| Number code | Cultivar name | Source of seed |
|---|---|---|
| 129 | Saloon | JHI |
| 130 | Sanette | Syn |
| 131 | Scandium | JHI |
| 132 | Scarlett | JHI |
| 133 | Scholar | Syn |
| 134 | Scrabble | Syn |
| 135 | Sebastian | JHI |
| 136 | Simba | JHI |
| 137 | Skittle | JHI |
| 138 | Sparkle | Syn |
| 139 | Spartan | JHI |
| 140 | Spey | JHI |
| 141 | Spire | JHI |
| 142 | Starlight | JHI |
| 143 | Static | JHI |
| 144 | Steffi | JHI |
| 145 | Steina | JHI |
| 146 | Sultan | JHI |
| 147 | SW Scania | JHI |
| 148 | SY Arderin | Syn |
| 149 | SY Cristal | Syn |
| 150 | SY Errigal | Syn |
| 151 | SY Solar | Syn |
| 152 | SY Stanza | Syn |
| 153 | Syn 1 | Syn |
| 154 | Syn 2 | Syn |
| 155 | Syn 3 | Syn |
| 156 | Syn 4 | Syn |
| 157 | Syn 5 | Syn |
| 158 | Syn 6 | Syn |
| 159 | Syn 7 | Syn |
| 160 | Syn 8 | Syn |
| 161 | Syn 9 | Syn |

| Number code | Cultivar name | Source of seed |
|---|---|---|
| 162 | Syn 10 | Syn |
| 163 | Syn 11 | Syn |
| 164 | Syn 12 | Syn |
| 165 | Syn 13 | Syn |
| 166 | Syn 14 | Syn |
| 167 | Syn 15 | Syn |
| 168 | Syn 16 | Syn |
| 169 | Syn 17 | Syn |
| 170 | Syn 18 | Syn |
| 171 | Syn 19 | Syn |
| 172 | Syn 20 | Syn |
| 173 | Syn 21 | Syn |
| 174 | Syn 22 | Syn |
| 175 | Syn 23 | Syn |
| 176 | Syn 24 | Syn |
| 177 | Syn 25 | Syn |
| 178 | Syn 26 | Syn |
| 179 | Syn 27 | Syn |
| 180 | Syn 28 | Syn |
| 181 | Syn 29 | Syn |
| 182 | Syn 30 | Syn |
| 183 | Tankard | JHI |
| 184 | Taphouse | JHI |
| 185 | Tartan | JHI |
| 186 | Tavern | JHI |
| 187 | Tocada | JHI |
| 188 | Torbellino | Syn |
| 189 | Tremois | JHI |
| 190 | Trinity | JHI |
| 191 | Triumph | JHI |
| 192 | Troon | JHI |
| 193 | Tyne | JHI |
| 194 | Union | JHI |

| Number code | Cultivar name | Source of seed |
|---|---|---|
| 195 | Valticky | JHI |
| 196 | Volla | JHI |
| 197 | Waggon | JHI |
| 198 | Westminster | JHI |
| 199 | Wisa | JHI |
| 200 | Zephyr 2RSB | JHI |